

See discussions, stats, and author profiles for this publication at: <https://www.researchgate.net/publication/228819984>

Numerical Methods in Meteorology and Oceanography

Article · November 2010

CITATIONS

2

READS

1,183

1 author:



Kristofer Döös
Stockholm University
79 PUBLICATIONS 1,774 CITATIONS

[SEE PROFILE](#)

Some of the authors of this publication are also working on these related projects:



Project TRACMASS [View project](#)

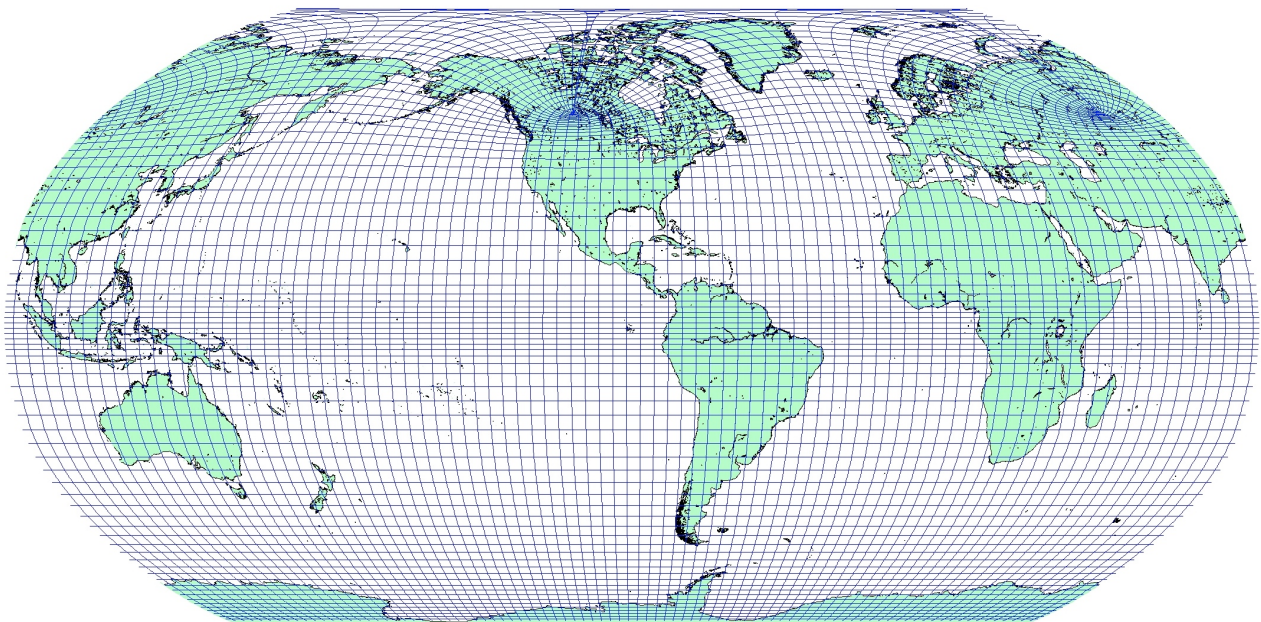


Project Eulerian and Lagrangian view of the coupled ocean-atmosphere hydrologic cycle [View project](#)

Numerical Methods in Meteorology and Oceanography



Kristofer Döös
Department of Meteorology
Stockholm University
<http://doos.misu.su.se/pap/compnum.pdf>
Email:doos@misu.su.se



6th October 2010

Contents

1	Introduction	5
2	Partial Differential Equations (PDE)	7
2.1	Elliptic	8
2.2	Parabolic	9
2.3	Hyperbolic	10
3	Finite differences	12
3.1	The grid point method	12
3.2	Finite difference schemes	12
3.3	Finite time differences	14
3.3.1	Two-level-schemes	15
3.3.2	Three-level-schemes	16
4	Numerical stability of the advection equation (hyperbolic)	18
4.1	The advection equation with leap-frog-scheme, i.e. $O[(\Delta x)]^2$	18
4.2	The advection equation with Euler (forward) scheme in time and centered scheme in space	20
4.3	The upstream or upwind scheme	21
4.4	The advection equation with a $O[(\Delta x)^4]$ scheme	25
5	The numerical mode	30
5.1	The numerical mode of the three level schemes	30
5.1.1	The computational initial condition	32
5.2	Suppression of the computational mode	32
6	Accuracy of the numerical phase speed	34
6.1	Dispersion due to the spatial discretisation	34
6.2	Dispersion due to the time discretisation	34
6.3	Dispersion due to both the spatial and time discretisation	36
7	Diffusion and friction terms (parabolic)	40
7.1	Rayleigh friction	40
7.2	The heat equation	42

CONTENTS	2
7.3 Advection-diffusion equation	47
8 Poisson and Laplace equations (elliptic)	51
8.1 Jacobi iteration	51
8.2 Gauss-Seidel iteration	51
8.3 Successive Over Relaxation (SOR)	52
9 The shallow water equations	54
9.1 One-dimensional gravity waves with centered space differencing	54
9.2 Two-dimensional gravity waves with centered space differencing	55
9.3 The linearised shallow water equations without friction	57
9.4 Conservation of mass, energy and enstrophy	62
9.4.1 The shallow water equations with non-linear advection terms	62
9.4.2 Discretisation	63
10 Implicit and semi-implicit schemes	66
10.1 The implicit scheme (trapezoidal rule)	66
10.2 The semi-implicit method of Kwizak and Robert	68
10.3 The semi-Lagrangian technique	69
10.3.1 Passive advection in 1-D	69
10.3.2 Interpolation and Stability	71
11 Spherical Harmonics	73
11.1 Spectral methods	73
11.2 Spherical harmonics	74
11.3 The spectral transform method	77
11.4 Application to the shallow water equations on a sphere	77
12 Different types of Coordinates	79
12.1 Fixed height or depth coordinates	79
12.2 Other vertical coordinates	80
12.2.1 Pressure coordinates	82
12.2.2 Sigma coordinates	83
12.2.3 Hybrid coordinates	84
12.2.4 Ocean GCM coordinates	85
12.3 Finite elements	85
12.4 Results from Ocean and Atmospheric General Circulation Models	86
13 Practical computer exercises	89
13.1 Purpose	89
13.2 Theory	89
13.3 Tools	90
13.4 Theoretical exercises	91

13.5 Experimental exercises	91
13.6 Shallow Water Exercise by Anders Engström	93
13.7 Theory	93
13.8 Tools	93
13.9 Report	93
13.10 Exercises	94
13.10.1 1D-model	94
13.10.2 2D-model	95
13.11 Optional exercises	95
13.11.1 Non-Linear	95
13.11.2 Spectral model	96
13.12 General code structure	97
14 Exams at Stockholm University 1999-2008	99

Preface

The purpose of this compendium is to give an introduction and an overview of numerical modelling of the ocean and the atmosphere. Numerical schemes for the most common equation in oceanography and meteorology are described. For simplicity the equations will often be referred as the *hydrodynamic* equations since the numerical methods described in this compendium are both for modelling of the ocean and the atmosphere. Because mainly of the non-linearities of the hydrodynamic equations, which describe the motion in the ocean and atmosphere it is not possible to find analytical solutions. We are therefore forced to make numerical approximations of the equations and solve them numerically by constructing numerical circulation models.

Kristofer Döös, associate professor in physical oceanography at the Department of Meteorology, Stockholm University

Chapter 1

Introduction

A numerical model of circulation of the atmosphere or the ocean is basically composed of three things:

1. A grid in space
2. Equations describing conservation of mass, heat, salt and momentum
3. Open boundaries

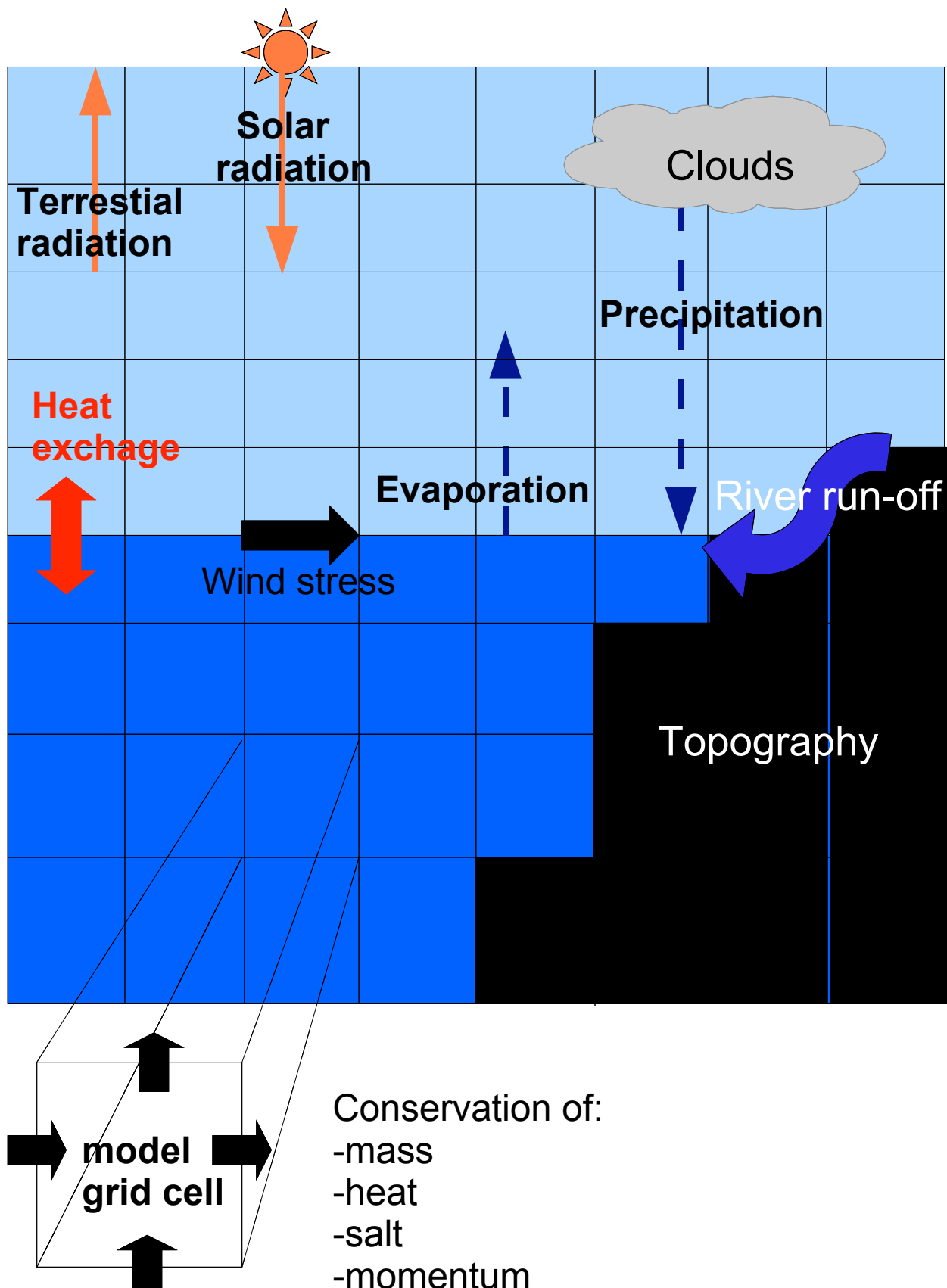


Figure 1.1: Schematic illustration of a numerical ocean-atmosphere circulation model

Chapter 2

Partial Differential Equations (PDE)

Before going into the numerics let us first classify the most usual types of PDE that occur in meteorology and oceanography. Partial differential equations are of vast importance in applied mathematics and engineering since so many real physical situations can be modelled by them. Second order linear PDEs can be classified into three categories - hyperbolic, parabolic and elliptic. These partial differential equations are the general linear homogeneous equations of the second order:

$$a \frac{\partial^2 u}{\partial x^2} + b \frac{\partial^2 u}{\partial x \partial y} + c \frac{\partial^2 u}{\partial y^2} + d \frac{\partial u}{\partial x} + e \frac{\partial u}{\partial y} + f u + g = 0 \quad (2.1)$$

Equation (2.1) resembles the equation for a conic section

$$ax^2 + bxy + cy^2 + dx + ey + f = 0 \quad (2.2)$$

where a, b, c, d, e, f are constants, Equation (2.2) represents an ellipse, parabola or a hyperbola according to $b^2 - 4ac <, = \text{ or } > 0$.

Thus one can classify the PDE according to Table 2.1.

These types of systems give rise to significantly different characteristic behaviour and, the solution scheme for each method can also differ. The three classes of PDEs require the specification of different kinds of boundary conditions. All three classes are represented among the most common equations in hydrodynamics.

We will now give examples of these equations.

Table 2.1: *Classification of the three PDEs and their different kinds of boundary conditions*

PDE	$b^2 - 4ac$	Boundary conditions
1. elliptic	$b^2 - 4ac < 0$	Dirichlet/Neumann/Robin
2. parabolic	$b^2 - 4ac = 0$	One initial+some boundary condition
3. hyperbolic	$b^2 - 4ac > 0$	Cauchy+some boundary condition

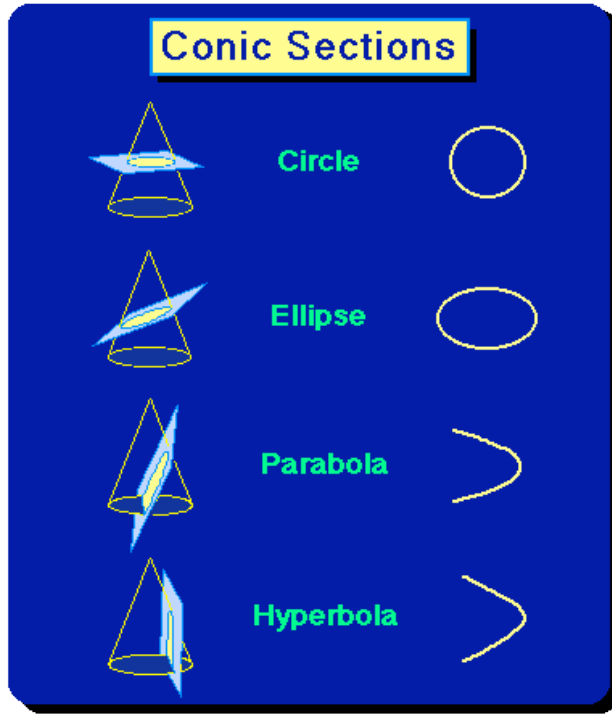


Figure 2.1: A diagram of conic sections, including a circle, an ellipse, a parabola and a hyperbola. Note that these geometrical representations of Equation (2.2) are not solutions to the PDE Equation (2.1).

2.1 Elliptic

Laplace's or Poisson's equations. Examples: steady state temperature of a plate, stream function/ vorticity relationship.

$$\frac{\partial^2 u}{\partial x^2} + \frac{\partial^2 u}{\partial y^2} = 0 \text{ (or } f(x, y))$$

From Eq. (2.1), we get $a = 1$, $b = 0$ and $c = 1$ which leads to that $b^2 - 4ac = -4 < 0$ and hence the PDE must be elliptic.

Helmholtz's equations. Many problems related to steady-state oscillations (mechanical, acoustical, thermal, electromagnetic) lead to the two-dimensional Helmholtz equation. For $f < 0$, this equation describes mass transfer processes with volume chemical reactions of the first order.

$$\frac{\partial^2 u}{\partial x^2} + \frac{\partial^2 u}{\partial y^2} + \lambda^2 u = 0$$

Schrödinger's equation describes the space- and time-dependence of quantum mechanical systems:

$$\frac{\partial^2 u}{\partial x^2} + \frac{\partial^2 u}{\partial y^2} + k(E - V)u = 0$$

Another example of an elliptic equation can be found from the simplest equation of motion in the atmosphere and the ocean. The linearised shallow water equations without friction. Note that the independent

variables x and y in 2.1 do not have anything with x and y in the equations below and must therefore be replaced in order to calculate $b^2 - 4ac$.

$$\frac{\partial u}{\partial t} - fv = -g \frac{\partial h}{\partial x} \quad (2.3)$$

$$\frac{\partial v}{\partial t} + fu = -g \frac{\partial h}{\partial y} \quad (2.4)$$

$$\frac{\partial h}{\partial t} + H \left(\frac{\partial u}{\partial x} + \frac{\partial v}{\partial y} \right) = 0 \quad (2.5)$$

From (2.3, 2.4, 2.5) we can deduce

$$\frac{\partial}{\partial t} \left[\frac{\partial^2}{\partial t^2} + f^2 - gH \left(\frac{\partial^2}{\partial x^2} + \frac{\partial^2}{\partial y^2} \right) \right] h = 0$$

If we integrate this in time we get

$$\frac{\partial^2 h}{\partial t^2} + f^2 h - gH \left(\frac{\partial^2}{\partial x^2} + \frac{\partial^2}{\partial y^2} \right) h = \xi(x, y)$$

If the problem is time independent then we get the geostrophic relationship

$$f^2 h - gH \left(\frac{\partial^2}{\partial x^2} + \frac{\partial^2}{\partial y^2} \right) h = \xi(x, y)$$

From Eq. (2.1), we get $a = -gH$, $b = 0$ and $c = -gH$ which leads to that $b^2 - 4ac = -4g^2H^2 < 0$ and hence the PDE must be elliptic.

Other elliptic PDEs are

There are three different types of possible boundary conditions for this class:

1. u to be specified on the boundary (Dirichlet).
2. $\frac{\partial u}{\partial n}$ to be specified on the boundary (Neumann)
3. $au + \frac{\partial u}{\partial x}$ to be specified on the boundary (Cauchy)

2.2 Parabolic

Diffusion equation. Example: temperature, salinity, passive tracers.

$$\frac{\partial T}{\partial t} = K \frac{\partial^2 T}{\partial x^2} \quad \text{where } K > 0$$

From Eq. (2.1), we get $a = K$, $b = 0$ and $c = 0$ which leads to that $b^2 - 4ac = 0$ and hence the PDE must be parabolic.

$T(x, t)$ is the temperature distribution along the x -axis as a function of time. To solve the equation in the interval $0 \leq x \leq L$ one must specify an initial condition $T(x, 0)$ on $0 \leq x \leq L$ and the boundary conditions $T(0, t)$ and $T(L, t)$ must be specified during the whole time period.

2.3 Hyperbolic

Wave equation. Examples: vibrating string, ocean and atmospheric gravity waves.

$$\frac{\partial^2 u}{\partial t^2} = c_0^2 \frac{\partial^2 u}{\partial x^2}$$

The first order PDE (advection equation) can also be classified as a hyperbolic, since its solutions satisfy the wave equation.

$$\frac{\partial u}{\partial t} = -c_0 \frac{\partial u}{\partial x}$$

By derivating the advection equation first with respect to t and then with respect to x , $(\frac{\partial}{\partial t} - c_0 \frac{\partial}{\partial x})$ it is possible to eliminate u_{tx} between the two equations and we obtain the wave equation.

From Eq. (2.1) we get $b^2 - 4ac = 4c_0^2 > 0$ i.e. hyperbolic. In order to obtain unique solutions for $0 \leq x \leq L$ we need two initial conditions and boundary conditions in both ends of u . E.g.

- $u(x, 0)$ specified initially on $0 \leq x \leq L$
- $\frac{\partial(u, 0)}{\partial t}$ specified initially on $0 \leq x \leq L$
- $u(0, t)$ specified on the boundary $x = 0$
- $\frac{\partial(L, t)}{\partial x}$ free or open boundary on $x = L$

The behaviour of the solutions, the proper initial and/or boundary conditions, and the numerical methods that can be used to find the solutions depend essentially on the type of PDE that we are dealing with. Although non-linear multidimensional PDEs cannot in general be reduced to these canonical forms, we need to study these prototypes of the PDEs to develop an understanding of their properties, and then apply similar methods to the more complicated equations.

Exercises:

1. Solve the following equation by separation of variables:

$$\frac{\partial u}{\partial t} = -c \frac{\partial u}{\partial x}$$

with the initial condition

$$u(x, 0) = -Ae^{ikx}$$

2. a) Show that the advection equation

$$\frac{\partial u}{\partial t} = -c \frac{\partial u}{\partial x}$$

has the general solution

$$u = f(x - ct)$$

where f is an arbitrary solution.

- b) Interpret the equation geometrically in the xt-plane.
- c) Solve the equation with the following initial condition: $u(x, 0) = g(x)$.

3. Derive the wave equation from the system

$$\frac{\partial \mathbf{V}}{\partial t} = -g \nabla h$$

$$\frac{\partial h}{\partial t} = -H \nabla (hV)$$

where g and H are constants.

Chapter 3

Finite differences

3.1 The grid point method

Let us study a function with one independent variable.

$$u = u(x)$$

Suppose we have an interval L which is covered with $N + 1$ equally spaced grid points. The grid length is then $\Delta x = L/N$ and the grid points are at $x_j = j\Delta x$ where $j = 0, 1, 2, \dots, N$ are integers. Let the value of u at x_j be represented by u_j .

3.2 Finite difference schemes

We are now going to derive expressions which can be used to give an approximate value of a derivative at a grid point in terms of grid-point values. The finite differences can be constructed between values of u_j over the grid length Δx . The first derivative of $u(x)$ can be approximated with

- forward difference: $(\frac{du}{dx})_j \rightarrow \frac{u_{j+1} - u_j}{\Delta x}$
- centered difference: $(\frac{du}{dx})_j \rightarrow \frac{u_{j+1} - u_{j-1}}{2\Delta x}$
- backward difference: $(\frac{du}{dx})_j \rightarrow \frac{u_j - u_{j-1}}{\Delta x}$

The is the same as the formal mathematical definition of a derivative of the function $u(x)$

$$\frac{du}{dx} = \lim_{\Delta x \rightarrow 0} \frac{u(x + \Delta x) - u(x)}{\Delta x}$$

with the difference that Δx does not tend to zero. This difference introduces an error that one can estimate by deriving the finite differences in a more rigorous way by using a Taylor expansion. The Taylor series for $f(y)$ about $y = a$ is

$$f(y) = f(a) + (y - a)f'(a) + \frac{1}{2}(y - a)^2 f''(a) + \dots + \frac{1}{n!}(y - a)^n f^{(n)}(a)$$

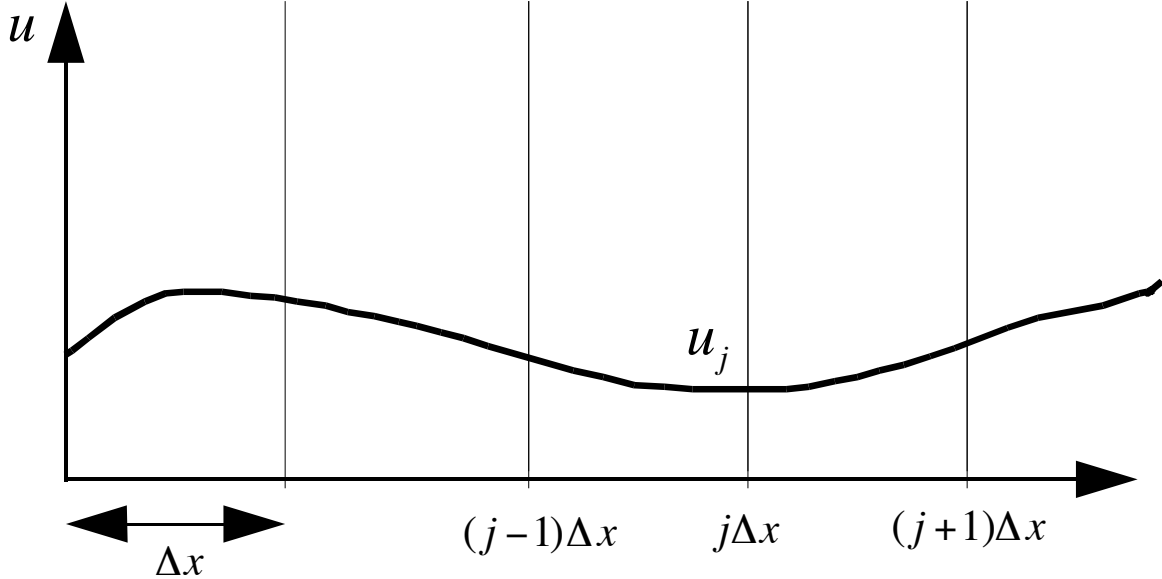


Figure 3.1: The approximation of $u(x)$ in the grid points $x = j\Delta x$ is $u_j = u(x=j\Delta x)$ where Δx is the grid length and $j = 0, 1, 2, \dots, I$ are integers.

Substituting $f(y)$ by $u(x)$, a by x_j and y by x_{j+1} , we obtain the Taylor expansion of the function $u(x)$ in the point $j + 1$.

$$u_{j+1} = u_j + \Delta x \left(\frac{du}{dx} \right)_j + \frac{1}{2} (\Delta x)^2 \left(\frac{d^2 u}{dx^2} \right)_j + \frac{1}{6} (\Delta x)^3 \left(\frac{d^3 u}{dx^3} \right)_j + \frac{1}{24} (\Delta x)^4 \left(\frac{d^4 u}{dx^4} \right)_j + \frac{1}{120} (\Delta x)^5 \left(\frac{d^5 u}{dx^5} \right)_j + \dots \quad (3.1)$$

The forward difference can now be expressed as

$$\frac{u_{j+1} - u_j}{\Delta x} = \left(\frac{du}{dx} \right)_j + \frac{1}{2} (\Delta x) \left(\frac{d^2 u}{dx^2} \right)_j + \frac{1}{6} (\Delta x)^2 \left(\frac{d^3 u}{dx^3} \right)_j + \frac{1}{24} (\Delta x)^3 \left(\frac{d^4 u}{dx^4} \right)_j + \frac{1}{120} (\Delta x)^4 \left(\frac{d^5 u}{dx^5} \right)_j + \dots \quad (3.2)$$

The difference between this expression and the approximated derivative $\left(\frac{du}{dx} \right)_j$ is

$$\varepsilon = \frac{1}{2} (\Delta x) \left(\frac{d^2 u}{dx^2} \right)_j + \frac{1}{6} (\Delta x)^2 \left(\frac{d^3 u}{dx^3} \right)_j + \frac{1}{24} (\Delta x)^3 \left(\frac{d^4 u}{dx^4} \right)_j + \frac{1}{120} (\Delta x)^4 \left(\frac{d^5 u}{dx^5} \right)_j + \dots$$

which is called the truncation error of the derivative approximation. These are the terms that have been truncated (erased). Hence we have an accuracy of the first order with

$$\varepsilon = O(\Delta x)$$

which is the lowest order of accuracy that is acceptable.

The accuracy of the centered difference can be obtained from 3.1 and a Taylor expansion in x of the function $u(x)$ at the point $j - 1$

$$u_{j-1} = u_j - \Delta x \left(\frac{du}{dx} \right)_j + \frac{1}{2} (\Delta x)^2 \left(\frac{d^2 u}{dx^2} \right)_j - \frac{1}{6} (\Delta x)^3 \left(\frac{d^3 u}{dx^3} \right)_j + \frac{1}{24} (\Delta x)^4 \left(\frac{d^4 u}{dx^4} \right)_j - \frac{1}{120} (\Delta x)^5 \left(\frac{d^5 u}{dx^5} \right)_j + \dots \quad (3.3)$$

so that

$$\frac{u_{j+1} - u_{j-1}}{2\Delta x} \rightarrow \left(\frac{du}{dx} \right)_j + \frac{1}{6} (\Delta x)^2 \left(\frac{d^3 u}{dx^3} \right)_j + \frac{1}{120} (\Delta x)^4 \left(\frac{d^5 u}{dx^5} \right)_j + \dots$$

The truncation error is of the second order:

$$\varepsilon = \frac{1}{6} (\Delta x)^2 \left(\frac{d^3 u}{dx^3} \right)_j + \dots = O((\Delta x)^2)$$

A scheme with fourth order accuracy can be obtained if we do a Taylor expansion for u_{j+2} :

$$u_{j+2} = u_j + 2\Delta x \left(\frac{du}{dx} \right)_j + \frac{1}{2} (2\Delta x)^2 \left(\frac{d^2 u}{dx^2} \right)_j + \frac{1}{6} (2\Delta x)^3 \left(\frac{d^3 u}{dx^3} \right)_j + \frac{1}{24} (2\Delta x)^4 \left(\frac{d^4 u}{dx^4} \right)_j + \frac{1}{120} (2\Delta x)^5 \left(\frac{d^5 u}{dx^5} \right)_j + \dots$$

and

$$u_{j-2} = u_j - 2\Delta x \left(\frac{du}{dx} \right)_j + \frac{1}{2} (2\Delta x)^2 \left(\frac{d^2 u}{dx^2} \right)_j - \frac{1}{6} (2\Delta x)^3 \left(\frac{d^3 u}{dx^3} \right)_j + \frac{1}{24} (2\Delta x)^4 \left(\frac{d^4 u}{dx^4} \right)_j - \frac{1}{120} (2\Delta x)^5 \left(\frac{d^5 u}{dx^5} \right)_j + \dots$$

so that

$$\frac{u_{j+2} - u_{j-2}}{4\Delta x} \rightarrow \left(\frac{du}{dx} \right) + \frac{4}{6} (\Delta x)^2 \left(\frac{d^3 u}{dx^3} \right)_j + \frac{16}{120} (\Delta x)^4 \left(\frac{d^5 u}{dx^5} \right)_j + \dots$$

This scheme is as the previous centered scheme accurate at the second order but if we combine the two centered schemes so that

$$\frac{4}{3} \frac{u_{j+1} - u_{j-1}}{2\Delta x} - \frac{1}{3} \frac{u_{j+2} - u_{j-2}}{4\Delta x} \rightarrow \left(\frac{du}{dx} \right) - \frac{1}{30} (\Delta x)^4 \left(\frac{d^5 u}{dx^5} \right)_j + \dots \quad (3.4)$$

we get an accuracy of the fourth order i.e. $\varepsilon = O((\Delta x)^4)$.

3.3 Finite time differences

The time schemes that are used for the PDEs are relatively simple, usually of the second and sometimes even only of the first order of accuracy. There are several reasons for this. First, it is a general experience that schemes constructed so as to have a high order of accuracy are mostly not very successful when solving PDEs.

This is in contrast to the experience with ordinary differential equations, where very accurate schemes, such as the Runge-Kutta method, are extremely rewarding. There is a basic reason for this difference. With an ordinary differential equation, the equation and a single initial condition is all that is required for an exact solution. Thus, the error of the numerical solution is entirely due the inadequacy of the scheme. With a PDE, the error of the numerical solution is brought about both by the inadequacy of the scheme and by insufficient information about the initial conditions, since they are known only at discrete space points. Thus, an increase in accuracy of the scheme improves only one of these two components, and the result is not too impressive.

Another reason for not requiring a scheme of high accuracy for approximations to the time derivative terms is that, in order to meet a stability requirement of the type discussed in the next chapter, it is usually necessary to choose a time step significantly smaller than that required for adequate accuracy. With the time step usually chosen, other errors, for example in the space differencing, are much greater than those due to the time differencing. Thus, computation effort is better spent in reducing these errors, and not in increasing the accuracy of the time differencing schemes. This, of course, does not mean that it is not necessary to consider carefully the properties of various possible time differencing schemes. Accuracy, is only one important consideration in choosing a scheme.

To define some schemes, we consider the equation:

$$\frac{du}{dt} = f(u, t) \quad \text{where } u = u(t)$$

The independent variable t is the time. f is a function of u and t , e.g. the advection equation where $f = -c\frac{\partial u}{\partial x}$

In order to discretise the equation we will divide the time axis into segments of equal length Δt . The approximated value of $u(t)$ at time $t = n\Delta t$ is u^n . In order to compute u^{n+1} we need to know at least u^n and often also u^{n-1} . There are many different time schemes.

3.3.1 Two-level-schemes

These are schemes that use two different time levels: n and $n + 1$ and that the time integration becomes

$$u^{n+1} = u^n + \int_{n\Delta t}^{(n+1)\Delta t} f(u, t) dt$$

The problem now is that f only exists as discrete values f^n and f^{n+1} .

Euler or forward scheme

$$u^{n+1} = u^n + \Delta t f^n$$

The truncation error of this scheme is $O(\Delta t)$, i.e. a first order accurate scheme. The scheme is said to be *uncentered* since the time derivative is at time level $n + 1/2$ and the function at time level n . In general, uncentered schemes are accurate to the first order and centered to the second order.

Backward scheme

$$u^{n+1} = u^n + \Delta t f^{n+1}$$

The backward scheme is uncentered in time and of $O(\Delta t)$. If, as here, a value of f is taken at time level $n + 1$ and that f depends of u , i.e. u^{n+1} then the scheme is said to be *implicit*. For an ordinary differential equation, it may be simple to solve for u^{n+1} .

But for a PDE it will require solving a set of simultaneous equations, with one equation for each of the grid points of the computation region. If no value of f depends of u^{n+1} on the right hand side the scheme is said to be *explicit*.

In the very simple cases when f only depends on t such as e.g. $du/dt = -\gamma u$ then the discretised equation becomes $u^{n+1} = u^n + \Delta t (-\gamma u^{n+1})$, which can be rearranged to $u^{n+1} = u^n/(1 + \gamma\Delta t)$ so that all there are no terms of $n + 1$ on the right hand side and the discretised equation can be easily integrated despite that it is still implicit.

Trapezoidal scheme

If we approximate f by an average between time level $n + 1$ and n we obtain the trapezoidal scheme

$$u^{n+1} = u^n + \frac{1}{2}\Delta t (f^n + f^{n+1})$$

This scheme is also *implicit*, its truncation error is however $O((\Delta t)^2)$.

Matsuno or Euler-backward scheme

To increase the accuracy we can construct iterative schemes such as the Matsuno scheme that first uses an Euler forward time step.

$$u^{n+1/2} = u^n + \Delta t f^n$$

Then the value of the obtained u^{n+1} is used for an approximation of f^{n+1} , which is then used to make a backward step to obtain a final u^{n+1} .

$$u^{n+1} = u^{n+1/2} + \Delta t f^{n+1/2}$$

This scheme is *explicit* and of $O(\Delta t)$.

3.3.2 Three-level-schemes

These schemes use the the time at three levels and the time integration becomes

$$u^{n+1} = u^{n-1} + \int_{(n-1)\Delta t}^{(n+1)\Delta t} f(u, t) dt$$

The simplest three level scheme is to take for f a constant value equal to that at the middle of the interval $2\Delta t$. This gives the leapfrog scheme :

$$u^{n+1} = u^{n-1} + 2\Delta t f^n$$

which is of $O((\Delta t)^2)$. This is the most widely used scheme in atmospheric and ocean models.

Exercises:

1. Determine the order of accuracy of the leapfrog scheme,

$$\frac{u_j^{n+1} - u_j^{n-1}}{2\Delta t} + c \frac{u_{j+1}^n - u_{j-1}^n}{2\Delta x} = 0$$

for the advection equation

$$\frac{\partial u}{\partial t} + c \frac{\partial u}{\partial x} = 0$$

2. Determine the order of accuracy of the Euler forward scheme for the heat equation:

$$\frac{\partial u}{\partial t} = A \frac{\partial^2 u}{\partial x^2} \quad \text{where } A > 0$$

$$\frac{u_j^{n+1} - u_j^n}{\Delta t} = A \frac{u_{j+1}^n - 2u_j^n + u_{j-1}^n}{(\Delta x)^2}$$

Chapter 4

Numerical stability of the advection equation (hyperbolic)

In this chapter we will study differential equations with one dependent variable and two independent variables, that is PDE. More specifically we shall consider various simplified forms of the advection equation, describing advection of a dependent variable. This is considered in practice to be the most important part of the hydrodynamic equations for the ocean and the atmosphere.

We will use the advection equation, which is one of the dominating hyperbolic equations in geophysical hydrodynamics, to investigate what is required of the numerical schemes to be give stable solutions to the PDE, i.e. so that the small perturbations do not grow in time.

4.1 The advection equation with leap-frog-scheme, i.e. $\mathcal{O}[(\Delta x)]^2$

$$\frac{\partial u}{\partial t} + c \frac{\partial u}{\partial x} = 0$$

where $u = u(x, t)$ and c is phase speed. Analytical solutions are of the form $u(x, t) = u_0 e^{ik(x-ct)}$ with $c \equiv \omega/k$.

Let us now consider one among many possible discretisations of the advection equation using a centred difference both in time (leap frog) and in space so that

$$\frac{u_j^{n+1} - u_j^{n-1}}{2\Delta t} + c \frac{u_{j+1}^n - u_{j-1}^n}{2\Delta x} = 0 \quad (4.1)$$

In order to study the stability we will use the so called von Neumann method, which is generally not possible to use on non linear equations and one is therefore limited to study the linearised version of the equations in a numerical model. A solution to a linear equation can be expressed as a Fourier series where each Fourier component is a solution. Thus, we can test the stability with one single Fourier component of the form

$$u_j^n = u_0 e^{ik(j\Delta x - C_D n \Delta t)}$$

Note that the phase speed C_D , has an index D for finite difference, which is an approximation of the phase speed c of the differential equation. It is this C_D that has been obtained as a solution to 4.1, and which will here

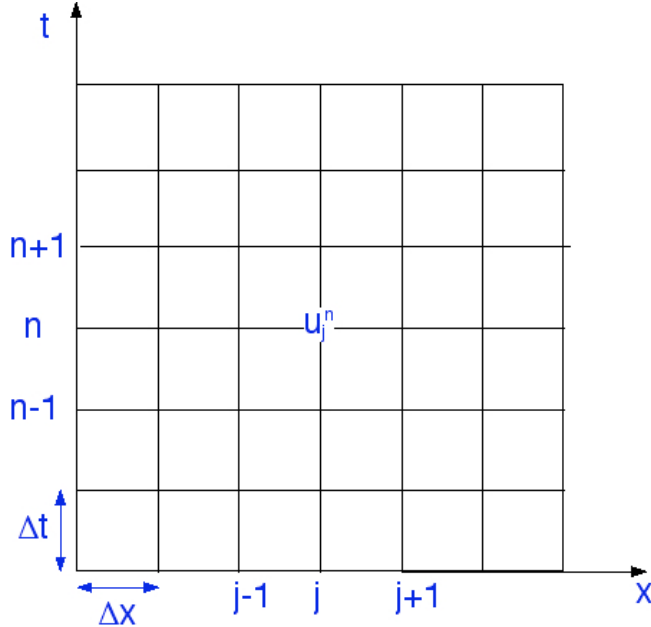


Figure 4.1: A finite difference grid in time and space.

be investigated. We observe that

$$u_j^{n+1} = u_0 e^{ik[j\Delta x - C_D(n+1)\Delta t]} = u_j^n e^{-ikC_D\Delta t} = u_j^n \lambda \quad \text{where } \lambda \equiv e^{-ikC_D\Delta t}$$

we can in the same way write for $n - 1$:

$$u_j^{n-1} = u_j^n \lambda^{-1}$$

that can be generalised as

$$u_j^{n+m} = u_j^n \lambda^m$$

and

$$u_j^n = \lambda^n u_0 e^{ikj\Delta x}$$

From this we can deduce that if $|u|$ is not going to “blow up” when integrating in time then one needs to require that

$$|\lambda| = \left| e^{-ikC_D\Delta t} \right| \leq 1 \tag{4.2}$$

and reversely if $|\lambda| > 1$ then it is unstable and it “blows up”. For that the condition 4.2 is fulfilled then C_D has to be real. This method based on studying the amplification factor λ is called the von Neumann method.

Let us now return to 4.1 and use λ so that

$$\lambda^2 + 2i \frac{c\Delta t}{\Delta x} \sin(k\Delta x) \lambda - 1 = 0 \tag{4.3}$$

Since $e^{i\alpha} - e^{-i\alpha} = 2i \sin \alpha$ and $x^2 + \alpha x + \beta = 0 \Rightarrow x = -\alpha/2 \pm \sqrt{\alpha^2/4 - \beta}$

4.3 has the solution:

$$\lambda = -i \frac{c\Delta t}{\Delta x} \sin(k\Delta x) \pm \sqrt{1 - \left(\frac{c\Delta t}{\Delta x} \sin(k\Delta x)\right)^2}$$

Since the absolute value of the complex number: $a + ib$ is $\sqrt{a^2 + b^2}$

If

$$\left[\frac{c\Delta t}{\Delta x} \sin(k\Delta x)\right]^2 \leq 1 \quad (4.4)$$

then

$$|\lambda|^2 = \left[\frac{c\Delta t}{\Delta x} \sin(k\Delta x)\right]^2 + \left\{ \sqrt{1 - \left[\frac{c\Delta t}{\Delta x} \sin(k\Delta x)\right]^2} \right\}^2 = 1$$

i.e. this scheme is stable if 4.4 is true and can also be written as

$$\frac{c\Delta t}{\Delta x} |\sin(k\Delta x)| \leq 1$$

and since $|\sin(k\Delta x)| \leq 1$ we have granted stability if

$$c \leq \frac{\Delta x}{\Delta t} \quad (4.5)$$

The Leap-frog is said to be *conditionally stable* with the so called *Courant-Fredrichs-Lowy or CFL criterion*. For a given spatial resolution (Δx) we need a time step (Δt) not exceeding $\frac{\Delta x}{c}$ so that 4.5 is valid for the fastest possible phase speed in the system. In the ocean this is set by the deepest depth H_{MAX} and the speed for long gravity waves so that for a chosen resolution Δx we get $\Delta t = \frac{\Delta x}{c} = \frac{\Delta x}{\sqrt{gH_{MAX}}}$.

4.2 The advection equation with Euler (forward) scheme in time and centered scheme in space

Let us now use another numerical scheme for the advection equation so that instead of 4.1 we have

$$\frac{u_j^{n+1} - u_j^n}{\Delta t} + c \frac{u_{j+1}^n - u_{j-1}^n}{2\Delta x} = 0 \quad (4.6)$$

Now we get

$$\lambda = 1 - i \frac{c\Delta t}{\Delta x} \sin(k\Delta x)$$

As before the criterion is that $|\lambda| \leq 1$ for stability and the absolute value of λ is now

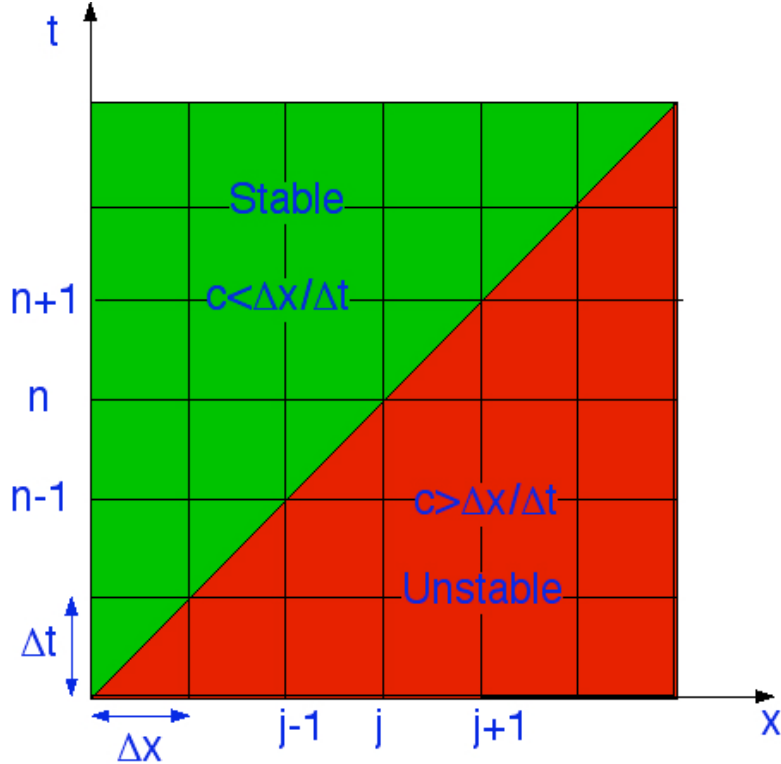


Figure 4.2: The Courant-Friedrichs-Lowy (CFL) stability criterion for centered schemes in time and space.

$$|\lambda|^2 = 1 + \left[\frac{c\Delta t}{\Delta x} \sin(k\Delta x) \right]^2$$

which is always $|\lambda| > 1$. Thus, the solution grows with time independently of how we choose the time step. This scheme is *unconditionally unstable*.

4.3 The upstream or upwind scheme

Let us now use a third numerical scheme for the advection equation

$$\begin{aligned} \frac{u_j^{n+1} - u_j^n}{\Delta t} + c \frac{u_j^n - u_{j-1}^n}{\Delta x} &= 0 \quad \text{if } c > 0 \\ \frac{u_j^{n+1} - u_j^n}{\Delta t} + c \frac{u_{j+1}^n - u_j^n}{\Delta x} &= 0 \quad \text{if } c < 0 \end{aligned} \tag{4.7}$$

The scheme is called upstream or upwind since it looks for information from where the wind or stream is coming in point $j - 1$. If $c > 0$ then one should use a backward scheme in space in order to have an upstream scheme.

The von Neumann stability analysis gives us

$$\lambda = 1 - \frac{c\Delta t}{\Delta x} [1 - \cos(k\Delta x) + i \sin(k\Delta x)]$$

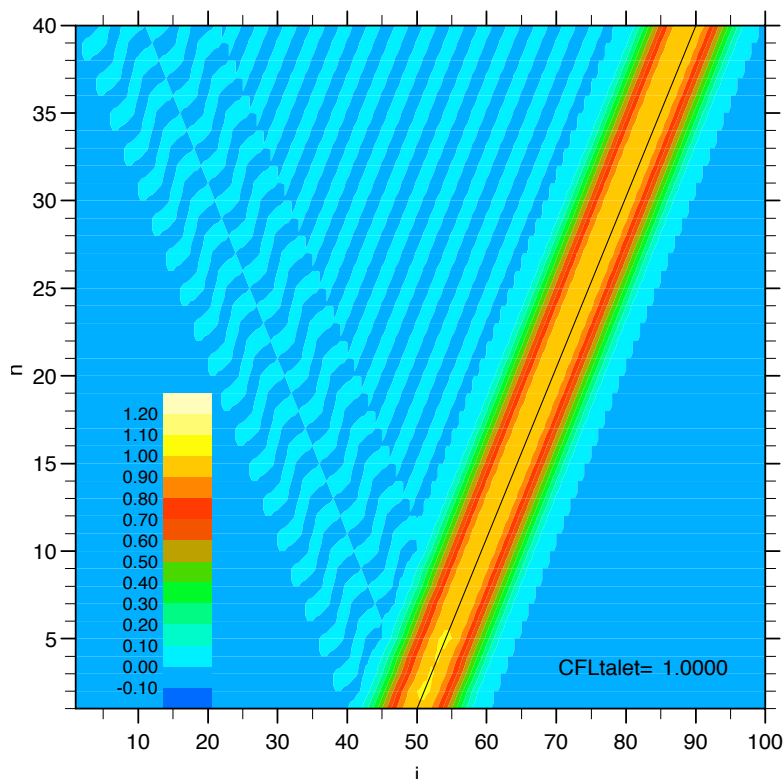


Figure 4.3: The advection equation integrated numerically with leap-frog and centered scheme in space 4.1. The first time step has been integrated with an Euler (forward) scheme. The CFL-number is $C_{FL} \equiv \frac{c\Delta t}{\Delta x} = 1$. The initial value is $u_j^{n=0} = \cos\left(\frac{\pi}{20}j\right)$ for $-10 \leq j \leq 10$ and $u_j^{n=0} = 0$ for the rest.

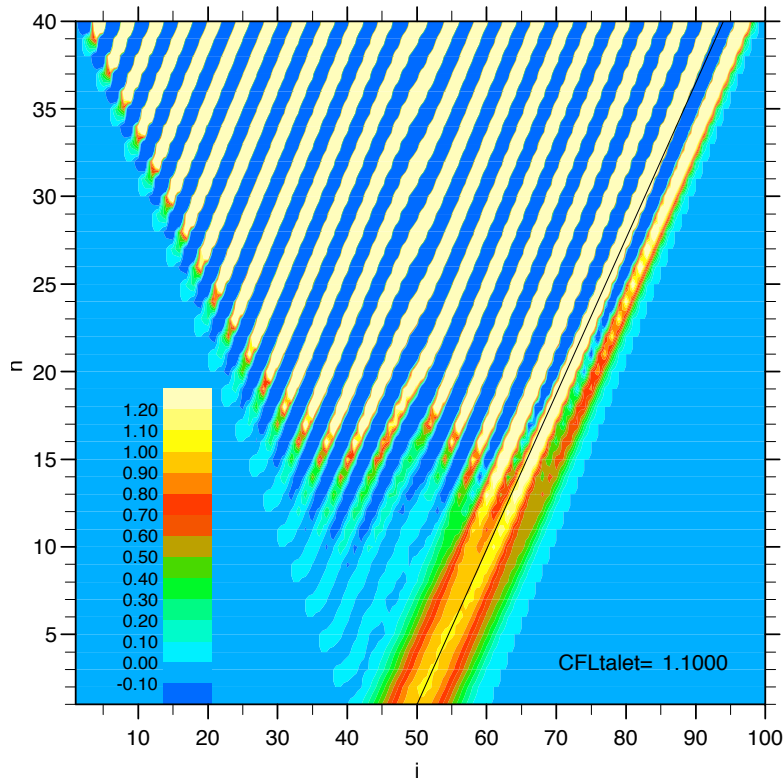


Figure 4.4: Same as Figure 4.3 but with $C_{FL} \equiv \frac{c\Delta t}{\Delta x} = 1.1$.

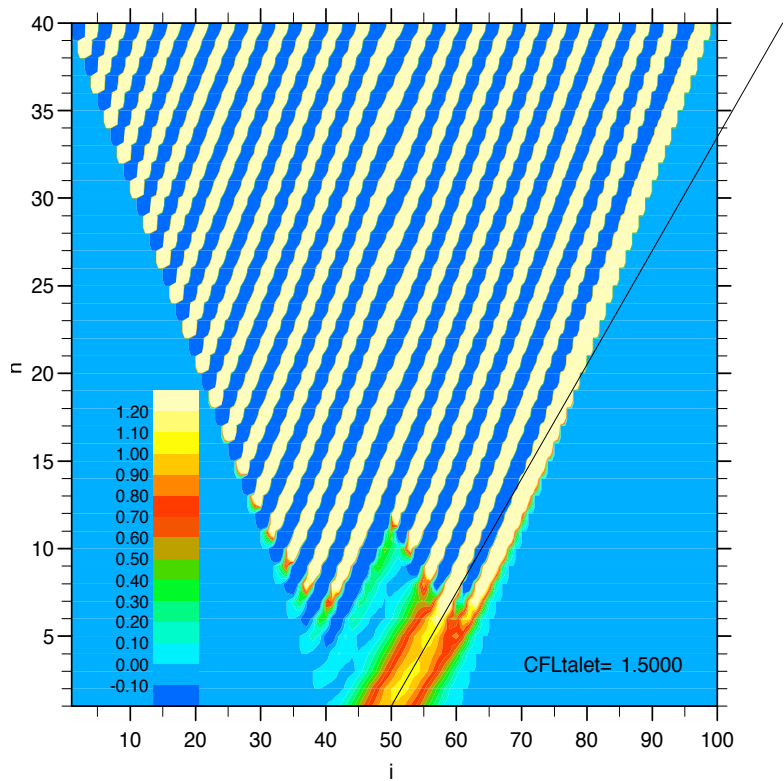


Figure 4.5: Same as Figure 4.3 but with $C_{FL} \equiv \frac{c\Delta t}{\Delta x} = 1.5$

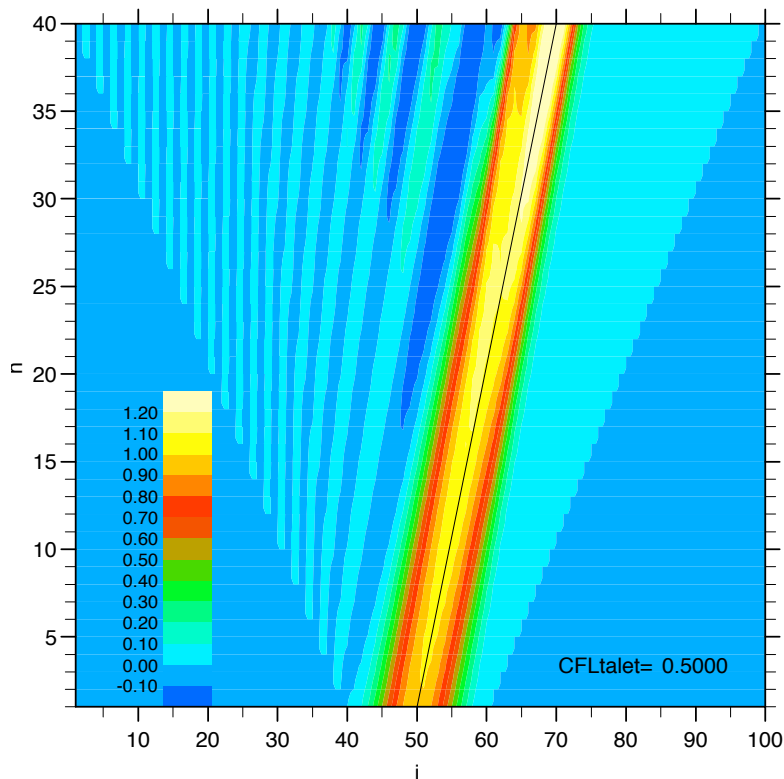


Figure 4.6: The advection equation integrated with Euler forward and a centered scheme in space. The CFL-number is $C_{FL} \equiv \frac{c\Delta t}{\Delta x} = 0.5$. Note that the solution does not seem to suddenly blow up but increases monotonically.

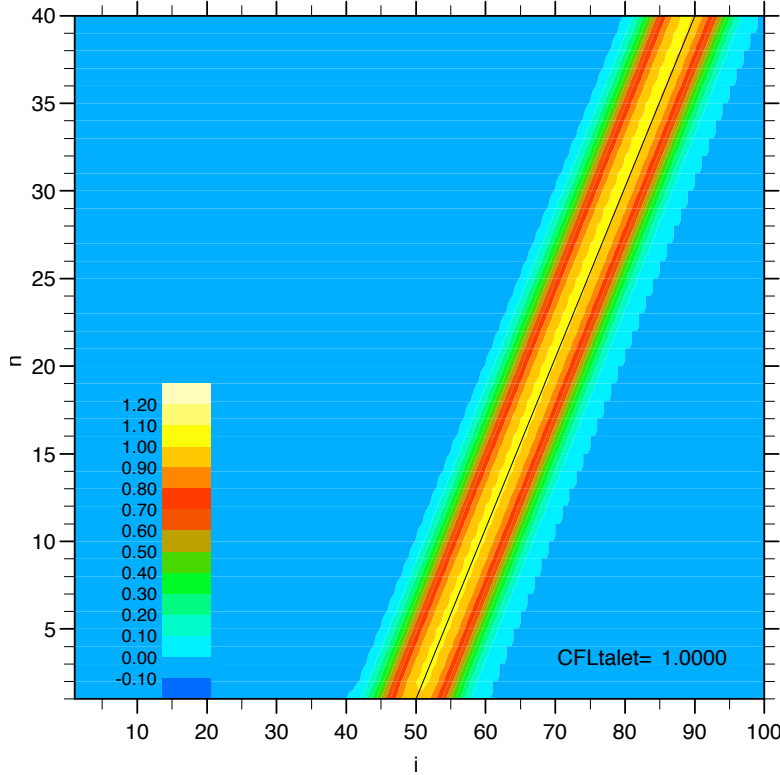


Figure 4.7: The advection Equation integrated numerically with the upstream scheme (Equation 4.7). The CFL-number is $C_{FL} \equiv \frac{c\Delta t}{\Delta x} = 1$.

and

$$|\lambda|^2 = \left\{ 1 - \frac{c\Delta t}{\Delta x} [1 - \cos(k\Delta x)] \right\}^2 + \left[\frac{c\Delta t}{\Delta x} \sin(k\Delta x) \right]^2 = 1 + 2\frac{c\Delta t}{\Delta x} [1 - \cos(k\Delta x)] \left(\frac{c\Delta t}{\Delta x} - 1 \right)$$

For $|\lambda|^2 < 1$ then we must have $0 \leq \frac{c\Delta t}{\Delta x} \leq 1$ which implies that c has to be positive to have stability. The scheme is hence conditionally stable. The criterion is otherwise similar to the one for the Leap frog scheme.

The upwind advection scheme was used in early numerical weather models due to its good stability properties, and it still finds use in idealised ocean box models as well as some general circulation models. When using upwind, however, one should realise that it is highly diffusive. The upwind scheme uses backward space differences if the velocity is in the positive x direction, and forward space differences for negative velocities. The name upwind denotes the use of upwind, or upstream, information in determining the form for the finite difference; downstream information is ignored.

4.4 The advection equation with a $O[(\Delta x)^4]$ scheme

Let us now study one final scheme of advection scheme which uses the forth order accurate spatial scheme 3.4.

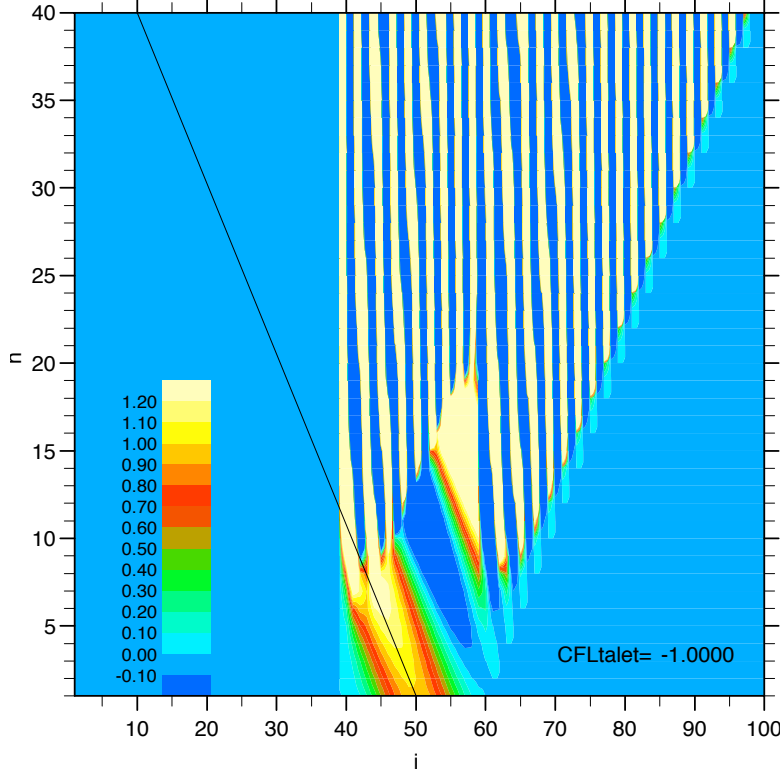


Figure 4.8: Same as Figure 4.7 but with $C_{FL} \equiv \frac{c\Delta t}{\Delta x} = -1$.

$$\frac{u_j^{n+1} - u_j^{n-1}}{2\Delta t} + c \left(\frac{4}{3} \frac{u_{j+1}^n - u_{j-1}^n}{2\Delta x} - \frac{1}{3} \frac{u_{j+2}^n - u_{j-2}^n}{4\Delta x} \right) = 0 \quad (4.8)$$

The von Neumann method gives

$$\lambda^2 + i \frac{c\Delta t}{3\Delta x} [8 \sin(k\Delta x) - \sin(2k\Delta x)] \lambda - 1 = 0$$

which has the solution

$$\lambda = -i \frac{c\Delta t}{6\Delta x} [8 \sin(k\Delta x) - \sin(2k\Delta x)] \pm \sqrt{1 - \left[\frac{c\Delta t}{6\Delta x} [8 \sin(k\Delta x) - \sin(2k\Delta x)] \right]^2}$$

If

$$\left[\frac{c\Delta t}{6\Delta x} [8 \sin(k\Delta x) - \sin(2k\Delta x)] \right]^2 < 1 \quad (4.9)$$

then

$$|\lambda|^2 = \left[\frac{c\Delta t}{6\Delta x} [8 \sin(k\Delta x) - \sin(2k\Delta x)] \right]^2 + \left\{ \sqrt{1 - \left[\frac{c\Delta t}{6\Delta x} [8 \sin(k\Delta x) - \sin(2k\Delta x)] \right]^2} \right\}^2 = 1$$

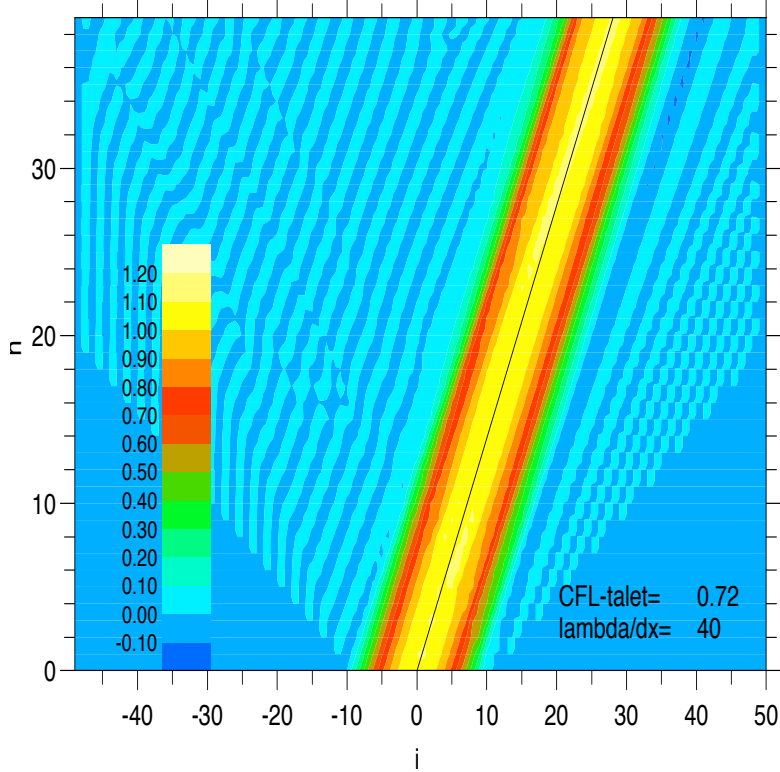


Figure 4.9: The advection equation integrated with the numerical scheme 4.8. The CFL number is $C_{FL} \equiv \frac{c\Delta t}{\Delta x} = 0.72$

i.e. this scheme is stable if 4.9 is fulfilled which can also be expressed as

$$\left| \frac{c\Delta t}{6\Delta x} [8 \sin(k\Delta x) - \sin(2k\Delta x)] \right| < 1$$

or

$$\frac{c\Delta t}{\Delta x} < \frac{6}{8 \sin(k\Delta x) - \sin(2k\Delta x)}$$

which has a minimum for $k\Delta x \approx 1$ so that the scheme is stable when $\frac{c\Delta t}{\Delta x} < 0.73$

Exercises:

1. Consider the leapfrog scheme for the advection equation,

$$\frac{u_j^{n+1} - u_j^{n-1}}{2\Delta t} + c \frac{u_{j+1}^n - u_{j-1}^n}{2\Delta x} = 0$$

Use

$$u_j^n = \lambda^n u_0 e^{ikj\Delta x}$$

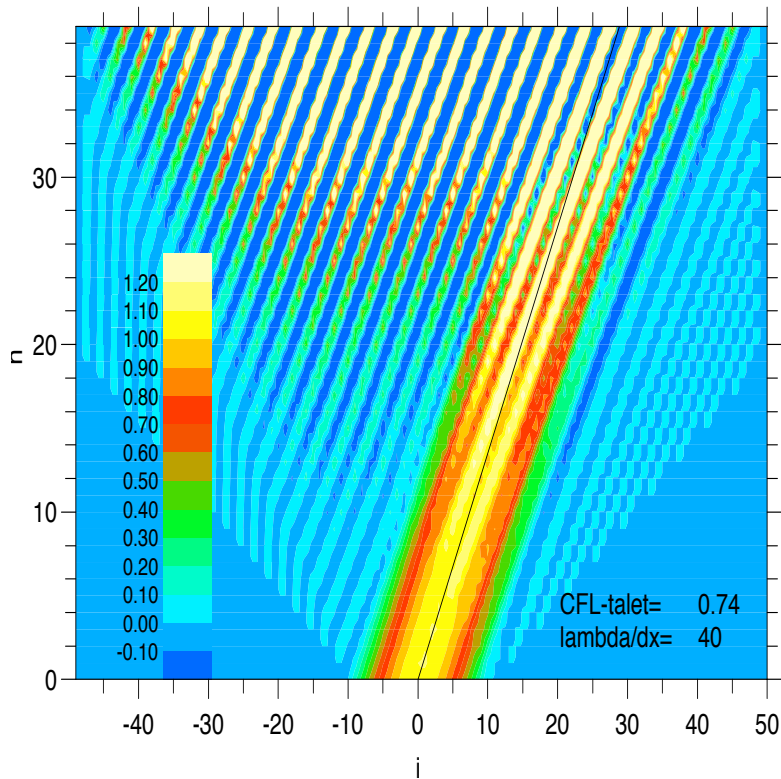


Figure 4.10: The advection equation integrated with the numerical scheme 4.8. The CFL number is $C_{FL} \equiv \frac{c\Delta t}{\Delta x} = 0.74$

and show that the amplification factor is

$$\lambda = -i \frac{c\Delta t}{\Delta x} \sin(k\Delta x) \pm \sqrt{1 - \left(\frac{c\Delta t}{\Delta x} \sin(k\Delta x) \right)^2}$$

2. Show that for $\frac{c\Delta t}{\Delta x} > 1$ in the previous exercise, we will have one of the solutions to the differential equation superior to one for at least some wave lengths, i.e. that the solution “blows up” .
3. Discretise the advection equation with Euler forward in both time and space. Show that for $c > 0$ (down stream scheme), the amplitude of the solutions will grow in time (unstable). But for $c < 0$ (up stream scheme) the amplitude will decrease in time, i.e. stable.
4. Make a stability analysis of the following discretisation of the advection equation

$$\frac{u_j^{n+1} - \frac{1}{2} (u_{j+1}^n + u_{j-1}^n)}{\Delta t} + c \frac{u_{j+1}^n - u_{j-1}^n}{2\Delta x} = 0$$

Chapter 5

The numerical mode

We shall in this chapter study some of the consequences of that the partial differential equations have been approximated with finite differences.

5.1 The numerical mode of the three level schemes

One problem with three level scheme such as the leap-frog-scheme is that they require more than one initial condition to start the numerical integration. From a physical standpoint a single initial condition for $u^{n=0}$ should have been sufficient. However in addition to the physical initial condition, three level schemes require a computational initial condition for $u^{n=1}$. This value cannot be calculated by a three level scheme, and, therefore, it will usually have to be obtained using two level schemes.

Consider the oscillation equation:

$$\frac{du}{dt} = i\omega u \text{ where } u = u(t)$$

which has the solution

$$u = u_0 e^{i\omega t}$$

The leap-frog scheme can be written as

$$u^{n+1} = u^{n-1} + 2i\omega \Delta t u^n \quad (5.1)$$

If we now study the amplification roots like in the previous chapter we get

$$\lambda^2 - 2i\omega \Delta t \lambda - 1 = 0$$

which has the solution

$$\lambda_{1,2} = i\omega \Delta t \pm \sqrt{1 - (\omega \Delta t)^2}$$

Thus there are two solutions of the form $u^{n+1} = \lambda u^n$.

Since we are solving a linear equation its solution will be a linear combination of the two solutions

$$u_1^n = \lambda_1^n u_1^0 \quad \text{and} \quad u_2^n = \lambda_2^n u_2^0$$

so that

$$u^n = a\lambda_1^n u_1^0 + b\lambda_2^n u_2^0$$

where a and b are constants. If $u^{n+1} = \lambda u^n$ should represent the approximation of the true solution then $\lambda \rightarrow 1$ when $\Delta t \rightarrow 0$. λ_1 does this but $\lambda_2 \rightarrow -1$. λ_1 is called the *physical mode* and λ_2 is called the *computational mode*, which has been introduced by the numerical scheme. This computational mode changes sign for each even and odd n .

A simple way to illustrate the computational mode is to study the simple case when $\omega = 0$ so that

$$\frac{du}{dt} = 0$$

which has the true solution

$$u(t) = \text{const}$$

The Leap-frog scheme gives

$$u^{n+1} = u^{n-1}$$

For a given physical initial condition $u^{n=0}$, we consider two special choices of $u^{n=1}$

1. Suppose calculating of $u^{n=1}$ happened to give the true value $u^{n=0}$ then we get for all n

$$u^{n+1} = u^n \tag{5.2}$$

or

$$u^{n+1} = \lambda_1 u^n$$

in this case we have obtained a numerical solution that is equal to the true solution and consists of the physical mode only.

2. Suppose now instead that when calculating $u^{n=1}$ we obtain $u^{n=1} = -u^{n=0}$. Then we obtain for all n

$$u^{n+1} = -u^n \tag{5.3}$$

or

$$u^{n+1} = \lambda_2 u^n$$

The numerical solution now consists entirely of the computational mode.

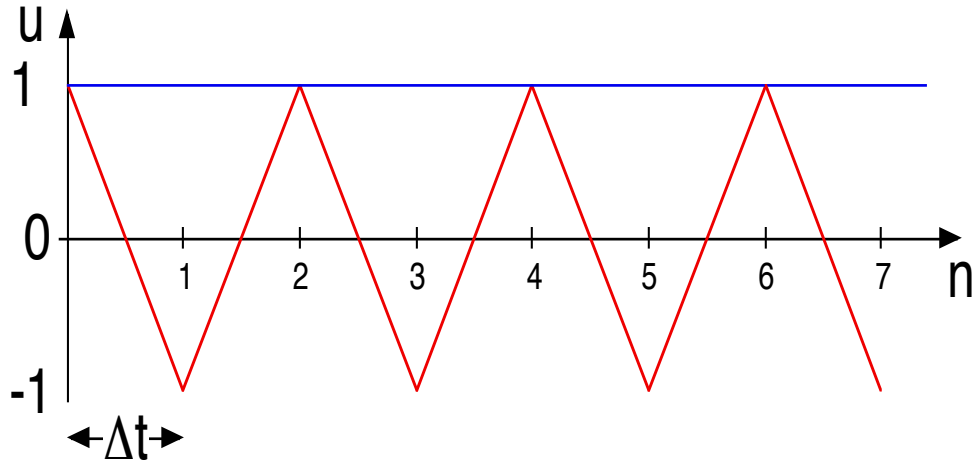


Figure 5.1: The physical mode in blue from Equation 5.2 and the numerical (or computational) mode in red from Equation 5.3. The initial physical condition is set to $u^{n=0} = 1$ and the computation initial condition is set to $u^{n=1} = 1$ in order to generate a constant physical mode and to $u^{n=1} = 0$ in order to illustrate a computational mode that changes sign at every time step.

5.1.1 The computational initial condition

A good choice of the computational initial condition is of vital importance for obtaining a satisfactory numerical solution for short simulations, where the initial condition is crucial which is the case for weather forecast predictions but less for long climate simulations. The computational initial condition ($u^{n=1}$), which is one Δt ahead of the physical condition ($u^{n=0}$) can be computed with a single Euler forward time step. Although this scheme is computationally unstable it can be used in a single time step since it requires many time steps before the solution grows and "blows up".

The computational initial condition for our academic case of the oscillation equation is then with an Euler forward time step:

$$u^{n=1} = u^{n=0} + i\omega\Delta t u^{n=0} \quad (5.4)$$

An alternative computational initial condition, when the solution is not so sensitive to the initial condition is just simply to set the same values to both time steps ($u^{n=1} = u^{n=0}$) but as shown above this can trigger immediately a computational mode.

5.2 Suppression of the computational mode

The computational mode which is introduced by the leap frog scheme can be suppressed in two different ways.
 1) The problem can be solved by integrating with an Euler forward or backward at regular intervals of a certain number of time steps (50 time steps or so is often used). This would imply that in the example of the previous paragraph that $u^{n+1} = u^n$ every 50 time steps, which eliminate the computational mode so that $a = 1$ and $b = 0$.

Another way, which is the most common way in atmospheric models, is to use a Robert-Asselin filter

(Robert,1966; Asselin,1972). First one applies the leap frog integration to obtain the solution at time level $n + 1$:

$$u^{n+1} = u_f^{n-1} + 2\Delta t F(u^n)$$

then the filter is applied as a time smoothing between the time levels $n - 1$, n and $n + 1$ so that

$$u_f^n = u^n + \gamma (u_f^{n-1} - 2u^n + u^{n+1}) \quad (5.5)$$

where the index f indicates the smoothed values and γ is the Asselin coefficient with a typical value around 0.1. The next frog jump will be

$$u^{n+2} = u_f^n + 2\Delta t F(u^{n+1})$$

Note that the added term is like smoothing in time, an approximation of an ideally time-centered smoother is

$$u_f^n = u^n + \gamma (u^{n-1} - 2u^n + u^{n+1}) \quad (5.6)$$

In our particular case of the discretised oscillation Equation 5.4 we can estimated the damping effect of the Robert-Asselin filter by introducing its discretised solution $u^n = u_0 e^{i\omega n \Delta t}$ into the smoother (Eq. 5.6) with the exception that u^{n-1} is taken as an unfiltered value. This results in

$$u_f^n = u^n [1 - 4\gamma \sin^2(\omega \Delta t / 2)] \quad (5.7)$$

The computational mode, whose period is $2\Delta t$ is hence reduced by $(1 - 4\gamma)$ every time step. Because the field at $n - 1$ is replaced by an already filtered value, the Rober-Asselin filter introduces a slight different compared to this simplified filter.

Chapter 6

Accuracy of the numerical phase speed

We will now investigate the accuracy of the numerical phase speed due to both the discretisation in space and time.

6.1 Dispersion due to the spatial discretisation

Let us first examine the advection equation with centred scheme in space

$$\frac{\partial u}{\partial t} + c \frac{u_{j+1}^n - u_{j-1}^n}{2\Delta x} = 0$$

by substituting wave solutions

$$u_j(t) = u_0 e^{ik(j\Delta x - C_D t)}$$

we get

$$C_D = c \frac{\sin(k\Delta x)}{k\Delta x}$$

where C_D is the numerical phase speed and c . the true phase speed. The ratio should ideally be as close as possible to one but is

$$\frac{C_D}{c} = \frac{\sin(k\Delta x)}{k\Delta x}$$

The numerical group speed is

$$C_{Dg} = \frac{d(\omega_D)}{dk} = \frac{d(kC_D)}{dk} = c \cos(k\Delta x)$$

6.2 Dispersion due to the time discretisation

The effects of the centred scheme is analysed in the same way as the effects of the centred scheme in space.

$$\frac{u_j^{n+1} - u_j^{n-1}}{2\Delta t} + c \frac{\partial u}{\partial x} = 0$$

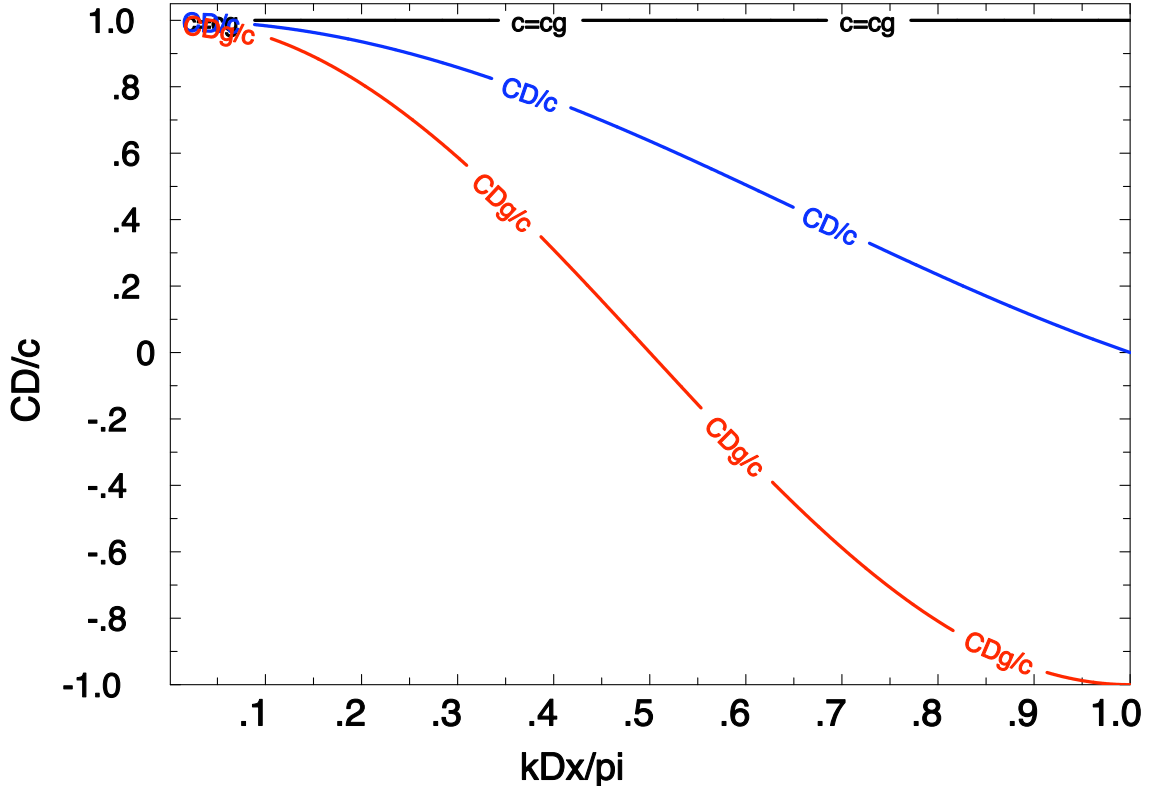


Figure 6.1: The numerical phase speed due to the centred finite difference in space compared to the analytical phase speed. The black line is the solution of the continuous equations which is the non dispersive analytical case, i.e. the phase speed is the same as the group velocity $c = c_g$. The blue line is the numerical phase speed normalised by dividing with c . Note that when the wave number increases (wave length decreases) then the numerical phase speed deviates from the analytical phase speed. The phase speed is clearly dispersive since the waves propagate at different speeds depending on their wave lengths. The red line shows the computational group velocity CD_g which at wave lengths shorter than 4 grid cells ($k\Delta x < \pi/2$) propagate in the wrong direction.

Substituting the wave solutions

$$u^n(x) = u_0 e^{ik(x - C_D n \Delta t)}$$

we get

$$C_D = \frac{\arcsin(\omega \Delta t)}{k \Delta t}$$

where C_D is the numerical phase speed and c . the true phase speed. The ratio should ideally be as close as possible to one but is

$$\frac{C_D}{c} = \frac{\arcsin(\omega \Delta t)}{\omega \Delta t}$$

The computational and physical group speeds differ also so that

$$\frac{C_{Dg}}{c_g} = \frac{d(\omega_D)}{c_g dk} = \frac{d(kC_D)}{c_g dk} = \frac{1}{\sqrt{1 - (\omega \Delta t)^2}}$$

The computation phase speed and group velocity is presented in Figure 6.2 where it is plotted normalised with c as a function of $\omega \Delta t$.

6.3 Dispersion due to both the spatial and time discretisation

Let us now investigate the effects of the leap-frog on the phase and group velocities by the advection equation with centered schemes in both time and space.

$$\frac{u_j^{n+1} - u_j^{n-1}}{2\Delta t} + c \frac{u_{j+1}^n - u_{j-1}^n}{2\Delta x} = 0$$

by substituting wave solutions

$$u_j^n = u_0 e^{ik(j \Delta x - C_D n \Delta t)}$$

we get

$$C_D = \frac{1}{k \Delta t} \arcsin \left[\frac{c \Delta t}{\Delta x} \sin(k \Delta x) \right]$$

where C_D is the numerical phase speed and c . the true phase speed. The ratio should ideally be as close as possible to one but is

$$\frac{C_D}{c} = \frac{1}{C_{FL} k \Delta x} \arcsin [C_{FL} \sin(k \Delta x)]$$

where the CFL-number is defined as $C_{FL} = \frac{c \Delta t}{\Delta x}$.

This phase speed is a function of the wave number k . Thus, the finite differencing in space causes a *computational dispersion*. As $k \Delta x$ increases, the computational phase speed C_D decreases from c to zero when $k \Delta x = \pi$, which corresponds to the shortest possible wave length of two grid cells ($\lambda = 2\Delta x$). Thus, all waves propagate at a speed that is less than the true phase speed c , with this decelerating effect increasing as

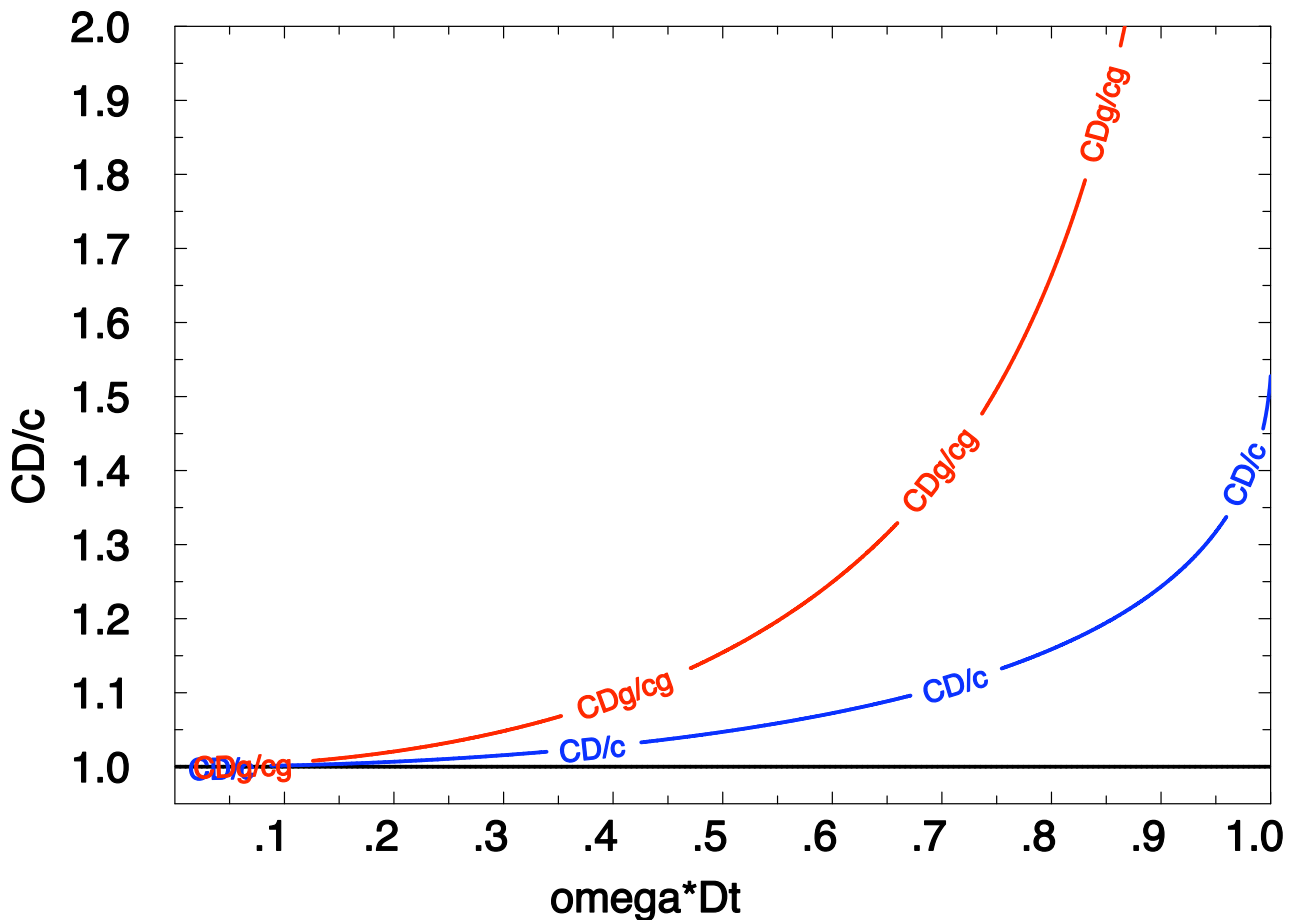


Figure 6.2: The numerical phase speed due to the centred finite difference in time compared to the analytical phase speed. The black line is the solution of the continuous equations which is the non dispersive analytical case, i.e. the phase speed is the same as the group velocity $c = c_g$. The blue line is the numerical phase speed normalised by dividing with c . Note that when the time step increases compared to the wave frequency (ω) then the numerical phase speed increases and deviates from the analytical phase speed. The red line shows the computational group velocity C_{Dg} .

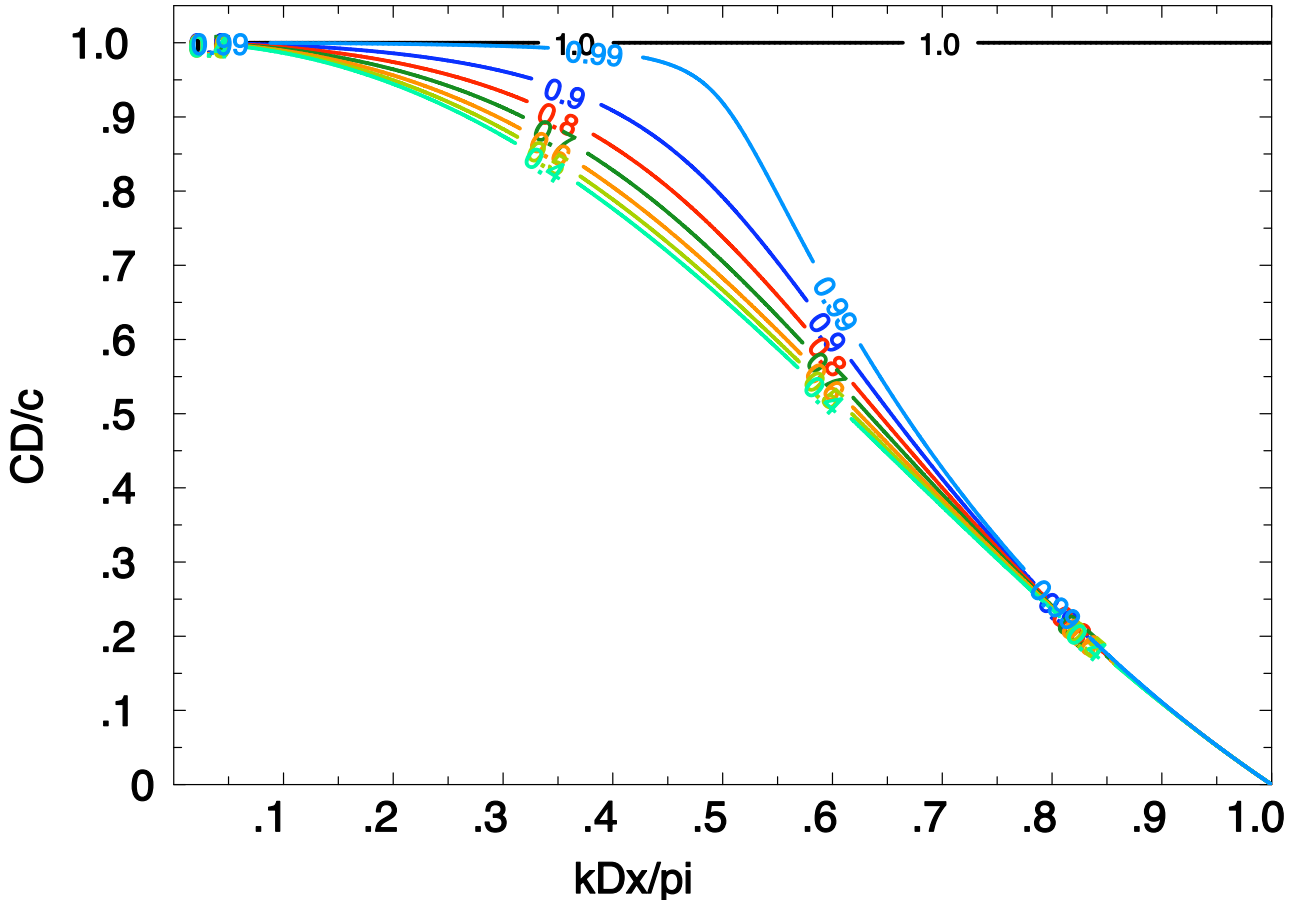


Figure 6.3: Numerical dispersion of the leap frog scheme. The lines show the ratio C_D/c as a function of the normalised wave number $\frac{k\Delta x}{\pi}$. The different lines correspond to different CFL-numbers ($C_{FL} = \frac{c\Delta t}{\Delta x}$), where these are indicated on the lines. The ideal solution is $C_D/c = 1$. Note that when the wave number increases (wave length decreases) then the numerical phase speed deviates from the analytical phase speed. The phase speed is clearly dispersive since the waves propagate at different speeds depending on their wave lengths.

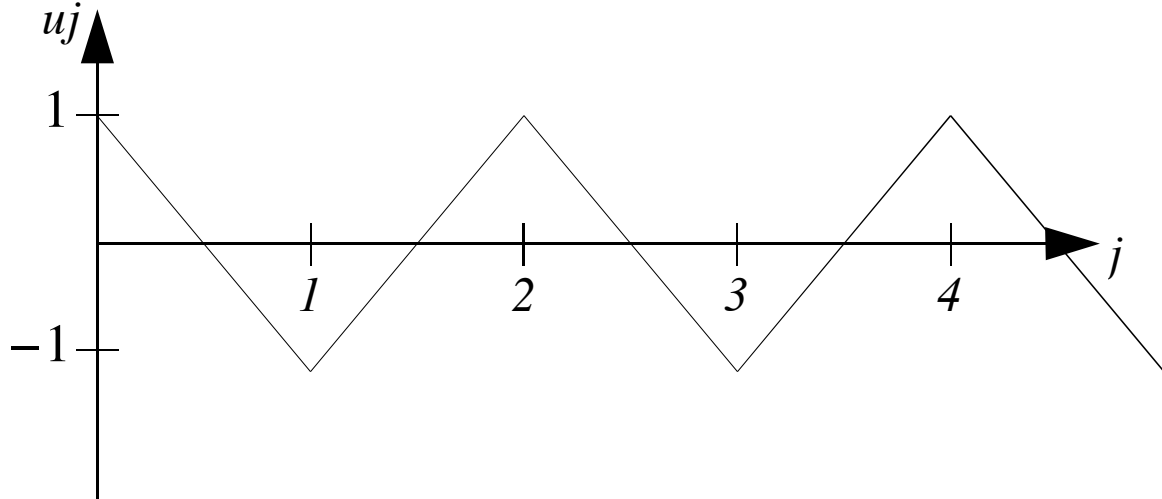


Figure 6.4: The two-grid-interval wave with a wave length of $\lambda = 2\Delta x$.

the wave length decreases. The two grid wave is stationary. Note that if $C_{FL} = 1$, which is the limit of stability for the advection equation then the the computation phase speed is the same as the analytical one ($C_D = c$).

The reason for the two grid wave to be stationary is obvious when we look at the wave illustrated in Figure 6.4. For this wave we have $u_{j+1} = u_{j-1}$ at all grid points which gives $\frac{\partial u_j}{\partial t} = 0$ in the advection equation.

We have encountered two effects in this section:

1. The advection speed is slower than the true advection speed.
2. The advection speed changes with the wave number.

Exercises

Derive the numerical phase speed :

$$C_D = \frac{1}{k\Delta t} \arcsin \left[\frac{c\Delta t}{\Delta x} \sin(k\Delta x) \right]$$

Chapter 7

Diffusion and friction terms (parabolic)

In this chapter we will investigate the discretisation of the friction and diffusion terms and how they affect the stability of the equation. Diffusion and friction terms are included in most models from the very simple shallow water models to the most complex ocean-atmosphere general circulation models.

7.1 Rayleigh friction

We will start by studying the simplest type of friction parameterisation, the Rayleigh friction::

$$\frac{\partial u}{\partial t} = -\gamma u \quad \text{where } \gamma > 0 \quad (7.1)$$

which has the solution

$$u(t) = u_0 e^{-\gamma t} \quad (7.2)$$

For centered time differences (leap-frog), which are the most common in equations with advection terms, the discretisation of Equation 7.1 is

$$\frac{u_j^{n+1} - u_j^{n-1}}{2\Delta t} = f = -\gamma u_j \quad (7.3)$$

If a stability analysis is performed in analogy with that of the advection equation in the previous chapter with $u_j^{n+m} = u_j^n \lambda^m$ one finds that

1. if the right hand side of Equation 7.3 is taken at the time step n , that is $f^n = -\gamma u_j^n$ then $\lambda_{1,2} = -\gamma\Delta t \pm \sqrt{1 + (\gamma\Delta t)^2}$, which has at least one root that is always greater than one for any $\gamma\Delta t > 0$. The scheme is hence unconditionally unstable.
2. if the right hand side of Equation 7.3 is taken at the time step $n-1$, that is $f^{n-1} = -\gamma u_j^{n-1}$ then $\lambda^2 = 1 - 2\gamma\Delta t$. The scheme is conditionally stable since $\lambda^2 \leq 1$ if $\gamma\Delta t \leq 1$. But since $\lambda^2 < 0$ for $1/2 < \gamma\Delta t < 1$, the roots of λ will be purely imaginary and the solution of u will oscillate and change sign for every second time step. If for instance $\gamma\Delta t = 1$ then $\lambda_{1,2} = \pm i$ and $u^n = i^n = 1, 0, -1, 0, 1, \dots$

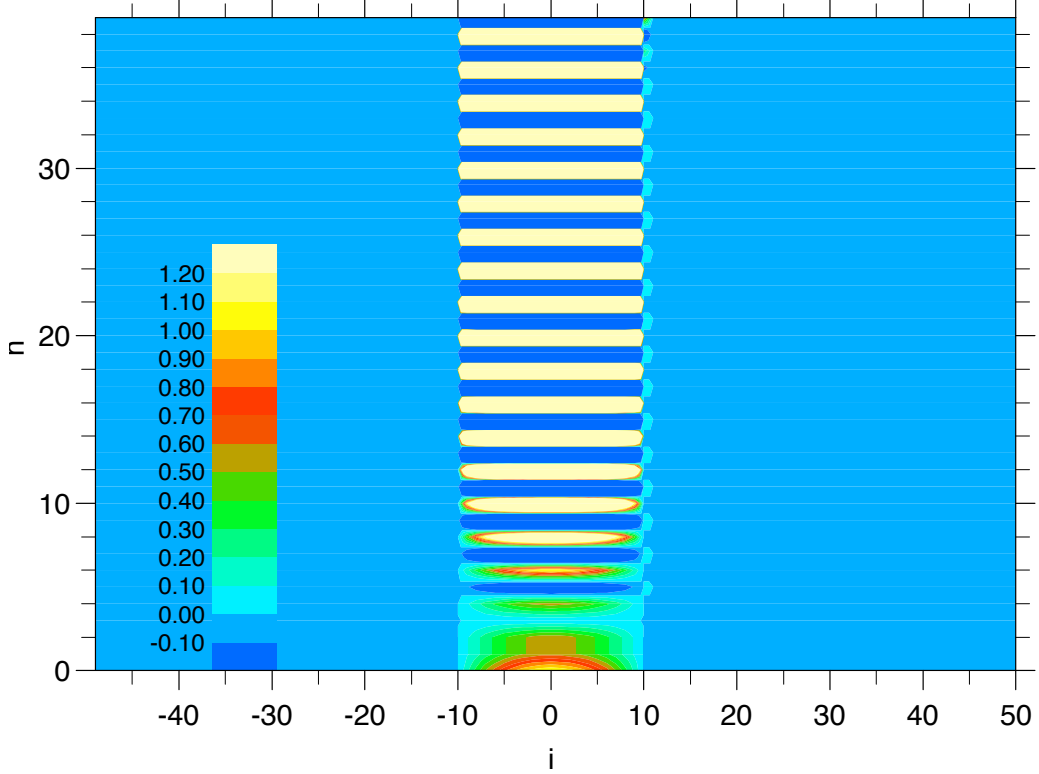


Figure 7.1: The Rayleigh friction equation 7.3 integrated with the the right hand side at time step n (case 1) and $\gamma\Delta t = 0.6$.

For a more strict condition $\gamma\Delta t < 1/2$ then λ will be real and u will have a more realistic evolution with no numerical oscillation.

3. if the right hand side of Equation 7.3 is taken as an average of $n - 1$ and $n + 1$ so that,

$$\frac{u_j^{n+1} - u_j^{n-1}}{2\Delta t} = -\frac{\gamma}{2} (u_j^{n+1} + u_j^{n-1})$$

This scheme, which is called Crank-Nicholson is said to be implicit because it includes a term $n + 1$ on the right hand side of Equation 7.3. This alternative gives the best approximation of Equation 7.2. The stability analysis gives $\lambda^2 = \frac{1-\gamma\Delta t}{1+\gamma\Delta t} < 1$ for all values of $\gamma\Delta t$. The scheme is hence absolute stable. But for the same reasons as in the previous alternative one needs $\gamma\Delta t < 1$ in order to have realistic evolution. Implicit schemes are often complicated to solve since they include values on the right hand side that one needs to solve simultaneously on the left hand side of the equation. But not in this particular case since the right hand side is in the same spatial grid point j as the left hand side of u^{n+1} and the equation can be rearranging so that:

$$u_j^{n+1} = \frac{1 - \gamma\Delta t}{1 + \gamma\Delta t} u_j^{n-1}$$

When using the Crank-Nicholson scheme as in this case with only a time integration on should use a two time step integration with Euler forward so that only two time steps are used and the equation now

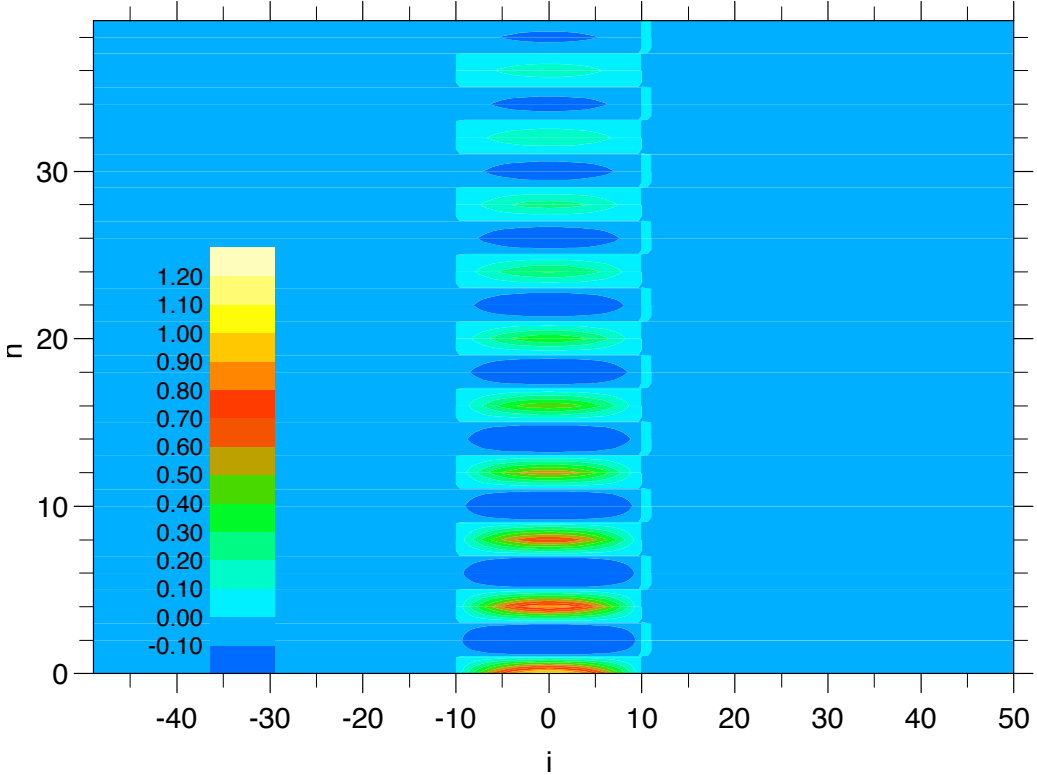


Figure 7.2: The Rayleigh friction equation 7.3 integrated with (2) i.e. the right hand side at time step $n - 1$ and $\gamma\Delta t = 0.95$.

becomes

$$u_j^{n+1} = \frac{1 - \gamma\Delta t}{1 + \gamma\Delta t} u_j^n$$

7.2 The heat equation

A somewhat more realistic friction parameterisation is the Laplace friction which is included in the heat equation

$$\frac{\partial u}{\partial t} = A \frac{\partial^2 u}{\partial x^2} \quad \text{where } A > 0 \quad (7.4)$$

which has the solution

$$u(x, t) = u_0 e^{\pm ikx - Ak^2 t} \quad (7.5)$$

A centered fintite difference of the of the Laplace operator (second order differential) can be obtianed by combining the two Taylor series we used in section 3.2:

$$u_{j+1} = u_j + \Delta x \left(\frac{du}{dx} \right)_j + \frac{1}{2} (\Delta x)^2 \left(\frac{d^2 u}{dx^2} \right)_j + \frac{1}{6} (\Delta x)^3 \left(\frac{d^3 u}{dx^3} \right)_j + \frac{1}{24} (\Delta x)^4 \left(\frac{d^4 u}{dx^4} \right)_j + \dots \quad (7.6)$$

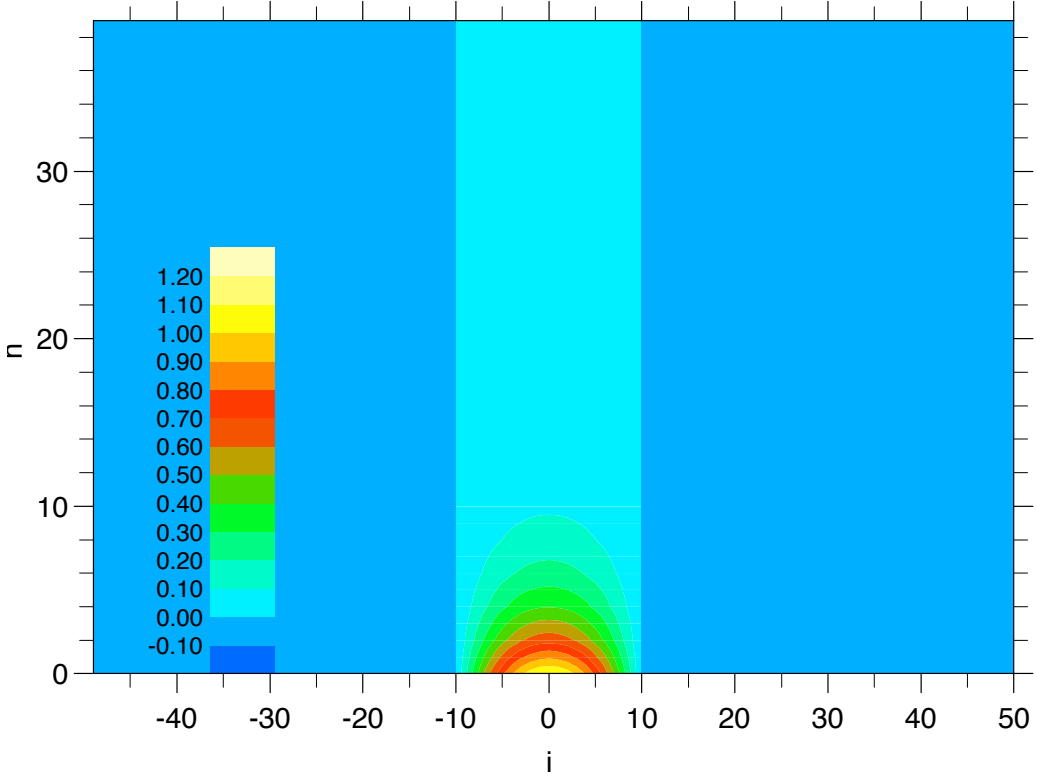


Figure 7.3: The Rayleigh friction equation 7.3 integrated with (2) i.e. the right hand side at time step $n - 1$ and $\gamma\Delta t = 0.2$.

$$u_{j-1} = u_j - \Delta x \left(\frac{du}{dx} \right)_j + \frac{1}{2} (\Delta x)^2 \left(\frac{d^2 u}{dx^2} \right)_j - \frac{1}{6} (\Delta x)^3 \left(\frac{d^3 u}{dx^3} \right)_j + \frac{1}{24} (\Delta x)^4 \left(\frac{d^4 u}{dx^4} \right)_j - \dots \quad (7.7)$$

We obtain by summing these two equations and dividing by $(\Delta x)^2$:

$$\frac{u_{j+1} - 2u_j + u_{j-1}}{(\Delta x)^2} = \frac{d^2 u}{dx^2} + \frac{1}{12} (\Delta x)^2 \left(\frac{d^4 u}{dx^4} \right)_j \quad (7.8)$$

This finite difference of the second order derivative is hence accurate to the second $O[(\Delta x)^2]$, which is the same as to say it has a truncation error of the second order.

The heat equation (7.4) can now be approximated by integrating in time with leap frog as

$$\frac{u_j^{n+1} - u_j^{n-1}}{2\Delta t} = A \frac{u_{j+1} - 2u_j + u_{j-1}}{(\Delta x)^2} \quad (7.9)$$

A stability analysis with the von Neumann method can be obtained by setting $u_j^n = u_0 \lambda^n e^{ikj\Delta x}$ into Equation (7.9). Depending on the time step of the right hand side we choose to have. Let us study the same three different cases as for the Rayleigh friction equation:

1. If the right hand side of Equation 7.9 is taken at the time step n then the equation for the amplification factor becomes

$$\lambda^2 + \frac{8A\Delta t}{(\Delta x)^2} \sin^2 \left(\frac{k\Delta x}{2} \right) \lambda - 1 = 0$$

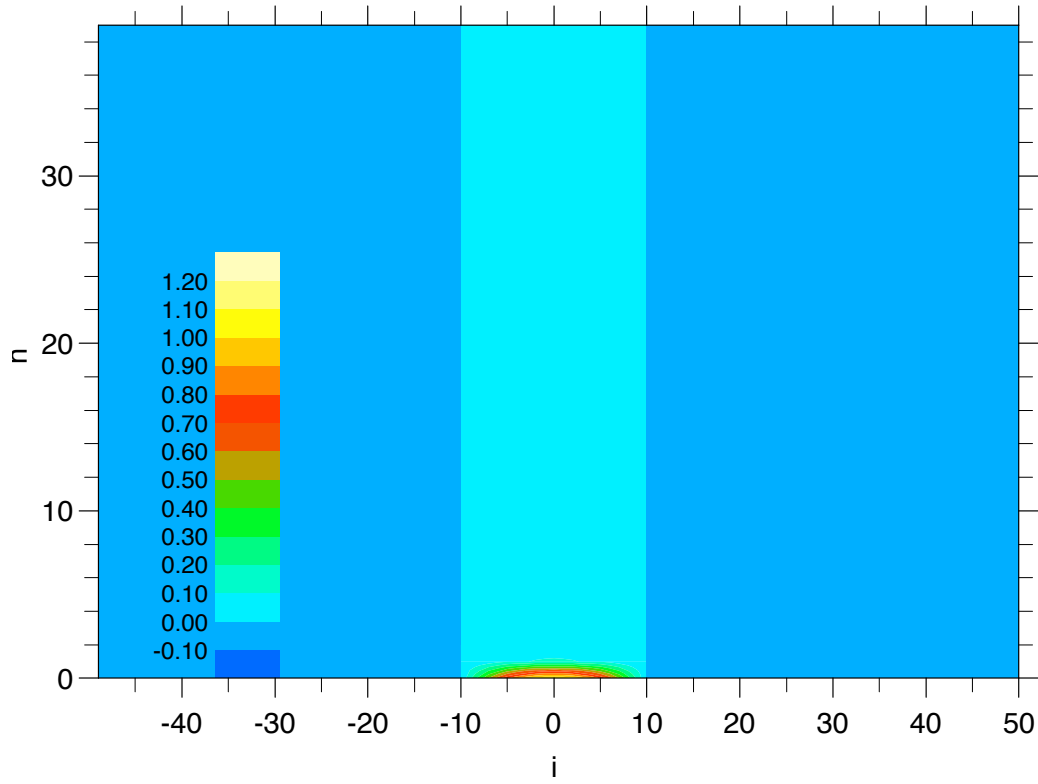


Figure 7.4: The Rayleigh friction equation 7.3 integrated with (3) i.e. the right hand side at time step $n - 1$ and $n + 1$ with $\gamma \Delta t = 0.9$.

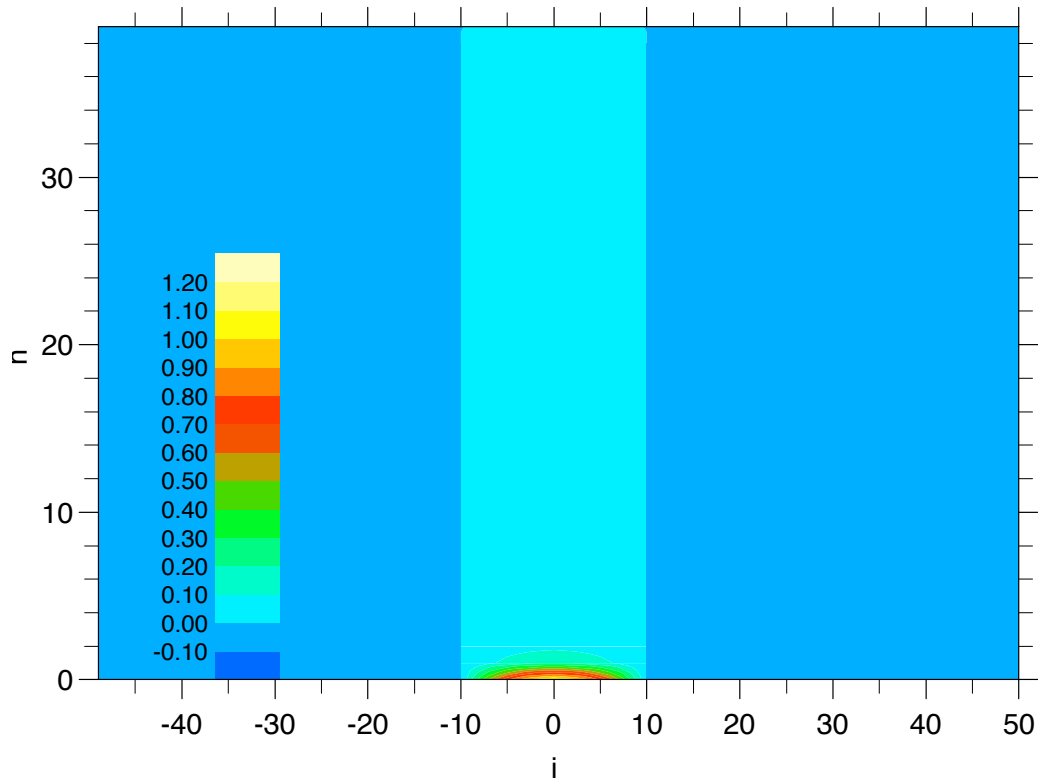


Figure 7.5: The Rayleigh friction equation 7.3 integrated with analytically with $\gamma \Delta t = 0.6$.

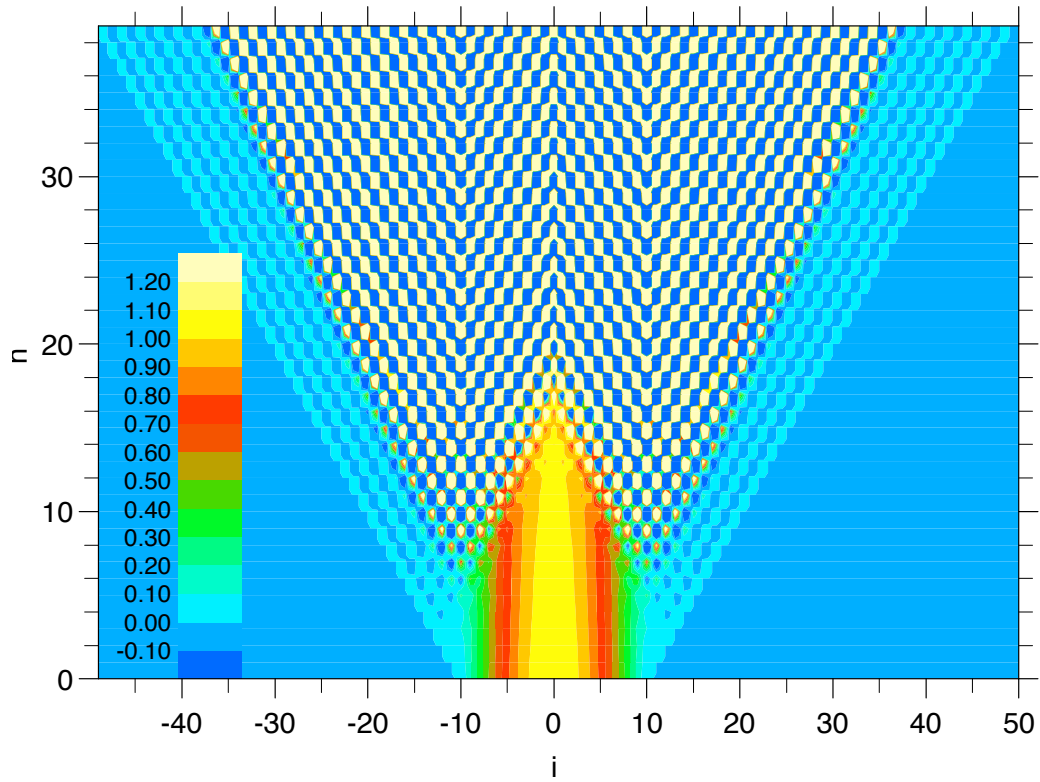


Figure 7.6: The heat equation (7.5) integrated with (7.9) with the right hand side at time step n and $\frac{A\Delta t}{(\Delta x)^2} = 0.24$

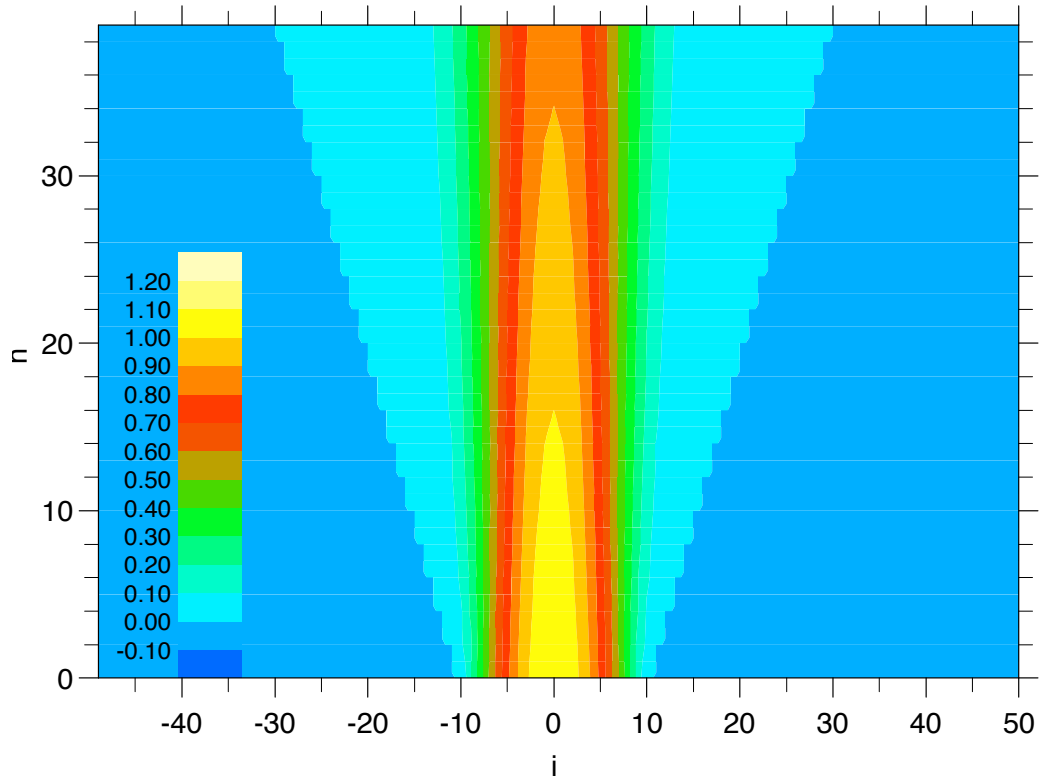


Figure 7.7: Same as Figure 7.6 but with the right hand side at time step $n-1$.

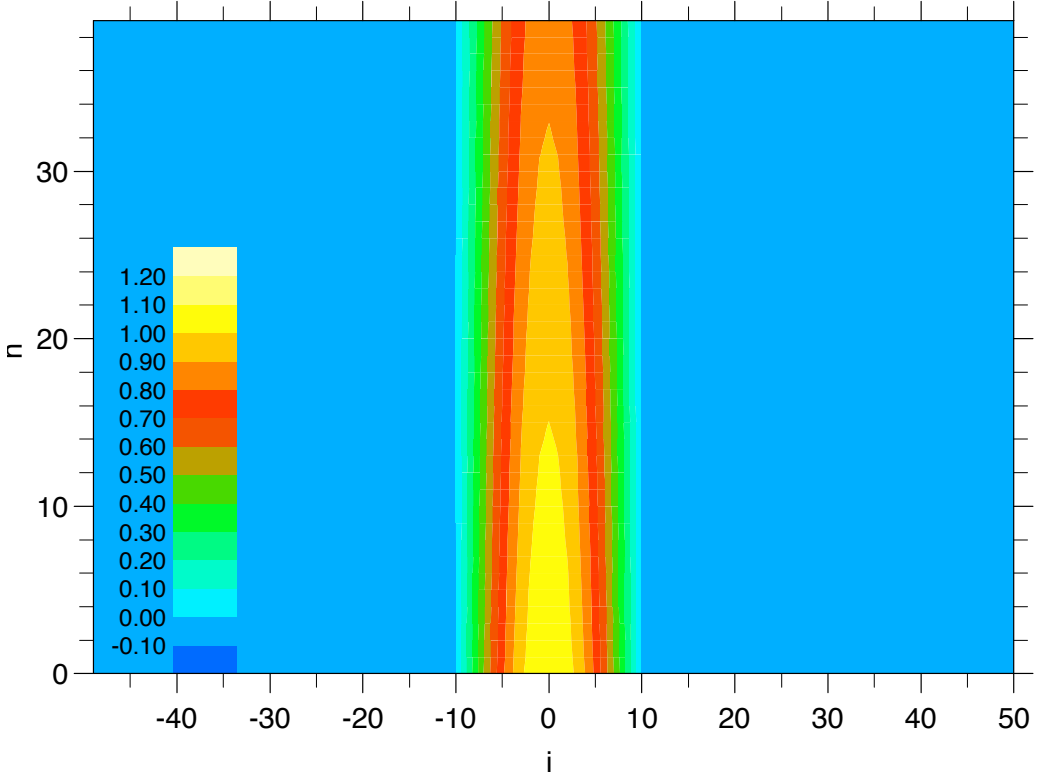


Figure 7.8: Same as Figure 7.6 but solved analytically.

which has the roots $\lambda_{1,2} = -a \pm \sqrt{1+a^2}$, where $a \equiv \frac{4A\Delta t}{(\Delta x)^2} \sin^2\left(\frac{k\Delta x}{2}\right)$. The second root will be $\lambda_2 < -1$ for any $\frac{A\Delta t}{(\Delta x)^2} > 0$, which implies that the scheme is unconditionally unstable.

2. If the right hand side of Equation 7.9 is taken at the time step $n-1$ then the equation for the amplification factor becomes

$$\lambda^2 = 1 - \frac{8A\Delta t}{(\Delta x)^2} \sin^2\left(\frac{k\Delta x}{2}\right)$$

the scheme is stable if $-1 \leq \lambda^2 \leq 1$, which is the case if $\frac{A\Delta t}{(\Delta x)^2} < 1/4$. The scheme is hence conditionally stable. However for the same reasons as for the Rayleigh equation we recommend the stricter condition $\frac{A\Delta t}{(\Delta x)^2} < 1/8$. In order to have $\lambda^2 > 0$ and avoiding time oscillations of the solution.

3. If the right hand side of Equation 7.9 is taken as an average of $n-1$ and $n+1$ (Crank-Nicholson scheme) then we have

$$\frac{u_j^{n+1} - u_j^{n-1}}{2\Delta t} = A \left(\frac{u_{j+1}^{n+1} - 2u_j^{n+1} + u_{j-1}^{n+1}}{(\Delta x)^2} + \frac{u_{j+1}^{n-1} - 2u_j^{n-1} + u_{j-1}^{n-1}}{(\Delta x)^2} \right) \quad (7.10)$$

The scheme is implicit as it includes terms at time step $n+1$ on the right hand. The equation can not be solved so easily as for the Rayleigh equation case since the $n+1$ terms on the right hand are at several spatial grid points ($j-1, j, j+1$). It is however possible to use algorithms that eliminates these terms.

We can nevertheless perform a stability analysis and calculate the amplification factor that becomes

$$\lambda^2 = \frac{1 - \frac{4A\Delta t}{(\Delta x)^2} \sin^2\left(\frac{k\Delta x}{2}\right)}{1 + \frac{4A\Delta t}{(\Delta x)^2} \sin^2\left(\frac{k\Delta x}{2}\right)} \quad (7.11)$$

which is always smaller than one and the is hence absolute stable. But in order to avoid imaginary roots that leads to oscillating solutions one should use $\frac{A\Delta t}{(\Delta x)^2} < 1/4$.

In most cases for the modelling of the atmosphere and the ocean γ and A are of such size that the stability criterion in the present chapter enables Δt to be much larger (5-10 times) than the CFL criterion $c < \frac{\Delta x}{\Delta t}$. The most common mistake is however to use the unconditionally unstable scheme with the friction taken at time step n when writing a code.

Note that the schemes in case 2 and 3 are in fact two level schemes since we do not use any values at time step n but only in $n - 1$ and $n + 1$. There is therefore no reason to use leap-frog here and we can instead use an Euler forward in time and replace all the $n - 1$ by n . The stability analysis remains the same but since the time step is halved we should replace Δt by $\Delta t/2$. It is nevertheless easier to demonstrate the differences between the three cases by using leap-frog for all cases.

7.3 Advection-diffusion equation

Let us now study an equation with both advection and diffusion terms so that

$$\frac{\partial u}{\partial t} + c \frac{\partial u}{\partial x} = A \frac{\partial^2 u}{\partial x^2} \quad (7.12)$$

which has the analytical solution

$$u(x, t) = u_0 e^{\pm ik(x-ct)-Ak^2t} \quad (7.13)$$

We have previously seen that a stable discretisation scheme for the advection equation is both centered in time and in space while for the diffusion equation the Laplace operator must be at time step $n - 1$. Let us now combine these schemes so that

$$\frac{u_j^{n+1} - u_j^{n-1}}{2\Delta t} + c \frac{u_{j+1}^n - u_{j-1}^n}{2\Delta x} = A \frac{u_{j+1}^{n-1} - 2u_j^{n-1} + u_{j-1}^{n-1}}{(\Delta x)^2} \quad (7.14)$$

Let us now perform a stability analysis by setting $u_j^n = \lambda^n e^{ikj\Delta x}$ into Equation (7.14) which after some calculation becomes

$$\lambda^2 + 2ia\lambda + b - 1 = 0 \quad (7.15)$$

where $a \equiv \frac{c\Delta t}{\Delta x} \sin(k\Delta x)$ and $b \equiv \frac{8A\Delta t}{(\Delta x)^2} \sin^2\left(\frac{k\Delta x}{2}\right)$.

The solution of equation (7.15) is

$$\lambda = -ia \pm \sqrt{1 - b - a^2}$$

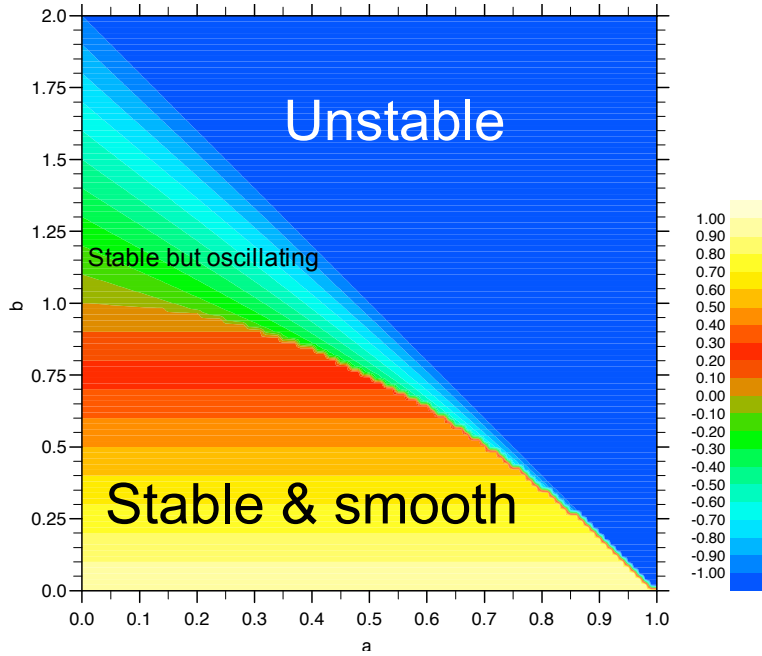


Figure 7.9: The stability function λ^2 as a function of $a \equiv \frac{c\Delta t}{\Delta x} \sin(k\Delta x)$ and $b \equiv \frac{8A\Delta t}{(\Delta x)^2} \sin^2\left(\frac{k\Delta x}{2}\right)$. The region in dark blue is where $\lambda^2 < -1$ and corresponds to unstable solutions. The green - light blue region where $-1 < |\lambda|^2 < 0$ is for stable solutions but oscillating ones. The yellow-red-brown region is for $0 < \lambda^2 < 1$, which correspond stable solutions and no oscillations.

If $1 - b - a^2 > 0$ then $|\lambda|^2 = a^2 + 1 - b - a^2 = 1 - b < 1$ (the scheme is stable for this root)

If $1 - b - a^2 < 0$ then $\lambda = -i\left(a \mp \sqrt{a^2 + b - 1}\right) \Rightarrow \lambda^2 = -\left(2a^2 + b - 1 \mp \sqrt{a^2 + b - 1}\right)$

This second root is not obvious to see when stable so we have plotted λ^2 as a function of a and b . in Figure 7.9.

Let us know integrate equation (7.14) so that

$$u_j^{n+1} = u_j^{n-1} - \frac{c\Delta t}{\Delta x} (u_{j+1}^n - u_{j-1}^n) + \frac{2A\Delta t}{(\Delta x)^2} (u_{j+1}^{n-1} - 2u_j^{n-1} + u_{j-1}^{n-1}) \quad (7.16)$$

From Figure 7.9 we can see that if $A \neq 0$ then we need to have a CFL-number ($\frac{c\Delta t}{\Delta x}$) well under 1. If we choose $\frac{2A\Delta t}{(\Delta x)^2} = \frac{1}{8}$ then $b = \frac{1}{2}$ and we can see in Figure 7.9 that $|\lambda|^2 < 1$ for a up to approximately 0.72. Let us therefore integrate Equation (7.16) and test if it is stable. It should be stable when $\frac{c\Delta t}{\Delta x} = 0.7$ and unstable when $\frac{c\Delta t}{\Delta x} = 0.8$.

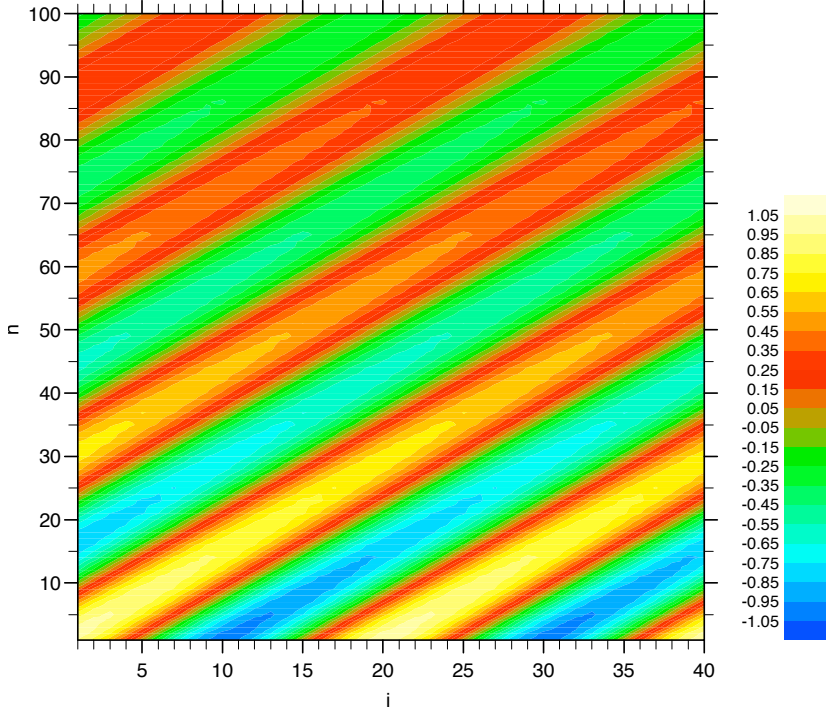


Figure 7.10: The integration of Equation (7.16) with $\frac{c\Delta t}{\Delta x} = 0.7$ and $\frac{2A\Delta t}{(\Delta x)^2} = \frac{1}{8}$. The integration is stable as it should according to our stability analysis.

Exercises

1. Perform a stability analysis for the Rayleigh friction equation with the right hand side of Equation 7.3 taken at the time step n
2. Same as previous but taken at the time step $n - 1$
3. Same as previous but taken at the time step $n + 1$
4. Calculate the stability criterion for

$$\frac{\partial u}{\partial t} = A \frac{\partial^2 u}{\partial x^2} \quad \text{where } A > 0$$

with

$$\frac{u_j^{n+1} - u_j^n}{2\Delta t} = A \frac{u_{j+1}^n - 2u_j^n + u_{j-1}^n}{(\Delta x)^2}$$

Estimate an upper limit for Δt for

- a) $A = 10^6 m^2/s$, $\Delta x = 400 km$ (large scale horizontal diffusion)
- b) $A = 1 m^2/s$, $\Delta x = 10 m$ (vertical diffusion in a boundary layer)

5. The diffusion equation is solved by the Crank-Nicholson scheme:

$$\frac{T_j^{n+1} - T_j^n}{\Delta t} = \frac{A}{2} \left[\frac{T_{j+1}^n - 2T_j^n + T_{j-1}^n}{(\Delta x)^2} + \frac{T_{j+1}^{n+1} - 2T_j^{n+1} + T_{j-1}^{n+1}}{(\Delta x)^2} \right]$$

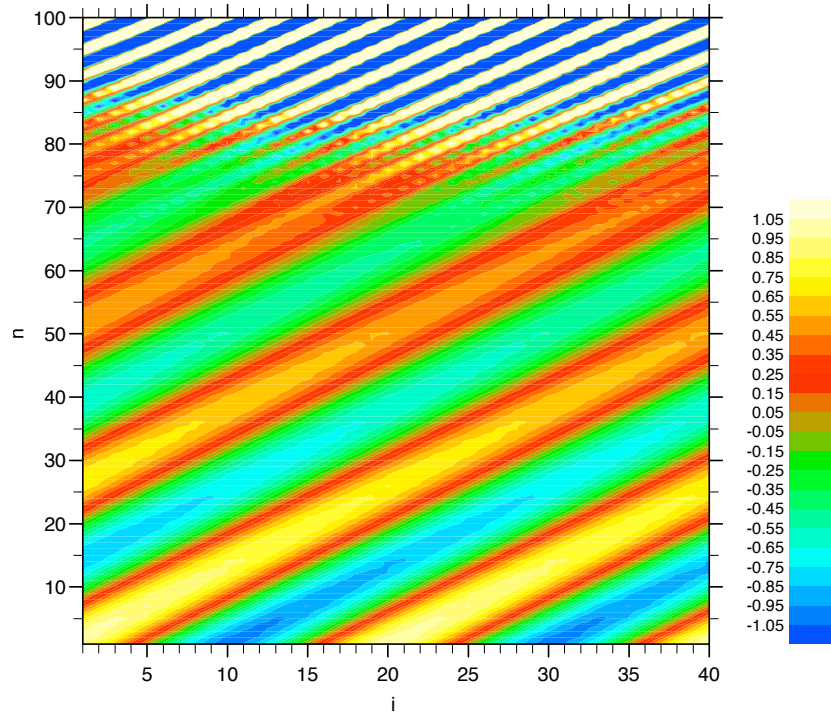


Figure 7.11: Same as Figure 7.11 but with $\frac{c\Delta t}{\Delta x} = 0.8$. The integration is clearly unstable as it should according to our stability analysis.

Examine the stability of this scheme.

Chapter 8

Poisson and Laplace equations (elliptic)

Consider Poisson's equation in two dimensions

$$\nabla^2 u = \left(\frac{\partial^2}{\partial x^2} + \frac{\partial^2}{\partial y^2} \right) u = f(x, y) \quad (8.1)$$

If $f(x, y) = 0$ then (8.1) is called the Laplace Equation.

Equation (6.8) and can be discretised as

$$\frac{u_{i-1,j} - 2u_{i,j} + u_{i+1,j}}{(\Delta x)^2} + \frac{u_{i,j-1} - 2u_{i,j} + u_{i,j+1}}{(\Delta y)^2} = f_{i,j} \quad (8.2)$$

If we consider a square grid in such a way that $\Delta x = \Delta y$, then Equation (8.2) simplifies to

$$u_{i,j} = \frac{1}{4} \left[u_{i-1,j} + u_{i+1,j} + u_{i,j-1} + u_{i,j+1} - (\Delta x)^2 f_{i,j} \right] \quad (8.3)$$

If the boundary values for the domain are known then it is possible to solve this by iteration.

In iterative methods we need initial values at iteration level $u_{i,j}^m$ ($m = 0$ initially) and the purpose is to calculate $u_{i,j}^{m+1}$.

8.1 Jacobi iteration

Values from previous iteration level are used, which results in

$$u_{i,j}^{m+1} = \frac{1}{4} \left[u_{i-1,j}^m + u_{i+1,j}^m + u_{i,j-1}^m + u_{i,j+1}^m - (\Delta x)^2 f_{i,j} \right]$$

The method works but is inefficient and is not used in solving practical problems.

8.2 Gauss-Seidel iteration

A clear improvement in efficiency of iterative methods is obtained if we use the the newly computed values in the iteration formula: iteration level $m + 1$ values are available for nodes $(i - 1, j)$ and $(i, j - 1)$ when calculating u for node (i, j) . Thus the Gauss-Seidel formula is:

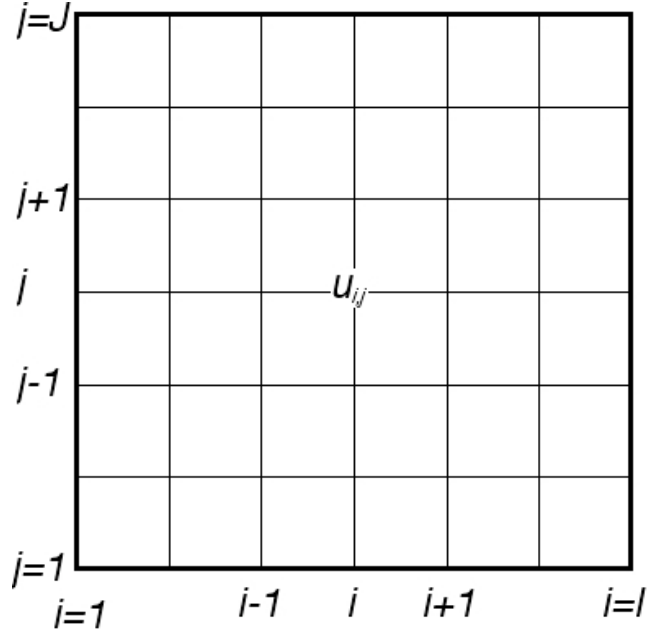


Figure 8.1: Grid for the Poisson and Laplace equations. Boundary values required for the four walls: $i = 1, j = 1, J; i = I, j = 1, J; i = 1, I, j = 1; i = 1, I, j = J$.

$$u_{i,j}^{m+1} = \frac{1}{4} [u_{i-1,j}^{m+1} + u_{i+1,j}^m + u_{i,j-1}^{m+1} + u_{i,j+1}^m - (\Delta x)^2 f_{i,j}] \quad (8.4)$$

The inclusion of the two newly computed values makes Gauss-Seidel iteration more efficient than Jacobi iteration.

8.3 Successive Over Relaxation (SOR)

Gauss-Seidel iteration method can be further improved by increasing the convergence rate using the method of SOR (Successive Over Relaxation). The change between two successive Gauss-Seidel iterations is called the residual c , which is defined as

$$c = u_{i,j}^{m+1} - u_{i,j}^m$$

In the method of SOR, the Gauss-Seidel residual is multiplied by a relaxation factor ω and new iteration value is obtained from

$$u_{i,j}^{m+1} = u_{i,j}^m + \omega c = u_{i,j}^m + \omega (\hat{u}_{i,j}^{m+1} - u_{i,j}^m) = (1 - \omega) u_{i,j}^m + \omega \hat{u}_{i,j}^{m+1} \quad (8.5)$$

where $\hat{u}_{i,j}^{m+1}$ denotes the new iteration value obtained from Gauss-Seidel method using Equation (8.4). It can be easily seen that if $\omega = 1$, SOR reduces to Gauss-Seidel iteration method. By substituting Equation (8.4) of the Gauss-Seidel iteration method to Equation (8.5), we obtain the equation used in the SOR method:

$$u_{i,j}^{m+1} = (1 - \omega) u_{i,j}^m + \frac{\omega}{4} [u_{i-1,j}^{m+1} + u_{i+1,j}^m + u_{i,j-1}^{m+1} + u_{i,j+1}^m - (\Delta x)^2 f_{i,j}] \quad (8.6)$$

Usually the numerical value of relaxation parameter can be obtained by trial and error and optimum value is around 1.5. In the case that $0 < \omega < 1$, the method is said to be "under relaxed". According to the selection of parameter ω , we either extrapolate $\omega > 1$ or $0 < \omega < 1$ interpolate between the old iteration value at level m and Gauss-Seidel value at level $m + 1$. If we extrapolate too much, i.e. ω is too high, the iteration starts to oscillate and probably collapses.

Exercises

- 1) Set up a numerical model with 10×10 points. Start with $u=0$ in the interior and with $u=1$ as boundary conditions. Test the convergence of the 3 different iterations schemes from this chapter.

Chapter 9

The shallow water equations

In this chapter we consider the equations describing the horizontal propagation of gravity and inertia-gravity waves. These equations are often referred to as the linearised shallow water equations. Mathematically, this means that we will be dealing with a system of two or three partial differential equations of the first order. Thus, we will now have two or three dependent variables (one or two velocities and pressure/height). The system of equations will always be equivalent to a single differential equation but of a higher order. This equation can be obtained from the system by elimination of dependent variables.

9.1 One-dimensional gravity waves with centered space differencing

For simplicity we shall start with the simplest case of gravity waves

$$\frac{\partial u}{\partial t} = -g \frac{\partial h}{\partial x} \quad \text{and} \quad \frac{\partial h}{\partial t} = -H \frac{\partial u}{\partial x}$$

where g is the gravity and H the depth/height. We seek solutions of the form

$$u(x, t) = \operatorname{Re} [u_0 e^{i(kx - \omega t)}] \quad \text{and} \quad h(x, t) = \operatorname{Re} [h_0 e^{i(kx - \omega t)}]$$

giving the frequency equation

$$\omega^2 = gHk^2$$

so that the phase speed is

$$c = \frac{\omega}{k} = \pm \sqrt{gH}$$

showing that the gravity waves can propagate along the x-axis in both directions with a speed of \sqrt{gH} . This speed is not a function of the wave number and consequently there is no dispersion of the waves.

Consider now the differential-difference equations with centered scheme

$$\frac{\partial u_j}{\partial t} = -g \frac{h_{j+1} - h_{j-1}}{2\Delta x} \quad \text{and} \quad \frac{\partial h_j}{\partial t} = -H \frac{u_{j+1} - u_{j-1}}{2\Delta x} \quad (9.1)$$

We seek solutions of the form

$$u_j = u_0 e^{i(jk\Delta x - \omega_D t)} \quad \text{and} \quad h_j = h_0 e^{i(jk\Delta x - \omega_D t)}$$

which are substituted in Equation (9.1) and gives the frequency equation

$$c_D = \frac{\omega_D}{k} = \pm \sqrt{gH} \frac{\sin(k\Delta x)}{k\Delta x}$$

and the numerical group speed is

$$C_{Dg} = \frac{d(kC_D)}{dk} = c \cos(k\Delta x)$$

This phase speed is function of the wave number, and thus, we see that the space differencing again results in computational dispersion. It is the same as the one obtained for the advection equation with centered schemes.

There are two types of possible grids for these types of equations as illustrated by Figure 9.1. We can have the two dependent variables in the same points as in Equation 9.1 or we can alternate them in space.

$$\frac{\partial u_j}{\partial t} = -g \frac{h_j - h_{j-1}}{\Delta x} \quad \text{and} \quad \frac{\partial h_j}{\partial t} = -H \frac{u_{j+1} - u_j}{\Delta x} \quad (9.2)$$

This is called a staggered grid. The phase speed becomes now

$$c_D = \frac{\omega_D}{k} = \pm \sqrt{gH} \frac{\sin(\frac{k\Delta x}{2})}{(\frac{k\Delta x}{2})}$$

and

$$C_{Dg} = \frac{d(\omega_D)}{dk} = \frac{d(kC_D)}{dk} = c \cos\left(\frac{k\Delta x}{2}\right)$$

The staggered grid has hence the advantage that

- the computational time is half as long or the number of grid points is halved
- the truncation error is half as big with $\Delta x \rightarrow \Delta x/2$
- waves with $k\Delta x > \pi/2$, which are the waves shorter than 4 grid cells, are eliminated. They are the ones that have a big error in the phase speed.

9.2 Two-dimensional gravity waves with centered space differencing

We now consider two dimensional gravity waves.

$$\begin{aligned} \frac{\partial u}{\partial t} &= -g \frac{\partial h}{\partial x} \\ \frac{\partial v}{\partial t} &= -g \frac{\partial h}{\partial y} \\ \frac{\partial h}{\partial t} &= -H \left(\frac{\partial u}{\partial x} + \frac{\partial v}{\partial y} \right) \end{aligned} \quad (9.3)$$

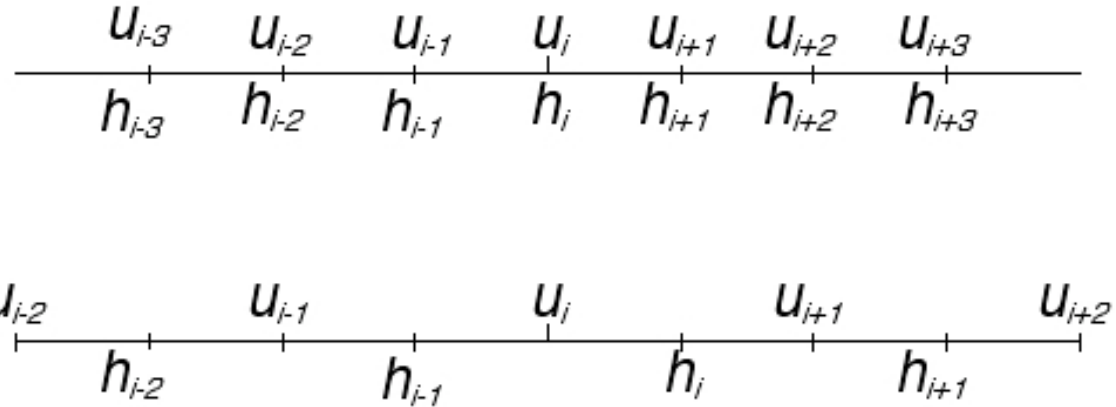


Figure 9.1: Top: grid with two dependent variables that are both carried at every grid point. Bottom: staggered grid with two dependent variables that are carried at alternate grid points

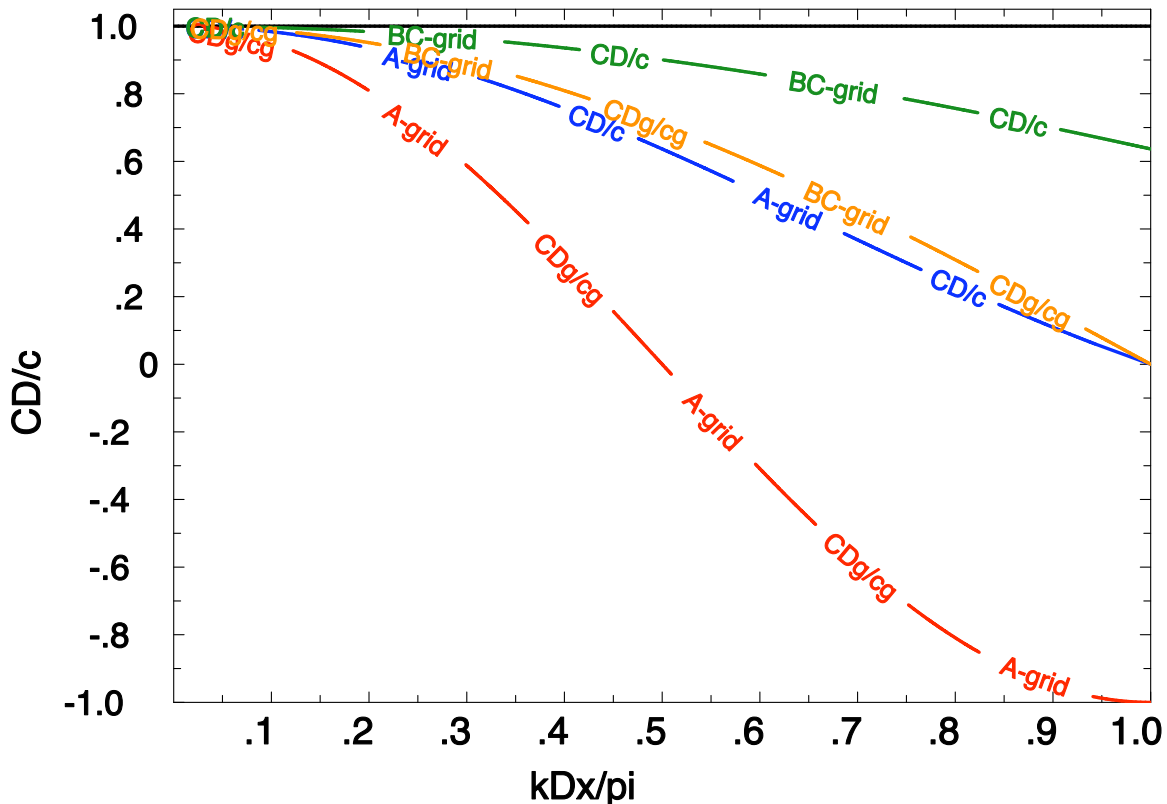


Figure 9.2: The numerical phase speed C_D due to the centred finite difference in space compared to the analytical phase speed c for one dimension shallow water equations (Eq. 9.1). The black line is the solution of the continuous equations which is the non dispersive analytical case, i.e. the phase speed is the same as the group velocity $c = c_g$. The blue line is the numerical phase speed normalised by dividing with c . Note that when the wave number increases (wave length decreases) then the numerical phase speed deviates from the analytical phase speed. The phase speed is clearly dispersive since the waves propagate at different speeds depending on their wave lengths. The red line shows the computational group velocity C_{Dg} which at wave lengths shorter than 4 grid cells ($k\Delta x < \pi/2$) propagate in the wrong direction. The green and orange lines are for the staggered BC-grid.

Substituting the wave solutions

$$\begin{aligned} u(x, y, t) &= \operatorname{Re} \left[u_0 e^{i(kx+ly-\omega t)} \right] \\ v(x, y, t) &= \operatorname{Re} \left[v_0 e^{i(kx+ly-\omega t)} \right] \\ h(x, y, t) &= \operatorname{Re} \left[h_0 e^{i(kx+ly-\omega t)} \right] \end{aligned} \quad (9.4)$$

we now obtain

$$\omega^2 = gH(k^2 + l^2)$$

There are now several possible grids that usually are identified with the letters A to E according to Arakawa (1972). The three most common ones are illustrated in Figure 9.3.

9.3 The linearised shallow water equations without friction

let us now consider one of the simplest possible sets of the Navier-Stokes equations in the atmosphere or the ocean. The linearised shallow water equations or the gravity-inertia wave equations.

$$\begin{aligned} \frac{\partial u}{\partial t} - fv &= -g \frac{\partial h}{\partial x} \\ \frac{\partial v}{\partial t} + fu &= -g \frac{\partial h}{\partial y} \\ \frac{\partial h}{\partial t} + H \left(\frac{\partial u}{\partial x} + \frac{\partial v}{\partial y} \right) &= 0 \end{aligned} \quad (9.5)$$

where f is Coriolis acceleration and is here assumed to be constant. We seek as before solutions of the wave form (9.4) and we obtain

$$\omega^2 = f^2 + gH(k^2 + l^2)$$

For each of the three grids we use the simplest centered approximations for the space derivative and the Coriolis terms. We do not need to study the time differencing since it has been studied previously and is the same as before.

A-grid:

$$\begin{aligned} \frac{\partial u_{i,j}}{\partial t} &= -g \frac{h_{i+1,j} - h_{i-1,j}}{2\Delta x} + fv_{i,j} \\ \frac{\partial v_{i,j}}{\partial t} &= -g \frac{h_{i,j+1} - h_{i,j-1}}{2\Delta y} - fu_{i,j} \\ \frac{\partial h_{i,j}}{\partial t} &= -H \left(\frac{u_{i+1,j} - u_{i-1,j}}{2\Delta x} + \frac{v_{i,j+1} - v_{i,j-1}}{2\Delta y} \right) \end{aligned} \quad (9.6)$$

B-grid:

$$\frac{\partial u_{i,j}}{\partial t} = -g \frac{h_{i+1,j} + h_{i+1,j+1} - h_{i,j} - h_{i,j+1}}{2\Delta x} + fv_{i,j}$$

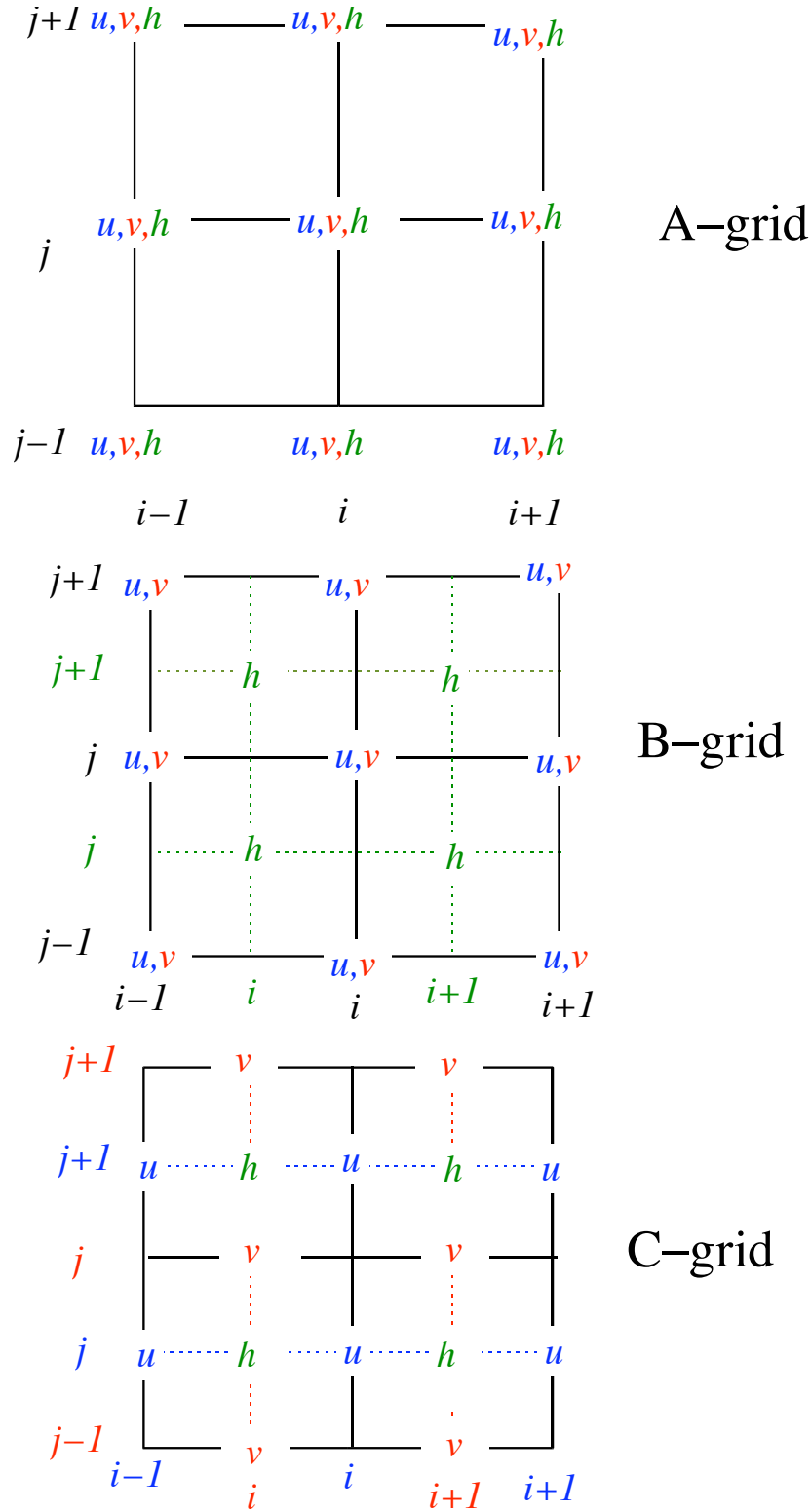


Figure 9.3: The three most common grids: A, B and C.

$$\begin{aligned}\frac{\partial v_{i,j}}{\partial t} &= -g \frac{h_{i,j+1} + h_{i+1,j+1} - h_{i,j} - h_{i+1,j}}{2\Delta y} - fu_{i,j} \\ \frac{\partial h_{i,j}}{\partial t} &= -H \left(\frac{u_{i,j} + u_{i,j-1} - u_{i-1,j} - u_{i-1,j-1}}{2\Delta x} + \frac{v_{i,j} + v_{i-1,j} - v_{i,j-1} - v_{i-1,j-1}}{2\Delta y} \right) \quad (9.7)\end{aligned}$$

C-grid:

$$\begin{aligned}\frac{\partial u_{i,j}}{\partial t} &= -g \frac{h_{i+1,j} - h_{i,j}}{\Delta x} + \frac{f}{4} (v_{i,j} + v_{i+1,j} + v_{i+1,j-1} + v_{i,j-1}) \\ \frac{\partial v_{i,j}}{\partial t} &= -g \frac{h_{i,j+1} - h_{i,j}}{\Delta y} - \frac{f}{4} (u_{i,j} + u_{i,j+1} + u_{i-1,j+1} + u_{i-1,j}) \\ \frac{\partial h_{i,j}}{\partial t} &= -H \left(\frac{u_{i,j} - u_{i-1,j}}{\Delta x} + \frac{v_{i,j} - v_{i,j-1}}{\Delta y} \right) \quad (9.8)\end{aligned}$$

For simplicity we shall first study the quasi-one-dimensional case where u , v and h do not depend on y so that the shallow water equations 9.5 are reduced to

$$\begin{aligned}\frac{\partial u}{\partial t} - fv &= -g \frac{\partial h}{\partial x} \\ \frac{\partial v}{\partial t} + fu &= 0 \\ \frac{\partial h}{\partial t} + H \frac{\partial u}{\partial x} &= 0 \quad (9.9)\end{aligned}$$

Substituting the wave solutions in equation 9.9, we obtain the frequency equation

$$\left(\frac{\omega}{f} \right)^2 = 1 + \frac{gH}{f^2} k^2 \quad (9.10)$$

Let us now look at the effect of the finite differencing in space in this case. As the variables are assumed not to depend on y , the system for the A-grid (9.6) is reduced to

$$\begin{aligned}\frac{\partial u_{i,j}}{\partial t} &= -g \frac{h_{i+1,j} - h_{i-1,j}}{2\Delta x} + fv_{i,j} \\ \frac{\partial v_{i,j}}{\partial t} &= -fu_{i,j} \\ \frac{\partial h_{i,j}}{\partial t} &= -\frac{H}{2\Delta x} (u_{i+1,j} - u_{i-1,j}) \quad (9.11)\end{aligned}$$

and for the B-grid:

$$\begin{aligned}\frac{\partial u_{i,j}}{\partial t} &= -g \frac{h_{i+1,j} + h_{i+1,j+1} - h_{i,j} - h_{i,j+1}}{2\Delta x} + fv_{i,j} \\ \frac{\partial v_{i,j}}{\partial t} &= -fu_{i,j}\end{aligned}$$

$$\frac{\partial h_{i,j}}{\partial t} = -\frac{H}{2\Delta x} (u_{i,j} + u_{i,j-1} - u_{i-1,j} - u_{i-1,j-1}) \quad (9.12)$$

and the C-grid:

$$\frac{\partial u_{i,j}}{\partial t} = -g \frac{h_{i+1,j} - h_{i,j}}{\Delta x} + \frac{f}{4} (v_{i,j} + v_{i+1,j} + v_{i+1,j-1} + v_{i,j-1})$$

$$\frac{\partial v_{i,j}}{\partial t} = -\frac{f}{4} (u_{i,j} + u_{i,j+1} + u_{i-1,j+1} + u_{i-1,j})$$

$$\frac{\partial h_{i,j}}{\partial t} = -\frac{H}{\Delta x} (u_{i,j} - u_{i-1,j}) \quad (9.13)$$

Substituting the wave solutions with no j dependency $(u_i, v_i, h_i) = (u_0, v_0, h_0)e^{I(ik\Delta x - \omega_D t)}$ into these systems (9.11, 9.12 and 9.13) gives the frequency equations:

$$A: \left(\frac{\omega_D}{f}\right)^2 = 1 + \frac{gH}{f^2} \frac{\sin^2(k\Delta x)}{(\Delta x)^2}$$

$$B: \left(\frac{\omega_D}{f}\right)^2 = 1 + \frac{gH}{f^2} \frac{\sin^2(k\Delta x/2)}{(\Delta x/2)^2}$$

$$C: \left(\frac{\omega_D}{f}\right)^2 = \cos^2\left(\frac{k\Delta x}{2}\right) + \frac{gH}{f^2} \frac{\sin^2(k\Delta x/2)}{(\Delta x/2)^2}$$

The non-dimensional frequency ω/f is now seen to depend on two parameters $k\Delta x$ and gH/f^2 (Rossby radius to the square) and is plotted in Figure 9.4 and validated against the non-discretised case of equation 9.10.

One can summarise the advantages and disadvantages of the grids by

- Grid A: The frequency reaches a maximum at $k\Delta x = \pi/2$, i.e. a wave length of 4 grids. Thus, the group velocity is zero for this wave length. If gravity-inertia waves of approximately that wave number are excited near a point inside the computational region, for example by non-linear effects or forcing through heating or ground topography, the wave energy stays near that point. Beyond this maximum value, for $\pi/2 < k\Delta x < \pi$, the frequency decreases as the wave number increases. Thus, for these waves the group velocity has wrong sign. Finally, the two-grid-interval wave with $k\Delta x = \pi$ behaves like a pure inertia oscillation, and its group velocity is again zero.
- Grid B: The frequency increases monotonically throughout the range $0 < k\Delta x < \pi$. However it reaches a maximum at the end of the range, so that the group velocity is zero for the two-grid-interval wave with $k\Delta x = \pi$.
- Grid C: The frequency increases monotonically in a similar way to the one for the B-grid if $gH/(f\Delta x)^2 > 1/4$ i.e. when the Rossby radius is longer than a half grid ($\sqrt{gH}/f > \frac{\Delta x}{2}$). If however the Rossby radius is exactly a half grid ($\sqrt{gH}/f = \frac{\Delta x}{2}$) then the group velocity is zero and for shorter Rossby radii then the frequency will decrease in an unrealistic way with increasing wave number throughout $0 < k\Delta x < \pi$. The advantage of the C-grid is however not seen here, but lies in that the velocities are perpendicular on the walls of the grid-box, which makes the differencing straightforward of 1) the scalar transport in the tracer equation and 2) the continuity equation.

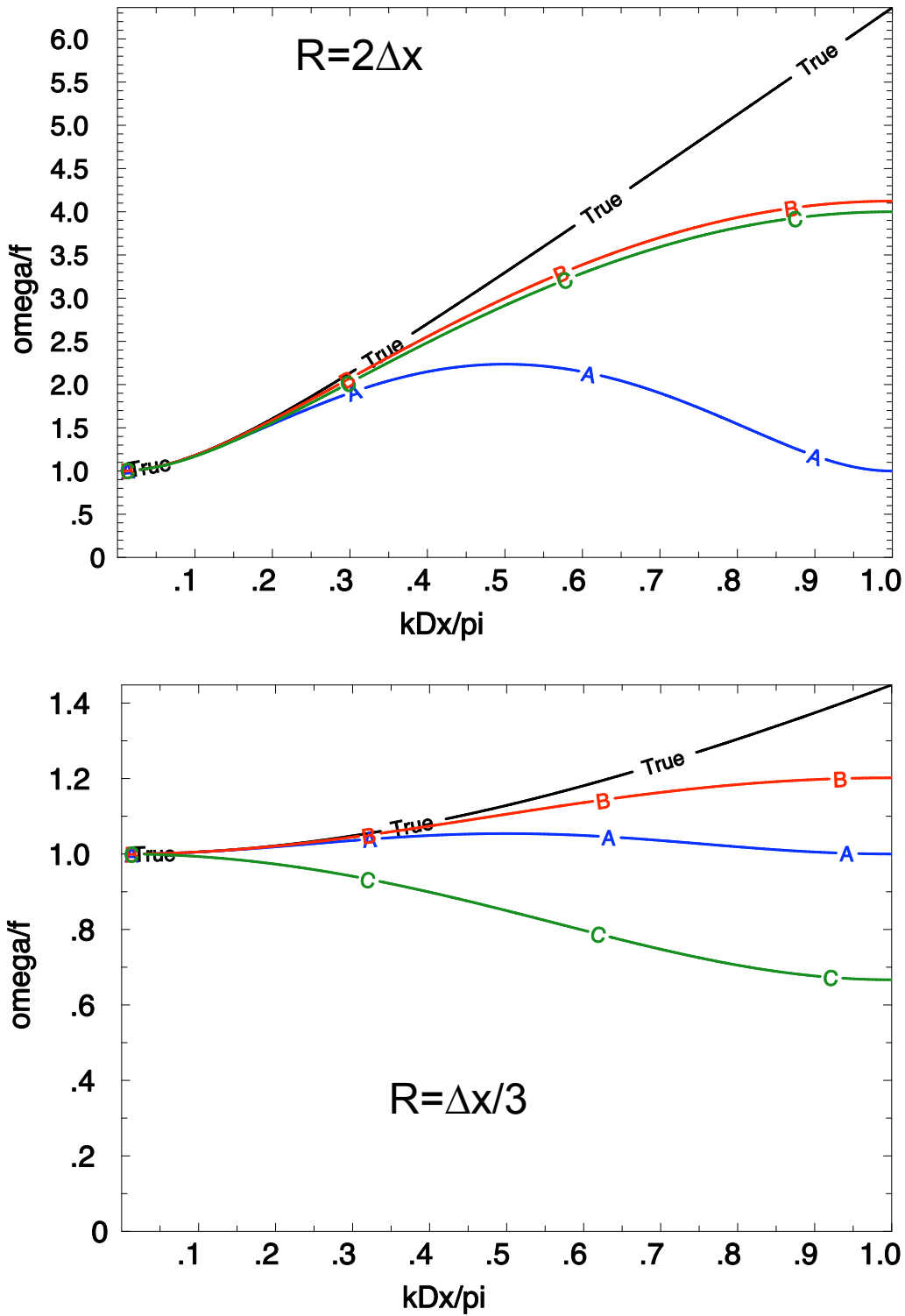


Figure 9.4: The function ω/f from (9.10) where at the top panel $gH/(f\Delta x)^2 = 4$, i.e. the Rossby radius set to two gridcells ($\sqrt{gH}/f = 2\Delta x$) and at the bottom panel $gH/(f\Delta x)^2 = 1/9$, i.e. the Rossby radius is set to a third of a grid cell ($\sqrt{gH}/f = \Delta x/3$). The black line corresponds to the true analytical solution, the blue line to the A-grid, the red line to the B-grid and the green line to the C-grid. NB: The B and C grid give similar results when the Rossby radius is well resolved but the C-grid degenerates when the grid resolution is coarse.

9.4 Conservation of mass, energy and enstrophy

There are several reasons why numerical schemes for models are often formulated to respect conservation properties of the governing equations. An important practical consideration is that satisfaction of conservation properties helps to ensure the computational stability of a model. Apart from this, the direct physical realism of a conservation property may be a desirable feature. For example, ensuring conservation of mass prevents the surface pressure from drifting to highly unrealistic values in long-term integrations of atmospheric models. Advection schemes which satisfy an appropriate dynamical conservation property may help to ensure the realism of a model's energy spectrum. There are, however, considerations other than conservation that might influence the choice of numerical scheme. Shape-preservation (avoidance of the generation of spurious maxima or minima) may be considered an important feature of an advection scheme, and the economy of a method (especially the ability to take long time steps) may be a critical factor. Indeed, semi-Lagrangian advection schemes, generally without formal conservation properties, are increasingly being developed for numerical weather prediction.

9.4.1 The shallow water equations with non-linear advection terms

Let us take the the shallow water momentum equation with the non-linear advection terms included

$$\frac{\partial \mathbf{V}}{\partial t} + \mathbf{V} \cdot \nabla \mathbf{V} + f \mathbf{k} \times \mathbf{V} = -g \nabla h$$

which can be rewritten as

$$\frac{\partial \mathbf{V}}{\partial t} + \xi \mathbf{k} \times (h \mathbf{V}) = -\nabla \left(gh + \frac{1}{2} \mathbf{V} \cdot \mathbf{V} \right)$$

The continuity equation with the non-linear terms is

$$\frac{\partial h}{\partial t} + \nabla \cdot (h \mathbf{V}) = 0$$

where \mathbf{V} is the horizontal velocity vector, $f \equiv 2\Omega \sin(\Phi)$ the Coriolis parameter, $\xi \equiv \left(f + \frac{\partial v}{\partial x} - \frac{\partial u}{\partial y} \right) / h$ the horizontal absolute potential vorticity, \mathbf{k} is the unit vector normal to the plane domain S and h the total water or air column and $H \equiv gh + \frac{1}{2}(u^2 + v^2) = gh + \frac{1}{2}\mathbf{V} \cdot \mathbf{V}$.

The equations can also be written on scalar form

$$\frac{\partial u}{\partial t} - \xi h v = -\frac{\partial H}{\partial x}$$

$$\frac{\partial v}{\partial t} + \xi h u = -\frac{\partial H}{\partial y}$$

$$\frac{\partial h}{\partial t} + \frac{\partial (hu)}{\partial x} + \frac{\partial (hv)}{\partial y} = 0$$

It can be verified that these equations are such that the following conservation relations hold:

1. Total mass: $M = \int_S h dS$

2. Total Energy: $E = \int_S \frac{1}{2} (gh + \mathbf{V} \cdot \mathbf{V}) hdS$
3. Absolute potential enstrophy: $Z = \int_S \frac{1}{2} \xi^2 hdS$

9.4.2 Discretisation

The discretisation is on a C-grid illustrated in Figure 9.5.

The space differencing operators are

$$\begin{aligned}\delta_x u &= \frac{1}{\Delta x} (u_{i+1/2,j} - u_{i-1/2,j}) \rightarrow \frac{u_{i,j} - u_{i-1,j}}{\Delta x} \\ \delta_y v &= \frac{1}{\Delta y} (v_{i,j+1/2} - v_{i,j-1/2}) \rightarrow \frac{v_{i,j} - v_{i,j-1}}{\Delta y} \\ \bar{u}^x &= \frac{1}{2} (u_{i+1/2,j} + u_{i-1/2,j}) \rightarrow \frac{1}{2} (u_{i,j} + u_{i-1,j}) \\ \bar{v}^y &= \frac{1}{2} (v_{i,j+1/2} + v_{i,j-1/2}) \rightarrow \frac{1}{2} (v_{i,j} + v_{i,j-1})\end{aligned}$$

The mass fluxes U and V are defined at the points where the velocity components u and v are located:

$$\begin{aligned}U_{i,j} &\equiv \bar{h}^x u = u_{i,j} \frac{1}{2} (h_{i,j} + h_{i+1,j}) \\ V_{i,j} &\equiv \bar{h}^y v = v_{i,j} \frac{1}{2} (h_{i,j} + h_{i,j+1})\end{aligned}$$

The gradient operator will act on a quantity H defined at the locations where h is defined:

$$H \equiv gh + \frac{1}{2} (\bar{u}^{2x} + \bar{v}^{2y}) = gh_{i,j} + \frac{1}{2} \left[\frac{1}{2} (u_{i,j}^2 + u_{i-1,j}^2) + \frac{1}{2} (v_{i,j}^2 + v_{i,j-1}^2) \right]$$

The potential absolute vorticity is redefined and located in the corners of the C-grid

$$\xi_{i,j} = \frac{f + \delta_x v - \delta_y u}{\bar{h}^x \bar{h}^y} = \frac{f + \frac{v_{i+1,j} - v_{i,j}}{\Delta x} - \frac{u_{i,j+1} - u_{i,j}}{\Delta y}}{\frac{1}{4} (h_{i,j} + h_{i+1,j} + h_{i,j+1} + h_{i+1,j+1})}$$

Simple expressions are chosen for

1. Total mass: $M = \sum h$
2. Total energy: $E = \frac{1}{2} \sum ((gh)^2 + h\bar{u}^{2x} + h\bar{v}^{2y})$
3. Absolute potential enstrophy: $Z = \frac{1}{2} \sum \xi^2 \bar{h}^x \bar{h}^y$

the symbol \sum referring to a summation over all grid points of same species. Note that due to symmetry:

$$\sum ab^x = \sum ba^x$$

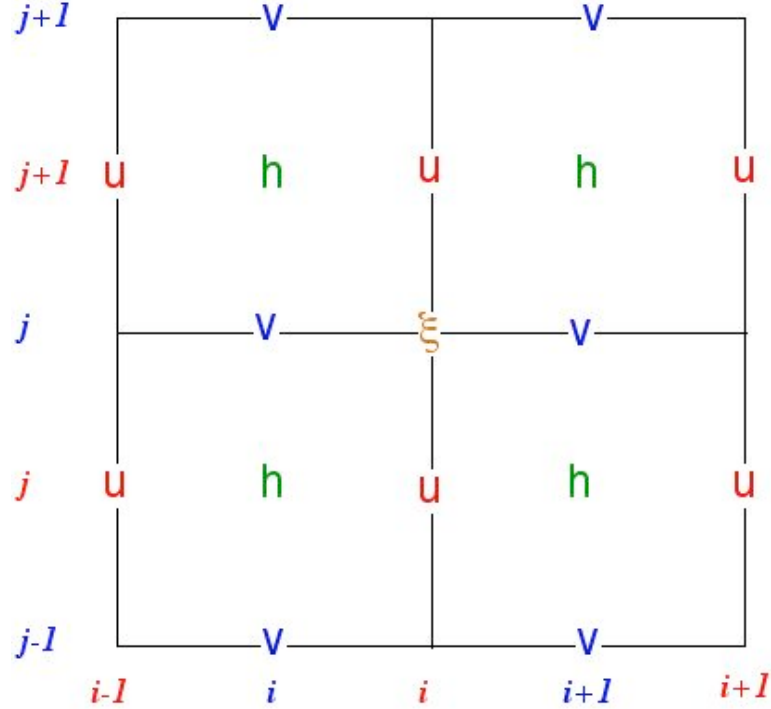


Figure 9.5: *C-grid with points for the zonal velocity u , meridional velocity v , water or air column height h and vorticity ξ .*

and that due to skew-symmetry

$$\sum a \delta_x b = - \sum b \delta_x a$$

The time derivative of the total energy is

$$\frac{dE}{dt} = \sum \left(U \frac{\partial u}{\partial t} + V \frac{\partial v}{\partial t} + H \frac{\partial h}{\partial t} \right) \quad (9.14)$$

A simple energy-conserving model can be defined as

$$\frac{\partial u}{\partial t} - \overline{\xi V^{xy}} + \delta_x H = 0$$

$$\frac{\partial v}{\partial t} + \overline{\xi U^{yx}} + \delta_y H = 0$$

$$\frac{\partial h}{\partial t} + \delta_x U + \delta_y V = 0$$

so that from Equation (9.14) we have

$$\frac{dE}{dt} = \sum \left(U \overline{\xi V^{xy}} - V \overline{\xi U^{yx}} \right) + \sum (-U \delta_x H - H \delta_x U) + \sum (-V \delta_y H - H \delta_y V) = 0$$

where each of the three summations cancel due to the symmetry or skew symmetry of the operators.

An absolute potential enstrophy model can be defined as

$$\frac{\partial u}{\partial t} - \bar{\xi}^y \bar{V}^{xy} + \delta_x H = 0$$

$$\frac{\partial v}{\partial t} + \bar{\xi}^x \bar{U}^{yx} + \delta_y H = 0$$

$$\frac{\partial h}{\partial t} + \delta_x U + \delta_y V = 0$$

In the corresponding vorticity equation, the discrete gradient vanishes $\delta_x \delta_y = \delta_y \delta_x$, so that

$$\frac{\partial}{\partial t} \left(\xi \bar{h}^{xy} \right) + \delta_x \left(\bar{\xi}^x \bar{U}^{yx} \right) + \delta_y \left(\bar{\xi}^y \bar{V}^{xy} \right) = 0$$

which when combined with the average continuity equation

$$\frac{\partial}{\partial t} \left(\bar{h}^{xy} \right) + \delta_x \left(\bar{U}^{yx} \right) + \delta_y \left(\bar{V}^{xy} \right) = 0$$

yields the conservative potential enstrophy equation

$$\frac{\partial}{\partial t} \left(\xi^2 \bar{h}^{xy} \right) + \delta_x \left(\bar{\xi}^2 \bar{U}^{yx} \right) + \delta_y \left(\bar{\xi}^2 \bar{V}^{xy} \right) = 0$$

Chapter 10

Implicit and semi-implicit schemes

The time step permitted by the economical explicit schemes, twice that prescribed by the CFL criterion, is still considerably shorter than that required for accurate integration of the quasi-geostrophic motions. Thus we consider implicit schemes which are stable for any choice of time step. We shall consider here only the simplest of the implicit schemes, the trapezoidal rule applied to the system (9.3) of pure gravity waves. For brevity it will simply be called the implicit scheme.

10.1 The implicit scheme (trapezoidal rule)

We consider the finite difference scheme

$$\begin{aligned} u^{n+1} &= u^n - \frac{g\Delta t}{2} (\delta_x h^n + \delta_x h^{n+1}) \\ v^{n+1} &= v^n - \frac{g\Delta t}{2} (\delta_y h^n + \delta_y h^{n+1}) \\ h^{n+1} &= h^n - \frac{H\Delta t}{2} (\delta_x u^n + \delta_y v^n + \delta_x u^{n+1} + \delta_y v^{n+1}) \end{aligned} \tag{10.1}$$

where the space differencing operator

$$\delta_x u = \frac{1}{\Delta x} (u_{i+1/2} - u_{i-1/2})$$

Substituting the wave solutions

$$u^n = \lambda^n u_0 e^{ik(j\Delta x + l\Delta y)}$$

`fig/relspeedgrav.pdf`

Figure 10.1: *Relative speed of gravity waves, with implicit time and centered space differencing, and a CFL-number equal to 5.*

$$v^n = \lambda^n v_0 e^{ik(j\Delta x + l\Delta y)}$$

$$h^n = \lambda^n h_0 e^{ik(j\Delta x + l\Delta y)}$$

we find

$$u_0(1-\lambda) = ig\Delta t(1+\lambda) \frac{\sin(k\Delta x/2)}{(\Delta x)} h_0$$

$$v_0(1-\lambda) = ig\Delta t(1+\lambda) \frac{\sin(l\Delta y/2)}{(\Delta y)} h_0$$

$$h_0(1-\lambda) = iH\Delta t(1+\lambda) \left[\frac{\sin(k\Delta x/2)}{(\Delta x)} u_0 + \frac{\sin(l\Delta y/2)}{(\Delta y)} v_0 \right]$$

One of the solutions is $\lambda = 1$ is associated with neutral a stationary solution. The remaining two are obtained by eliminate u_0, v_0, h_0 so that

$$\lambda = \frac{1 - A \pm 2i\sqrt{A}}{1 + A} \quad \text{where} \quad A \equiv gH(\Delta t)^2 \left[\frac{\sin^2(k\Delta x/2)}{(\Delta x)^2} + \frac{\sin^2(l\Delta y/2)}{(\Delta y)^2} \right]$$

Examination of these shows that it always gives amplification factors satisfying $|\lambda| = 1$ and so the scheme is unconditionally stable and neutral. Using

$$\lambda = |\lambda| e^{-i\omega\Delta t}$$

we find for the relative phase speed of the non-stationary solutions,

$$\frac{c^*}{\sqrt{gH}} = \frac{(\Delta x)^2}{2\sqrt{A}} \arctan \left(\frac{2\sqrt{A}}{1-A} \right)$$

Implicit time differencing is seen to result in a considerable retardation of gravity waves of the same order of the magnitude as that due to centred space differencing. The solution of the implicit scheme for new variables u^{n+1}, v^{n+1} is no longer trivial.

To apply an implicit method it is necessary to solve the difference system for variables at level $n+1$. For the system (10.1) it is more complex. The quantities $\delta_x u^{n+1}$ and $\delta_y v^{n+1}$ can be eliminated from the third equation by applying operators δ_x and δ_y to the first and second of these equations and substituting the results in to the third equation. This gives an equation for the height which can be solved using a number of standard methods: the most popular is the relaxation method.

1. A first guess h^{n+1} which is usually h^n .
2. At each of the grid points the value of h^{n+1} so as to satisfy the difference equation.
3. The preceding step is repeated as many times as needed to make the change at every point less than some pre-assigned small value.

10.2 The semi-implicit method of Kwizak and Robert

There is no advantage in using an implicit method for advection, Coriolis, and other terms of governing equations in atmospheric models. They are associated with slower phase speeds, and should not require excessively small time steps for linear stability when calculated explicitly. Since the trapezoidal implicit scheme is a two level scheme like the forward-backward scheme, it is convenient to use Adams-Basforth scheme for this purpose. Kwizak and Robert (1971) chose, however, to use the leapfrog scheme. The usual procedure used for solving the semi-implicit difference system for variables at time level $n + 1$ will be illustrated for the shallow water equations. These equations can be written in a compact form

$$\begin{aligned} \frac{\partial u}{\partial t} - fv &= -g \frac{\partial h}{\partial x} + A_u \\ \frac{\partial v}{\partial t} + fu &= -g \frac{\partial h}{\partial y} + A_v \\ \frac{\partial h}{\partial t} &= -H \left(\frac{\partial u}{\partial x} + \frac{\partial v}{\partial y} \right) + A_h \end{aligned} \quad (10.2)$$

where A_u , A_v and A_h denote the terms that were omitted in the system (9.5) describing the propagation of pure gravity waves. These additional terms, and implicit differencing over a time interval $2\Delta t$ for the gravity wave terms and centred space differencing (10.2) is replaced by

$$\begin{aligned} u^{n+1} &= u^{n-1} - g\Delta t (\delta_x h^{n-1} + \delta_x h^{n+1}) + 2\Delta t A_u^n \\ v^{n+1} &= v^{n-1} - g\Delta t (\delta_y h^{n-1} + \delta_y h^{n+1}) + 2\Delta t A_v^n \\ h^{n+1} &= h^{n-1} - H\Delta t (\delta_x u^{n-1} + \delta_y v^{n-1} + \delta_x u^{n+1} + \delta_y v^{n+1}) + 2\Delta t A_h^n \end{aligned} \quad (10.3)$$

We now apply the operator δ_x to the first and δ_y to the second of these equations, respectively and add the results. We introduce the notation

$$\delta_{xx}h = \delta_x(\delta_x h) \quad \text{and} \quad \delta_{yy}h = \delta_y(\delta_y h)$$

We obtain

$$(\delta_x u + \delta_y v)^{n+1} = (\delta_x u + \delta_y v)^{n-1} - g\Delta t [(\delta_{xx} + \delta_{yy}) h^{n-1} + (\delta_{xx} + \delta_{yy}) h^{n+1}] + 2\Delta t (\delta_x A_u + \delta_y A_v)^n$$

Substituting the right-hand side into the third of Eqs. (10.3), and defining the “finite difference Laplacian” by

$$\nabla_*^2 \equiv \delta_{xx} + \delta_{yy}$$

we find that

$$h^{n+1} = h^{n-1} - 2H\Delta t (\delta_x u + \delta_y v)^{n-1} + gH (\Delta t)^2 (\nabla_*^2 h^{n-1} + \nabla_*^2 h^{n+1}) + 2\Delta t [A_h - H\Delta t (\delta_x A_u + \delta_y A_v)]^n$$

Using, in addition the definitions

$$F^{n-1} \equiv h^{n-1} - 2H\Delta t (\delta_x u + \delta_y v)^{n-1} + gH (\Delta t)^2 \nabla_*^2 h^{n-1}$$

$$G^n \equiv 2\Delta t [A_h - H\Delta t (\delta_x A_u + \delta_y A_v)]^n$$

this can be written as

$$h^{n+1} - gH (\Delta t)^2 \nabla_*^2 h^{n+1} = F^{n-1} + G^n \quad (10.4)$$

The terms have been arranged to show that at time level n the right hand side is known at all space grid points. Once the equation has been solved for the values h^{n+1} then u^{n+1} and v^{n+1} can be obtained directly from the first and the second of Eqs. (10.3). The algebraic system (10.4) is an approximation to an elliptic equation

$$\nabla^2 h + ah + b(x, y) = 0$$

10.3 The semi-Lagrangian technique

In an Eulerian Advection scheme an observer watches the world evolve around him at a fixed geographical point. Such schemes work well on regular Cartesian meshes, but often lead to overly restrictive time steps due to considerations of computational stability. In a Lagrangian advection scheme observer watches the world evolve around himself as he travels with a fluid particle. Such schemes can often use much larger time steps than Eulerian ones but have disadvantage that an initially regularly spaced set of particles will generally evolve to a highly irregularly spaced set at later times and important features of the flow may consequently not be well represented. The idea behind the semi-Lagrangian advection schemes is to try to get the best of both worlds: the regular resolution of the Eulerian schemes and the enhanced stability of the Lagrangian ones. This is achieved by using a different set of particles at each time step, the set of particles being chosen such that they arrive exactly at the pints of a regular Cartesian mesh at the end of the time step.

So far we have taken an Eulerian view and considered what was the evolution in time of a dependent variable at fixed points in space and in the spectral and finite elements we will consider what is the time evolution of some coefficients multiplying some basis functions also fixed in space; in other words, we used the partial time derivative $\partial/\partial t$.

A few years ago, several attempts were made to build stable time integration schemes permitting large time steps. Robert (1981) proposed using the quasi-Lagrangian technique for the treatment of the advective part of the equations.

10.3.1 Passive advection in 1-D

To present the basic idea behind the semi-Lagrangian method in its simplest context let us apply the one-dimensional advection equation

$$\frac{dF}{dt} = \frac{\partial F}{\partial t} + \frac{\partial x}{\partial t} \frac{\partial F}{\partial x} = 0 \quad (10.5)$$

where F is the advected property and

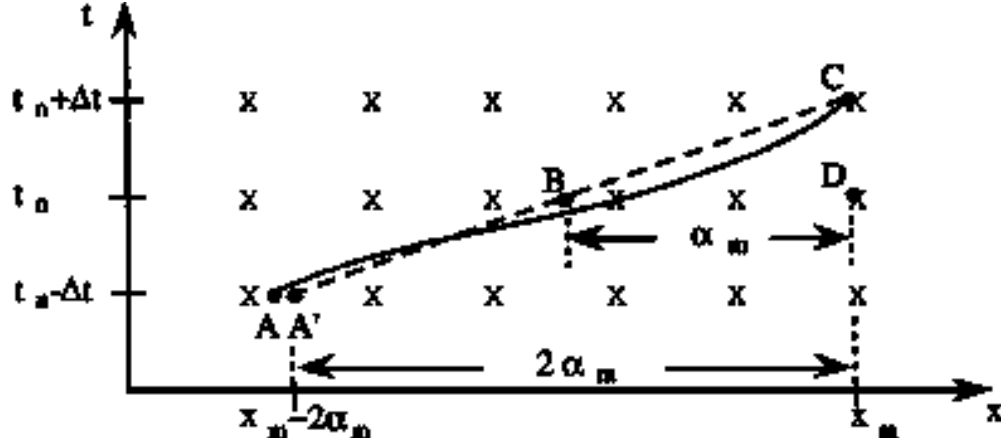


Figure 10.2: Schematic for three time level advection. Actual (solid curve) and approximate (dashed line) trajectories that arrive at mesh point x_m at time $t^n + \Delta t$. Here α_m is the distance the particle is displaced in x in time Δt .

$$\frac{\partial x}{\partial t} = U(x, t) \quad (10.6)$$

is given advection velocity. Equation (10.5) states that the scalar F is constant along a fluid path or trajectory. In Figure 10.2, the exact trajectory in the $x - t$ plane of the fluid particle that arrives at mesh point x_m at time $t^n + \Delta t$ is denoted by the solid curve AC , and an approximate straight line trajectory by the dashed line AC' . Let us assume that we know $F(x, t)$ at all mesh points x_m at times $t^n - \Delta t$ and t^n , and that we wish to obtain values at the same mesh points at time $t^n + \Delta t$. The essence of semi-Lagrangian advection is to approximately integrate Equation (10.5) along the approximated fluid trajectory AC' . Thus,

$$\frac{F(x_m, t^n + \Delta t) - F(x_m - 2\alpha_m, t^n - \Delta t)}{2\Delta t} = 0 \quad (10.7)$$

where α_m is the distance BD the particle travels in x in time Δt , when following the approximated space-time trajectory AC' . Thus we know α_m , then the value of F at the arrival point x_m at the time $t^n + \Delta t$ is just its value at the upstream point $x_m - 2\alpha_m$ at the time $t^n - \Delta t$. However, we have not as yet determined α_m ; even if we had, we only know F at mesh points, and generally it still remains to evaluate F somewhere between mesh points.

To determine α_m , note that U evaluated at the point B of Figure 10.2 is just the inverse of the slope of the straight line AC' , and this gives the following approximation to equation (10.6):

$$\alpha_m = \Delta t U(x_m - \alpha_m, t^n) \quad (10.8)$$

Equation (10.8) may be iteratively solved for the displacement α_m , for example by

$$\alpha_m^{k+1} = \Delta t U(x_m - \alpha_m^k, t^n) \quad (10.9)$$

with some initial guess for α_m^0 , provided U can be evaluated between the grid points. To evaluate F and U

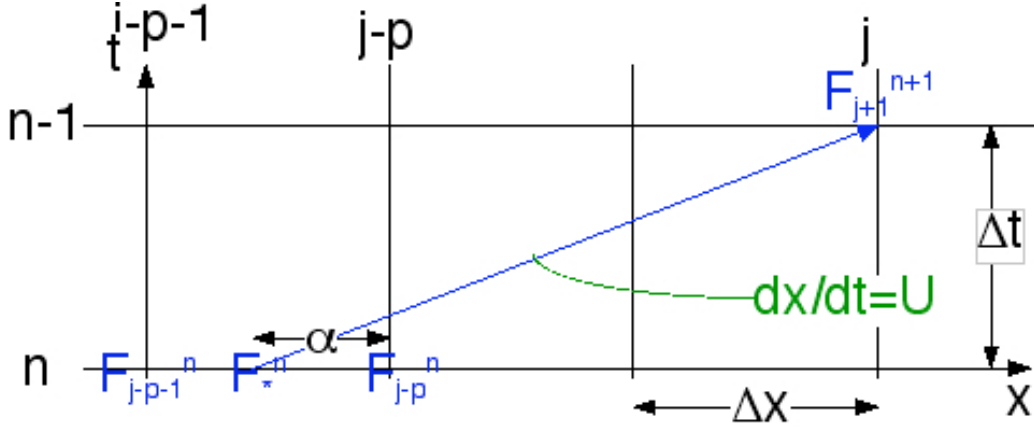


Figure 10.3: Schematic for the space interpolation.

b between mesh points, spatial interpolation is used.. The semi-Lagrangian algorithm for passive advection in one-dimension in summary is thus:

1. Solve Equation (10.9) iteratively for the displacement α_m for all mesh points x_m , using some initial guess (usually its value at the previous time step), and an interpolation formula.
2. Evaluate F at upstream points $x_m - 2\alpha_m$ at time $t^n - \Delta t$ using an interpolation formula.
3. Evaluate F at arrival points x_m at time $t^n + \Delta t$ using Equation (10.7).

10.3.2 Interpolation and Stability

Let us consider the linear advection equation

$$\frac{dF}{dt} = \frac{\partial F}{\partial t} + U \frac{\partial F}{\partial x} = 0$$

The distance traveled during the last interval by Δt an air or water parcel arriving at point x_j is $U\Delta t$, therefore it comes from a point

$$x_* = x_j - U\Delta t$$

If this point lies between grid points $j - p$ and $j - p - 1$, and we call α the fraction of grid length from point x_* to x_{j-p} point we have

$$U\Delta t = (p + \alpha)\Delta x$$

and using linear interpolation to find F_*^n we get

$$F_j^{n+1} = F_*^n = (1 - \alpha) F_{j-p}^n + \alpha F_{j-p-1}^n \quad (10.10)$$

Note that when $p = 0$, and $\alpha = 0$ then 10.10 becomes identical to the upstream differencing scheme.

We study the stability using the von Neumann method and, therefore, assume a solution of the form

$$F_j^n = F_0 \lambda^n e^{ijk\Delta x}$$

substituting we get

$$\lambda = \left[1 - \alpha \left(1 - e^{-ik\Delta x} \right) \right] e^{-ipk\Delta x}$$

and

$$|\lambda|^2 = 1 - 2\alpha(1-\alpha)[1 - \cos(k\Delta x)]$$

Therefore $|\lambda| \leq 1$ as long as $\alpha(1-\alpha) \geq 0$ or

$$0 \leq \alpha \leq 1$$

The scheme is, therefore, stable if the interpolation points are the two nearest ones to the departure point, but it is neutral only if $\alpha = 0$ or $\alpha = 1$, that is to say when no interpolation is needed. We will come to this point later.

We find that heavy damping occurs for the shortest wavelengths with a complete extinction when $k\Delta x = \pi$ (*wavelength* = $2\Delta x$) and when $\alpha = 1/2$. But the damping decreases as the wavelength increases. A strange feature of this scheme (peculiar to the case of constant wind) is that for a given α the phase errors and dissipation decrease as p increases. This happens because the departure point can be located precisely using only the wind at the arrival point.

A similar analysis to the above can be carried out for quadratic interpolation. Once again the scheme is absolutely stable provided F_*^n is computed by interpolation from the nearest three grid points. This scheme has less damping than the linear interpolation, but the phase representation is not improved. It is easy to show that when the departure point is within half a grid length from the grid point (i.e. $p = 0$), this scheme becomes identical to the Lax-Wendroff scheme.

These ideas can be extended to two-dimensional flow. It has been found that bi-quadratic interpolation is absolutely stable for constant flow (provided the nine grid points nearest the departure point are used for interpolation) and that the characteristics of this scheme are superior to those of a bilinear interpolation scheme.

Chapter 11

Spherical Harmonics

In modern atmospheric general circulation models (AGCMs), the horizontal spatial representation of scalar dynamic and thermodynamic fields is based on truncated series of spherical harmonic functions, the nature of the underlying two-dimensional horizontal physical grid, also known as a transform grid, is tightly coupled to the parameters of the spherical harmonic expansion itself.

11.1 Spectral methods

The numerical integration methods discussed thus far are based on the discrete representation of the data on a grid or mesh of points covering the space over which a prediction of the variables is desired. Then a local time derivatives of the quantities to be predicted are determined by expressing the horizontal and vertical advection terms, sources etc., in finite difference form. Finally, the time extrapolation is achieved by one of many possible algorithms, for example leapfrog. The finite difference technique has a number of associated problems such as truncation error, linear and non-linear instability. Despite these difficulties, the finite difference method has been the most practical method of producing forecasts numerically from the dynamical equations. There is another approach called the spectral method which avoids some of the difficulties cited previously, in particular, non-linear instability; however the method is less versatile and the required computations are comparatively time consuming. In a general sense, the mode of representation of data depends on the nature of the data and the shape of the region over which the representation is desired. An alternative to depiction on a mesh or grid of discrete points is a representation in the form of a series of orthogonal functions. This requires the determination of the coefficients of these functions, and the representation is said to be spectral representation or a series expansion in wave number space. When such functions are used, the space derivatives can be evaluated analytically, eliminating the need for approximating them with finite differences.

The operational ECMWF forecast model uses a spectral technique for its horizontal discretisation. Over the past decade or so this technique has become the most widely used method of integrating the governing equations of numerical weather prediction over hemispheric or global domains. Following the development of efficient transform methods by Eliassen et al. (1970) and Orszag (1970), and the construction and testing of multi-level primitive-equation models (e.g. Bourke, 1974; Hoskins and Simmons, 1975; Daley et al., 1976), spectral models were introduced for operational forecasting in Australia and Canada during 1976. The technique has been utilized operationally in the USA since 1980, in France since 1982, and in Japan and at ECMWF since

1983. The method is also extensively used by groups involved in climate modelling.

A comprehensive account of the technique has been given by Machenhauer (1979), and a further description of the method has been given by Jarraud and Simmons (1984). Reference should be made to these or other reviews for further discussion of most of the points covered below.

Associated Legendre polynomials

In mathematics, the associated Legendre functions are the canonical solutions of the general Legendre equation

$$\frac{d}{dx} \left[(1 - x^2) \frac{d}{dx} P_n^m(x) \right] = -n(n+1) P_n^m \quad (11.1)$$

where the indices n and m are referred to as the degree and order of the associated Legendre function respectively. The argument can be reparameterized in terms of angles, letting $x = \cos\theta$ and $\theta = \pi/2 - \varphi$, which is presented in Table 11.1 and in Figure 11.1.

Table 11.1: The associated Legendre polynomials P_n^m in $x = \cos\theta$, where $\theta = \pi/2 - \varphi$ is the colatitude.

	$m = 0$	$m = 1$	$m = 2$	$m = 3$
$n = 0$	1			
$n = 1$	$\cos\theta$	$-\sin\theta$		
$n = 2$	$\frac{1}{2}(3\cos^2\theta - 1)$	$-3\cos\theta\sin\theta$	$-3\sin^2\theta$	
$n = 3$	$\frac{1}{2}(5\cos^3\theta - 3\cos\theta)$	$-\frac{3}{2}(5\cos^2\theta - 1)\sin\theta$	$15\cos\theta\sin^2\theta$	$-15\sin^3\theta$

11.2 Spherical harmonics

Global atmospheric models use as basis functions spherical harmonics, which are the eigenfunctions of the Laplace equation on the sphere:

$$\nabla^2 Y_n^m = \frac{1}{a^2} \left[\frac{1}{\cos^2\varphi} \frac{\partial^2 Y_n^m}{\partial\lambda^2} + \frac{1}{\cos\varphi} \frac{\partial}{\partial\varphi} \left(\cos\varphi \frac{\partial Y_n^m}{\partial\varphi} \right) \right] = -\frac{n(n+1)}{a^2} Y_n^m \quad (11.2)$$

The spherical harmonics are products of Fourier series in longitude (λ) and associated Legendre polynomials in latitude (φ):

$$Y_n^m(\lambda, \varphi) = P_n^m(\mu) e^{im\lambda} \quad (11.3)$$

where $\mu = \sin\varphi$, m is the zonal wavenumber and n is the "total" wavenumber in spherical coordinates (as suggested by the Laplace equation).

In the usual application of the method, the basic prognostic variables are vorticity, divergence, temperature, a humidity variable, and the logarithm of surface pressure. Their horizontal representation is in terms of truncated series of spherical harmonic functions, whose variation is described by sines and cosines in the east-west

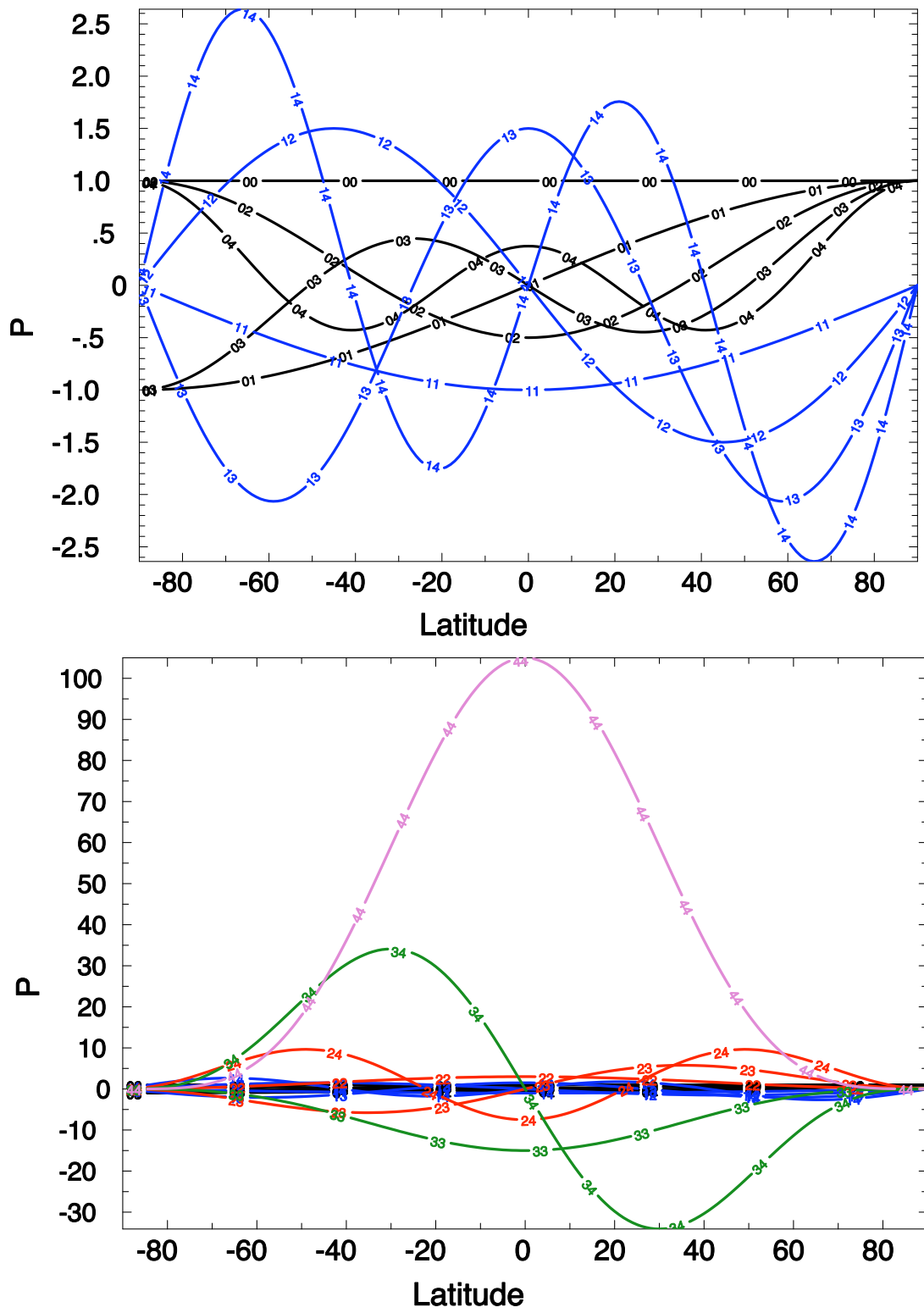


Figure 11.1: The first 15 associated Legendre polynomials P_n^m . The first index on the curves indicate the order of the polynomial and the second index the degree. The top figure shows $m = 1, 2$ for $n = 1, 2, 3, 4$. The bottom figure shows $m = 1, 2, 3, 4$ for $n = 1, 2, 3, 4$. Each colour correspond to a separate order (m) of the polynomial P_n^m .

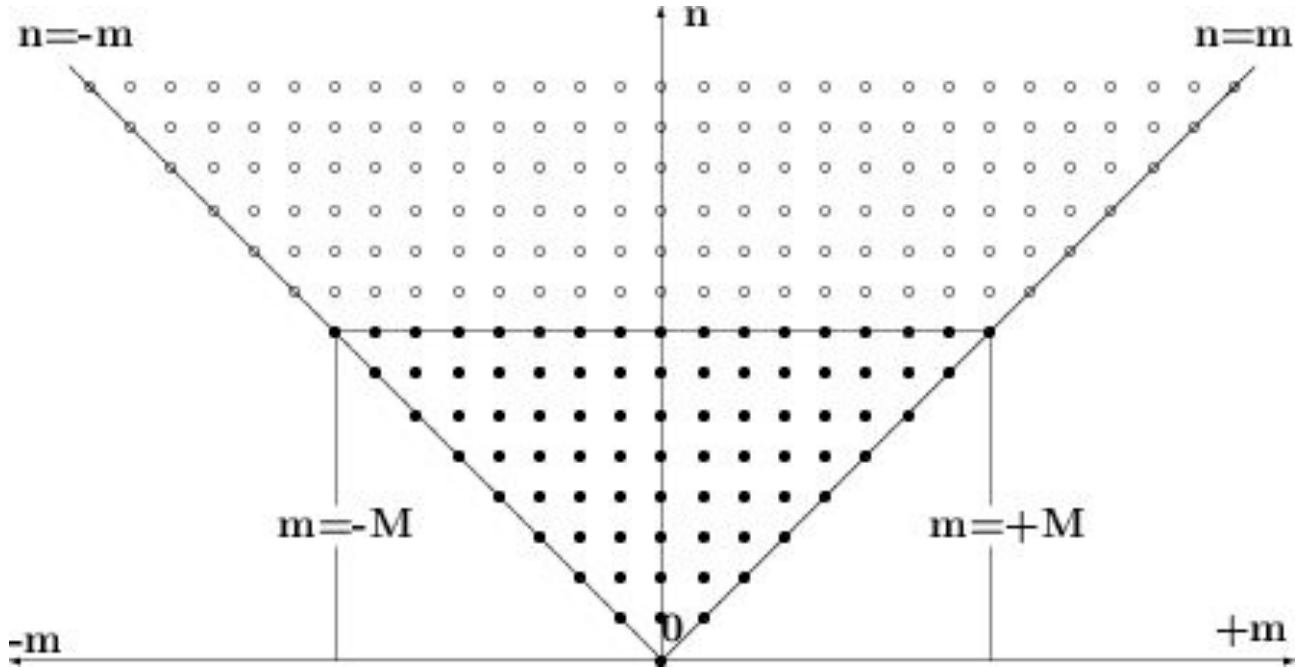


Figure 11.2: The triangular truncation in the (m, n) wavenumber space prescribes a triangular region of spherical harmonic modes indicated by the filled squares. Modes outside of this triangle are set to \circ (open circles).

and by associated Legendre functions in the north-south. The horizontal variation of a variable U is thus given by

$$U(\lambda, \varphi, t) = \sum_{n=0}^N \sum_{m=-n}^n U_n^m(t) Y_n^m(\lambda, \varphi) \quad (11.4)$$

the spatial resolution is uniform throughout the sphere. This has a major advantage over finite differences based on a latitude-longitude grid, where the convergence of the meridians at the poles requires very small time steps. Although there are solutions for this "pole problem" for finite differences, the natural approach to solve the pole problem for global models is the use of spherical harmonics.

It is becoming increasingly common for the so-called "triangular" truncation of the expansion to be used (Figure 11.2). This truncation is defined by $M = N = \text{constant}$, and gives uniform resolution over the sphere. The symbol "TN" is the usual way of defining the resolution of such a truncation; being the smallest total wave number retained in the expansion. The smallest resolved half-wavelength in any particular direction is then $\pi a/N$ (320 km for T63, 190 km for T106), although the corresponding lateral variation is of larger scale.

Derivatives of a spectral represented variable U are known analytically

$$\frac{\partial U}{\partial \lambda} = \sum_{n=0}^N \sum_{m=-n}^n i m U_n^m Y_n^m$$

and

$$\frac{\partial U}{\partial \varphi} = \sum_{n=0}^N \sum_{m=-n}^n U_n^m \frac{\partial P_n^m}{\partial \varphi} e^{im\lambda}$$

11.3 The spectral transform method

In a spectral model, a variable, $\xi(\lambda, \phi)$, is represented by a truncated series of spherical harmonic functions. This can be expressed as

$$\xi_n^m = \sum_{j=1}^J \xi^m(\phi_j) P_n^m(\phi_j), \quad (11.5)$$

where j is the latitudinal index, $\xi^m(\phi_j)$ is obtained by a fast fourier transform of $\xi(\lambda, \phi)$ and $P_n^m(\phi_j)$ is the associated Legendre functions.

The grid point values are obtained by the inverse transform

$$\xi^m(\phi) = \sum_{n=|m|}^{N(m)} \xi_n^m P_n^m(\phi), \quad (11.6)$$

followed by an inverse fast fourier transform to obtain $\xi(\lambda, \phi)$.

In a spectral model, the explicit time steps and horizontal gradients are performed in spectral space. The tendencies of the equations are however evaluated in grid point space. One benefit when representing the variables in spectral space is that horizontal derivatives are continuously represented, i.e. no finite differencing is needed to evaluate gradients. The methods used to perform the spherical harmonic transforms are however well out of the scope of this project. We have therefore chosen to use an already existing library to carry out the spectral transforms.

11.4 Application to the shallow water equations on a sphere

The momentum and mass continuity equations governing the motion of a rotating, homogenous, incompressible and hydrostatic fluid can be written on vector form as

$$\frac{d\mathbf{V}}{dt} = -f\mathbf{k} \times \mathbf{V} - \nabla\Phi + \nu\nabla^2\mathbf{V}, \quad (11.7)$$

$$\frac{d\Phi}{dt} = -\Phi\nabla \cdot \mathbf{V}, \quad (11.8)$$

where $\mathbf{V} = (u, v)$ is the horizontal velocity vector, Φ is the geopotential height, f is the coriolis parameter and ν is the horizontal diffusion coefficient. Furthermore,

$$\frac{d}{dt} = \frac{\partial}{\partial t} + \mathbf{V} \cdot \nabla, \quad (11.9)$$

and the ∇ operator is defined in spherical coordinates as

$$\nabla = \frac{1}{a \cos \phi} \frac{\partial}{\partial \lambda} + \frac{1}{a} \frac{\partial}{\partial \phi}, \quad (11.10)$$

where a is the earth radius, λ is the longitude coordinate and ϕ is the latitude coordinate.

The above equations describe the shallow-water equations in the u, v, Φ system. In the model, we use another form of these equations. By introducing the relative vorticity ζ and horizontal divergence δ , the equations can be transformed into the the ζ, δ, Φ system. We do not derive these equations here since it is relatively straightforward.

By introducing

$$\xi = \mathbf{k} \cdot (\nabla \times \mathbf{V}), \quad (11.11)$$

and

$$\delta = \nabla \cdot \mathbf{V}, \quad (11.12)$$

one can obtain the following set of equations (with $\mu = \sin \phi$)

$$\frac{\partial \eta}{\partial t} = -\frac{1}{a(1-\mu^2)} \frac{\partial}{\partial \lambda} U\eta + \frac{1}{a} \frac{\partial}{\partial \mu} V\eta, \quad (11.13)$$

$$\frac{\partial \delta}{\partial t} = \frac{1}{a(1-\mu^2)} \frac{\partial}{\partial \lambda} U\eta - \frac{1}{a} \frac{\partial}{\partial \mu} V\eta + \nabla^2 \left(\Phi + \frac{U^2 + V^2}{2(1-\mu^2)} \right), \quad (11.14)$$

$$\frac{\partial \Phi}{\partial t} = -\frac{1}{a(1-\mu^2)} \frac{\partial}{\partial \lambda} U\Phi + \frac{1}{a} \frac{\partial}{\partial \mu} V\Phi, \quad (11.15)$$

where now $\eta = \xi + f$ (absolute vorticity including earth rotation) and $(U, V) = (u, v) \cos \phi$.

Chapter 12

Different types of Coordinates

12.1 Fixed height or depth coordinates

A simple example of a vertical discretisation is the one of the continuity equation, which is used in many OGCMs (Ocean General Circulation Model), which uses the B-grid and fixed depth levels, as in Figure 12.1.

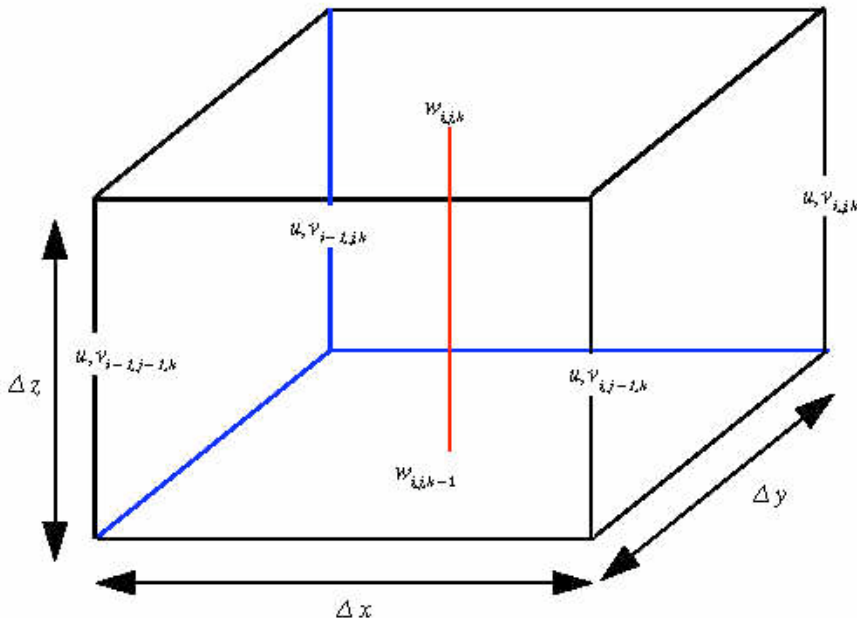


Figure 12.1: *Finite difference box for B-grid and fixed depth level coordinates.*

The continuity equation then becomes:

$$\frac{\partial u}{\partial x} + \frac{\partial v}{\partial y} + \frac{\partial w}{\partial z} = 0 \quad (12.1)$$

can be discretised into

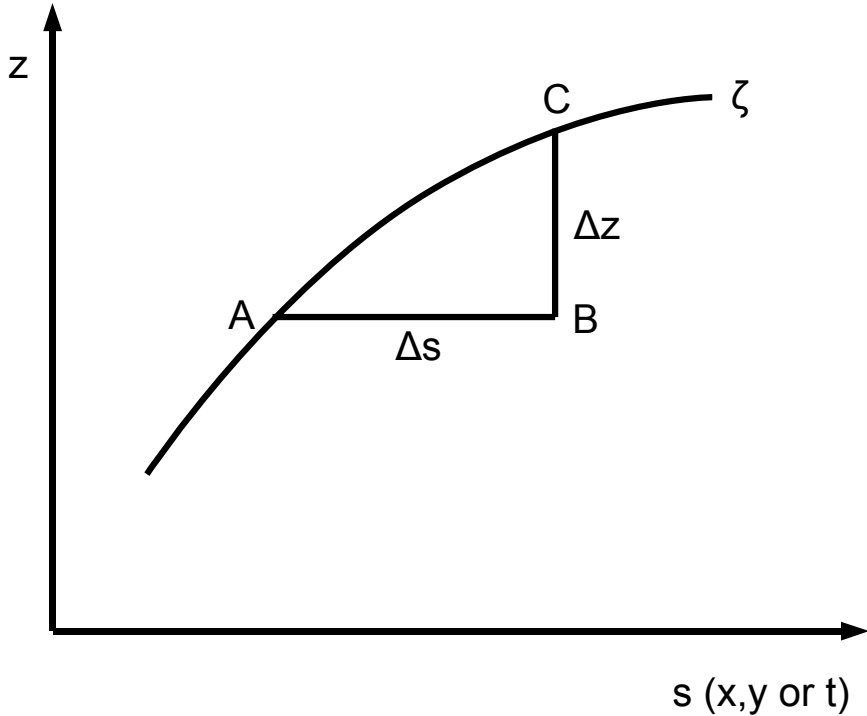


Figure 12.2: Schematic showing the vertical coordinate transformation.

$$w_{i,j,k} = w_{i,j,k-1} - \Delta z \left[\frac{(u_{i,j,k} + u_{i,j-1,k}) - (u_{i-1,j,k} + u_{i-1,j-1,k})}{2\Delta x} + \frac{(v_{i,j,k} + v_{i-1,j,k}) - (v_{i,j-1,k} + v_{i-1,j-1,k})}{2\Delta y} \right] \quad (12.2)$$

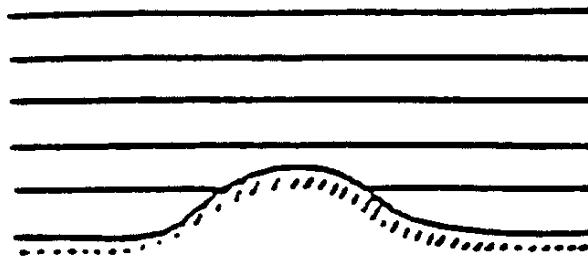
and is integrated from the bottom and upwards with the boundary condition $w=0$ where k increases with depth. Equation (12.2) can be explained by that the sum of all the volume fluxes in or out of the grid box is zero.

12.2 Other vertical coordinates

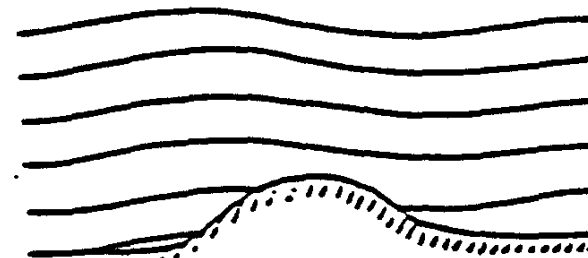
Instead of depth/height as vertical coordinate in our system of equations it is possible to use other quantities. The density varies with latitude and height/depth which make the equations sometimes less easy to use with than an alternative system which uses other quantities such as pressure, sigma or isentropic for the atmosphere and density or sigma for the ocean as the vertical coordinate. These coordinates can be more useful for numerical techniques in solving the complete equations of motion. We can derive a system of equations for a generalised vertical coordinate which is assumed to be related to the height/depth by a single-valued monotonic function. When we transform the vertical coordinate a variable $u(x, y, z, t)$ becomes $a(x, y, \zeta(x, y, z, t), t)$. The horizontal coordinates remain the same. Let s represent x, y or t . From Figure 12.2 we see that

$$\frac{C - A}{\Delta s} = \frac{B - A}{\Delta s} + \frac{C - B}{\Delta z} \frac{\Delta z}{\Delta s} \quad (12.3)$$

z -coordinates



p -coordinates



σ -coordinates

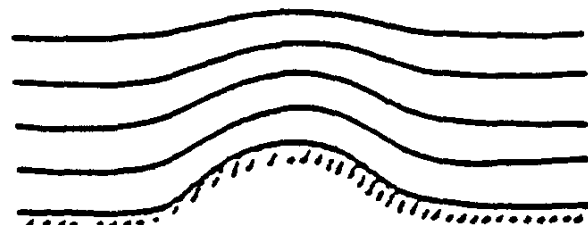


Figure 12.3: Schematic illustration of height, pressure and sigma coordinates in the atmosphere..

so that

$$\left(\frac{\partial a}{\partial s} \right)_{\zeta} = \left(\frac{\partial a}{\partial s} \right)_z + \left(\frac{\partial a}{\partial z} \right)_s \left(\frac{\partial z}{\partial s} \right)_{\zeta} \quad (12.4)$$

where

$$\frac{\partial a}{\partial \zeta} = \frac{\partial a}{\partial z} \frac{\partial z}{\partial \zeta} \quad (12.5)$$

or

$$\frac{\partial a}{\partial z} = \frac{\partial a}{\partial \zeta} \frac{\partial \zeta}{\partial z} \quad (12.6)$$

Substituting Eq. 12.6 in Eq. 12.4, we obtain

$$\left(\frac{\partial a}{\partial s} \right)_{\zeta} = \left(\frac{\partial a}{\partial s} \right)_z + \frac{\partial a}{\partial \zeta} \frac{\partial \zeta}{\partial z} \left(\frac{\partial z}{\partial s} \right)_{\zeta} \quad (12.7)$$

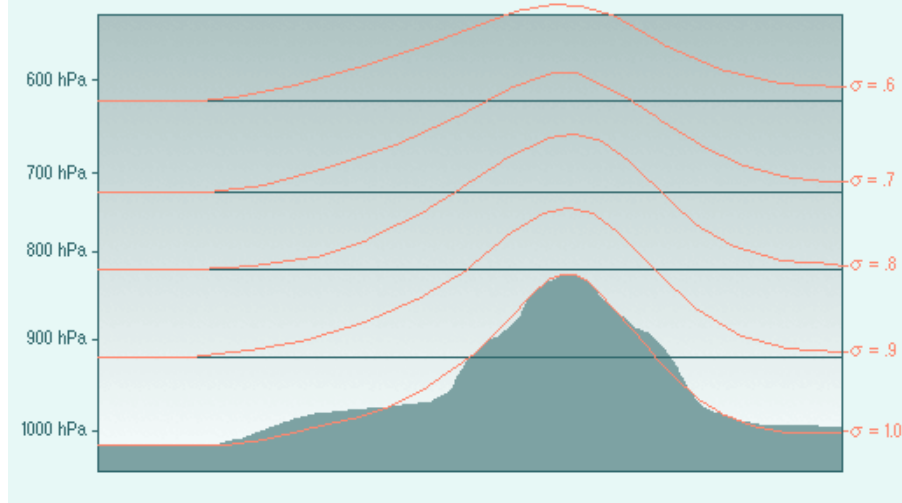


Figure 12.4: Atmospheric sigma coordinates.

From this relationship, if $s = x, y$, we can get an equation for a horizontal gradient of the scalar a in ζ coordinates:

$$\nabla_\zeta a = \nabla_z a + \frac{\partial a}{\partial \zeta} \frac{\partial \zeta}{\partial z} \nabla_\zeta z \quad (12.8)$$

and for the horizontal divergence of a vector \mathbf{V} :

$$\nabla_\zeta \cdot \mathbf{V} = \nabla_z \cdot \mathbf{V} + \frac{\partial \mathbf{V}}{\partial \zeta} \cdot \frac{\partial \zeta}{\partial z} \nabla_\zeta z \quad (12.9)$$

The total derivative of $a(x, y, \zeta, t)$ becomes

$$\frac{da}{dt} = \left(\frac{\partial a}{\partial t} \right)_\zeta + \mathbf{V} \cdot \nabla_\zeta a + \dot{\zeta} \frac{\partial a}{\partial \zeta} \quad (12.10)$$

12.2.1 Pressure coordinates

Pressure or isobaric coordinates can be used in atmosphere although not very often anymore in atmospheric GCMs. In pressure coordinates where $\partial p / \partial \zeta \equiv 1$, the total derivative (Eq. 12.10) is given by

$$\frac{da}{dt} = \frac{\partial a}{\partial t} + \mathbf{V} \cdot \nabla a + \omega \frac{\partial a}{\partial p} \quad (12.11)$$

where the vertical velocity in pressure coordinates is $\omega \equiv dp/dt$. The continuity equation 12.1 can now be written as

$$\nabla_p \cdot \mathbf{V} + \frac{\partial \omega}{\partial p} = 0 \quad (12.12)$$

Most Atmospheric GCMs today use however terrain-following vertical coordinates, which is described beneath.

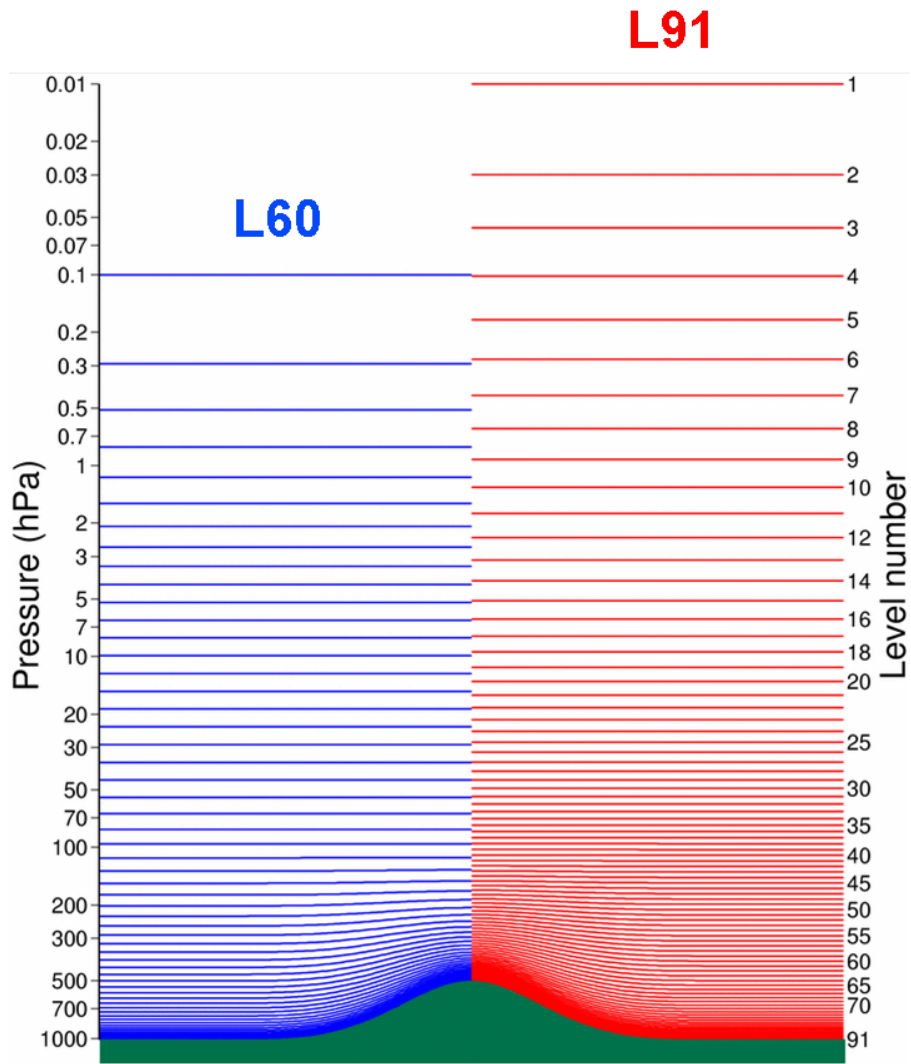


Figure 12.5: Two different vertical resolution of the hybrid-coordinate model at the ECMWF (The European Centre for Medium-Range Weather Forecasts).

12.2.2 Sigma coordinates

The sigma coordinate system defines the base at the model's ground level. The surfaces in the sigma coordinate system follow the model terrain and are steeply sloped in the regions where terrain itself is steeply sloped. the sigma coordinate system defines the vertical position of a point in the atmosphere as a ratio of the pressure difference between that point and the top of the domain to that of the pressure difference between a fundamental base below the point and the top of the domain. Because it is pressure based and normalised, it is easy to mathematically cast governing equations of the atmosphere into a relatively simple form. The sigma coordinate is hence $\sigma = p/p_S$ where $p_S(x, y, z, t)$ is the pressure at the surface of the Earth. The Boundary values are hence $\sigma = 0$ at the top of the atmosphere where $p = 0$ and $\sigma = 1$ at the surface of the Earth. The relationship between pressure and sigma coordinates is presented in Figure 12.4.

```

=====
TOP OF MODEL ATMOSPHERE ===== i = 1      a (Pa)      b (Pa Pa-1)
----- model level ----- (data) ----- j = 1      a = 0.00000   b = 0.00000
=====
interface ===== i = 2      a = 10.00000   b = 0.00000
----- model level ----- (data) ----- j = 2      a = 20.00000   b = 0.00000
=====
interface ===== i = 3      a = 28.21708   b = 0.00000
                                         a = 38.42530   b = 0.00000

----- model level ----- (data) ----- j - 1
=====
interface ===== i - 1
----- model level ----- (data) ----- j
=====
interface ===== i
----- model level ----- (data) ----- j + 1

=====
interface ===== i = 59      a = 7.36774   b = 0.99402
----- model level ----- (data) ----- j = 59      a = 3.68387   b = 0.99582
=====
interface ===== i = 60      a = 0.00000   b = 0.99763
----- model level ----- (data) ----- j = 60 = J      a = 0.00000   b = 0.99881
=====
MODEL SURFACE ===== i = 61 = I      a = 0.00000   b = 1.00000

```

Figure 12.6: Model levels for the 60 layers presented in Figure 12.5, with a_k and $a_{k+1/2}$ at interfaces are highlighted in red.

12.2.3 Hybrid coordinates

The hybrid coordinate system has the properties of sigma coordinates in the lower atmosphere and pressure in the stratosphere.

Following Simmons and Burridge (1981) the atmosphere is divided into $NLEV$ layers, which are defined by the pressures at the interfaces between them and these pressures are given by

$$p_{k+1/2} = a_{k+1/2} + b_{k+1/2} p_S \quad (12.13)$$

for $k = 0, 1, \dots, NLEV$, with $k = 0$ at the top of the atmosphere and $k = NLEV$ at the Earth's surface. The $a_{k+1/2}$ and $b_{k+1/2}$ are constants, whose values effectively define the vertical coordinate and p_S is the surface pressure. The dependent variables, which are the zonal wind (u), the meridional wind (v), the temperature (T) and the specific humidity (q) are defined in the middle of the layers, where the pressure is defined by

$$p_k = \frac{1}{2}(p_{k-1/2} + p_{k+1/2}) \quad (12.14)$$

for $k = 1, 2, \dots, NLEV$. The vertical coordinate is $\eta = \eta(p, p_S)$ and has the boundary value $\eta(0, p_S) = 0$ at the top of the atmosphere and $\eta(p_S, p_S) = 1$ at the Earth's surface. Two different vertical resolutions with hybrid

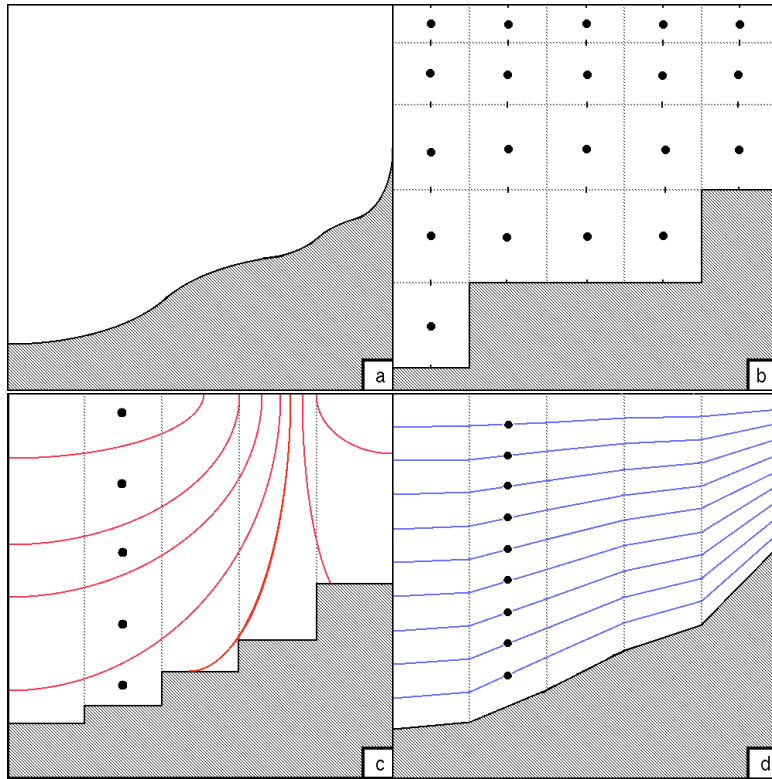


Figure 12.7: a) Ocean model vertical coordinates. The real topography, b) depth level coordinates, c) density coordinates, d) sigma coordinates.

coordinates are presented in Figure 12.5.

12.2.4 Ocean GCM coordinates

The three most common vertical coordinate systems in the ocean circulation models are presented in Figure 12.7.

12.3 Finite elements

In designing a numerical weather prediction model, one of the most fundamental aspects is the choice of discretisation technique in each of the spatial dimensions. In the vertical, by far the most popular choice is the finite difference method; while in the horizontal, both finite-difference and (especially for global models) spectral methods are widely employed. A third possibility is the finite element method.

The essence of the finite element method can be seen by considering various ways of representing a function $u(x)$ on an interval $a \leq x \leq b$. In the finite-difference method the function is defined only on a set of grid points; i.e. $u(x_j)$ is defined for a set of x_j , but there is no explicit information about how the function behaves between the grid points. In the spectral method, on the other hand, the function is defined in terms of a finite

set of basis functions:

$$u(x) = \sum_{k=0}^N a_k e_k \quad (12.15)$$

where the basis functions $e_k(x)$ are global (e.g. Fourier series, or spherical harmonics for two-dimensional functions on the surface of a sphere), and the a_k are the spectral coefficients. Equation (12.15) defines $u(x)$ everywhere on the interval, and the representation is independent of any set of grid points.

In the finite-element method, the function is again in terms of a finite set of basis functions:

$$u(x) = \sum_{k=0}^N a_k e_k$$

but this time basis functions $e_k(x)$ are local, i.e. they are non-zero only on a small-sub-interval. As in the spectral method, the a_k are the coefficients of the basis functions, and $u(x)$ is defined everywhere; but as in the finite-difference method, there is an underlying mesh of grid points (nodes) involved in the representation.

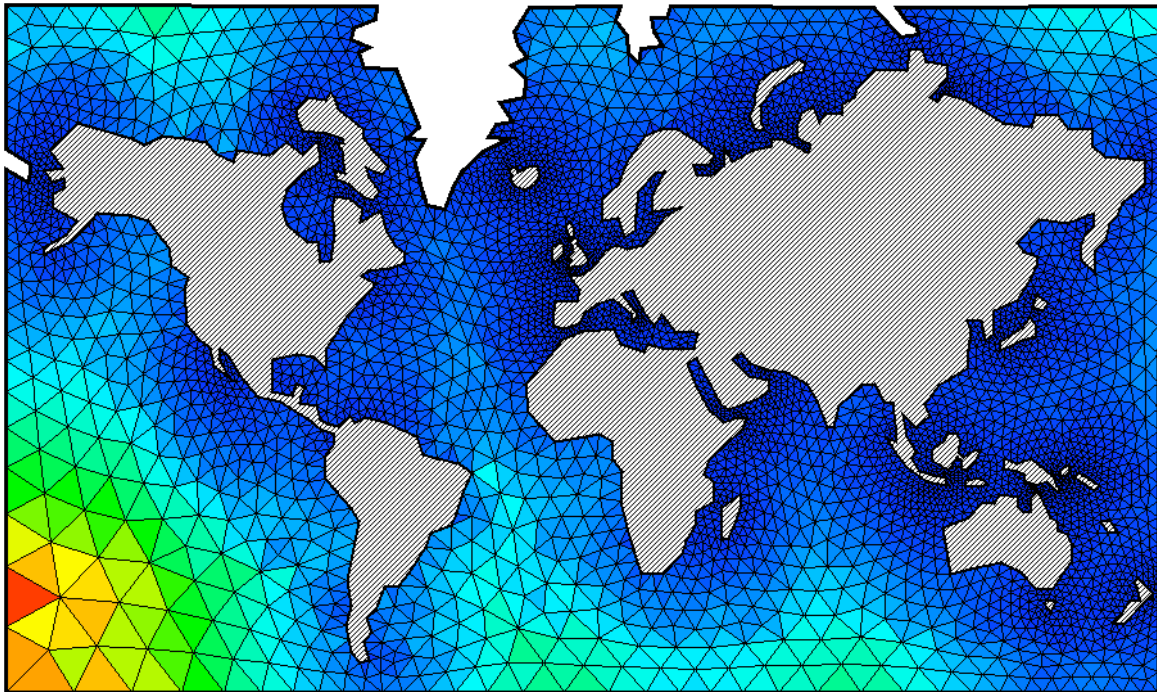


Figure 12.8: Finite elements for an ocean general circulation model

12.4 Results from Ocean and Atmospheric General Circulation Models

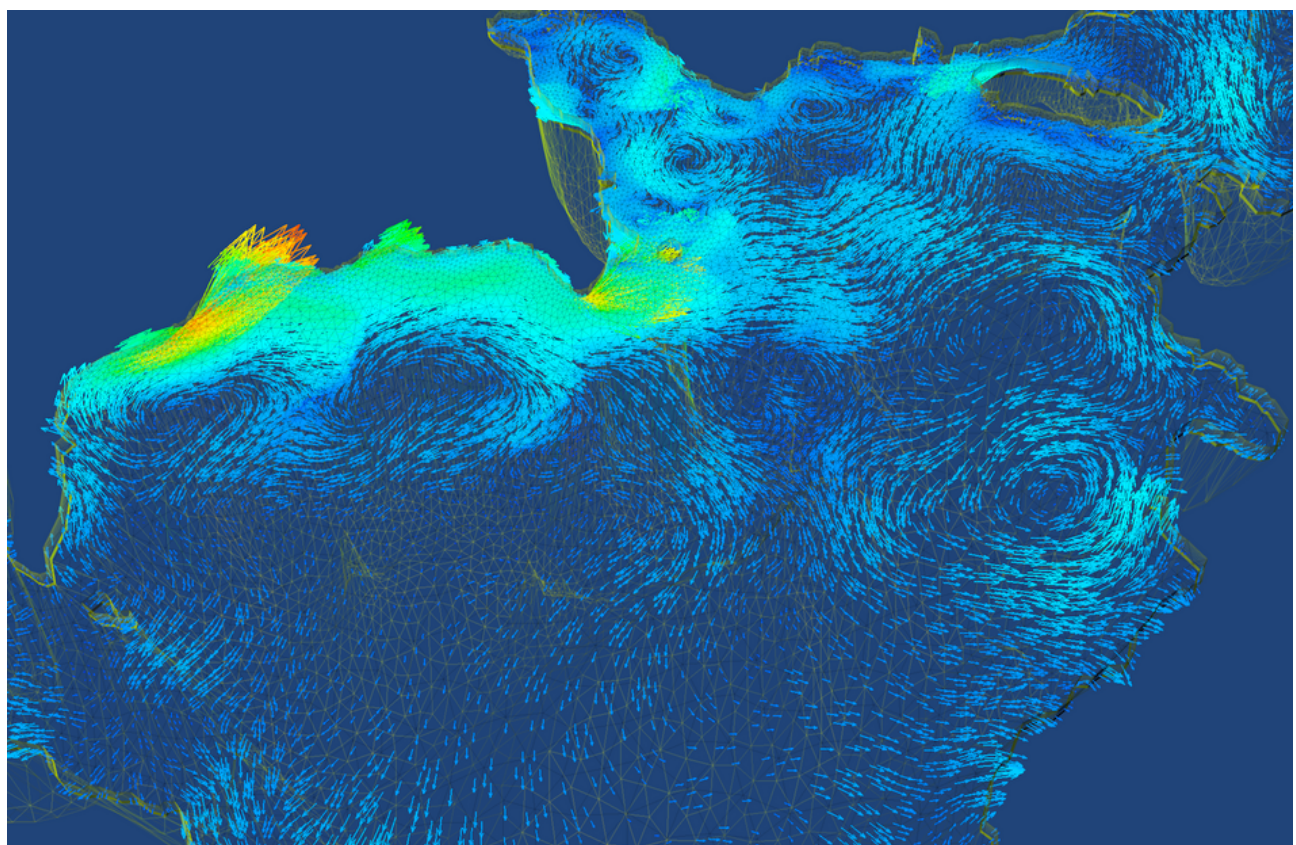


Figure 12.9: The ICOM finite element model with time and space adaptive mesh.

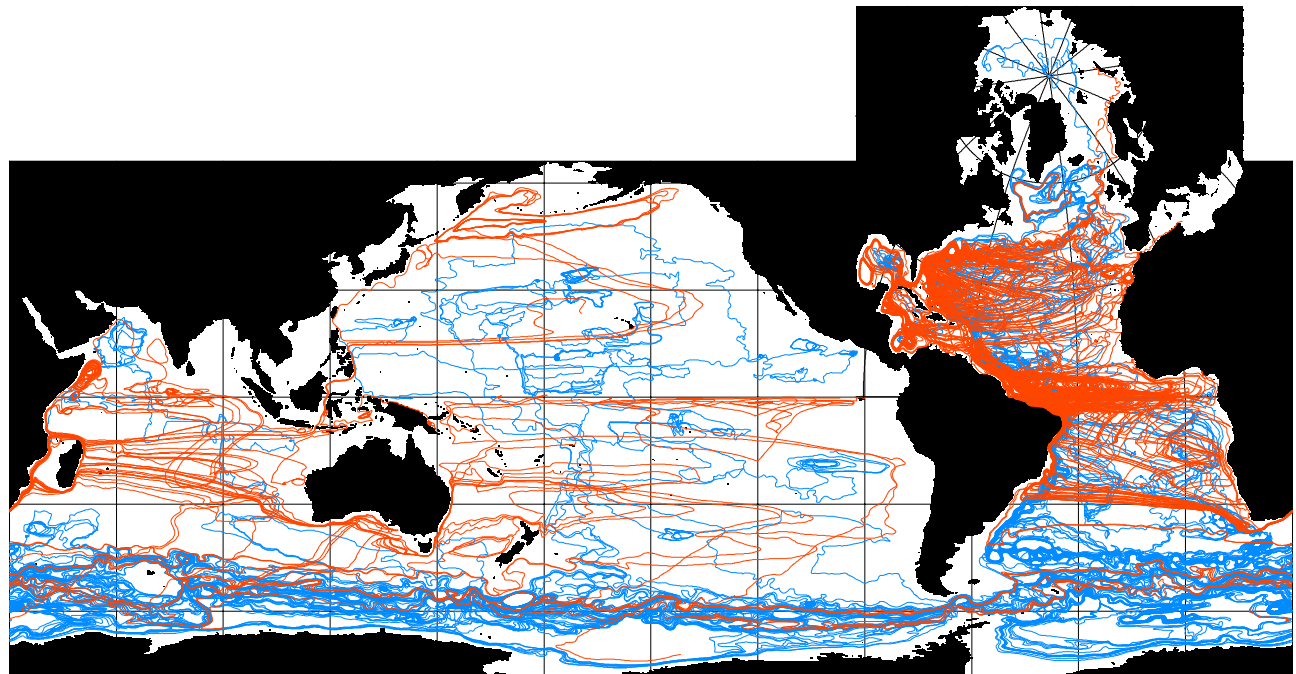


Figure 12.10: Lagrangian trajectories of the World Thermohaline Conveyor Belt by Döös (2000).

EC-Earth atmosphere model (IFS) - Meridional overturning analysis

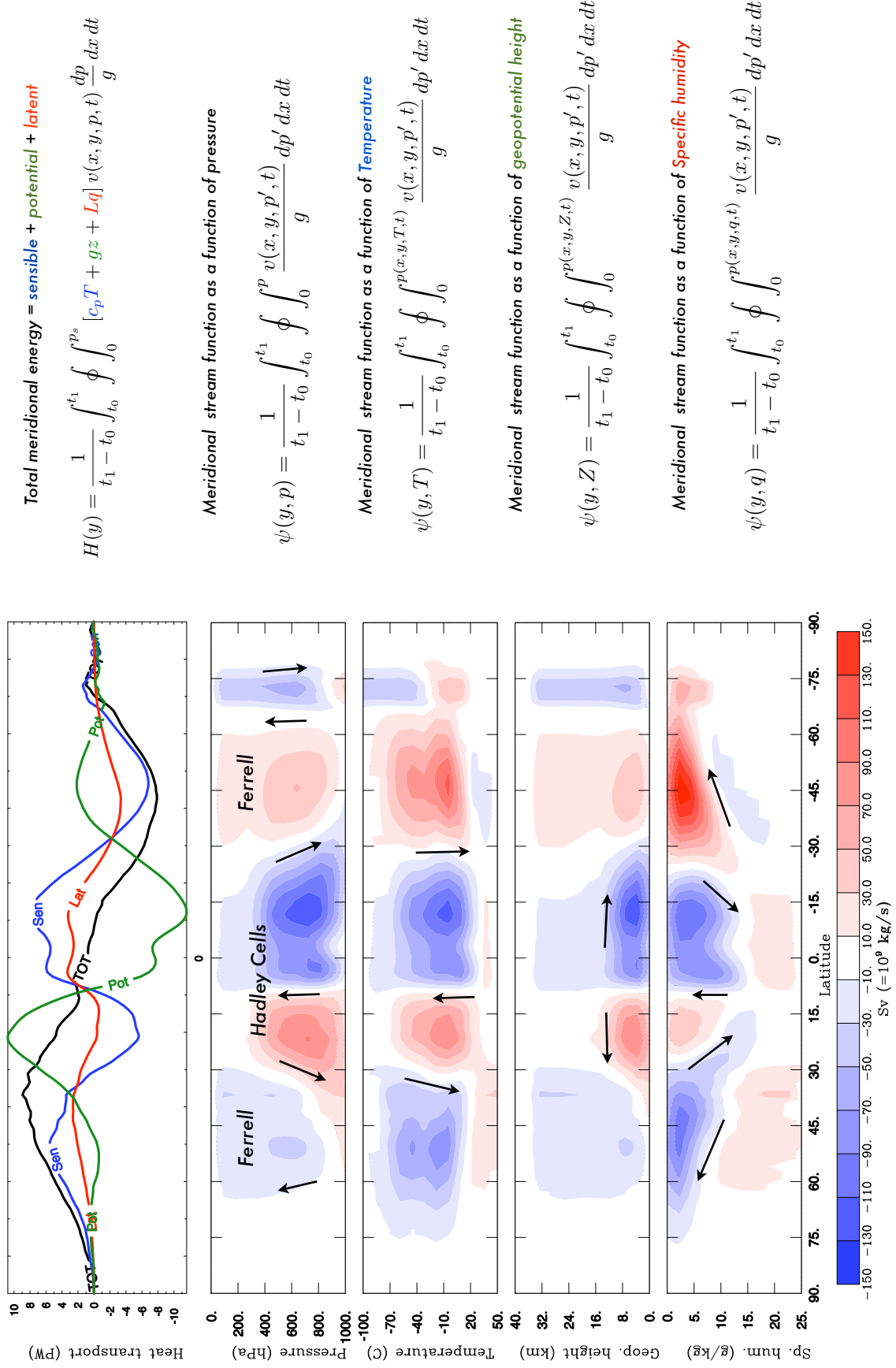


Figure 12.11: Meridional energy transport and overturning stream functions in the EC-earth (IFS) atmosphere.

Chapter 13

Practical computer exercises

13.1 Purpose

The aims of these exercises are to concretise the theory presented in the lectures and to give a better understanding of basic numerical methods. The leapfrog scheme, Euler forward scheme and upwind scheme will be studied applied on the advection equation, diffusion equation and shallow-water equations.

Each student should write a lab report. The numerical experiments should be documented with figures of u (and, for the shallow-water equations, of h) as a function of x for appropriate fixed values of t . In some cases 3D plots with u as a function of x, t are also useful. It should be clear what the figures show. The results should be analysed and commented.

13.2 Theory

a compact form

$$\frac{\partial u}{\partial t} - fv = -g \frac{\partial h}{\partial x} + A_u$$

The solution interval is in all cases $0 \leq x < 1$, with the periodic boundary condition $u(0, t) = u(1, t)$. The relative error is defined as $\|u - v\|/\|v\|$, where $v(x, t)$ is the analytic solution, and the norm is defined by

$$\|f\| = \left(\Delta x \sum_{i=1}^I |f_i|^2 \right)^{1/2}.$$

The advection equation is

$$\frac{\partial u}{\partial t} + c \frac{\partial u}{\partial x} = 0,$$

the diffusion equation is

$$\frac{\partial u}{\partial t} - \mu \frac{\partial^2 u}{\partial x^2} = 0$$

and the shallow-water equations in the one-dimensional case, are

$$\begin{cases} \frac{\partial u}{\partial t} = -g \frac{\partial h}{\partial x}, \\ \frac{\partial h}{\partial t} = -H \frac{\partial u}{\partial x}. \end{cases}$$

13.3 Tools

We will use fortran or MATLAB to solve the numerical exercises. It is convenient that everyone uses the same notation. Therefore use this variable convention.

u	velocity in x-direction
v	velocity in y-direction
h	the height of the field
i	index in x-direction
j	index in y-direction
n	index in time
nx	number of points in x-direction
ny	number of points in y-direction
nt	number of time steps
dx	grid spacing in x-direction
dy	grid spacing in y-direction
dt	length of time step
g	gravity
H	mean depth

A simple way of programming the advection equation discretized on a leapfrog scheme in MATLAB is as follows.

```

i      = 2:nx-1;
ip1   = i+1;
im1   = i-1;

for n = 2:nt-1
    u(i,n+1) = u(i,n-1) - cfl * (u(ip1,n) - u(im1,n));
end

```

Notice that the boundary points are not included, these has to be iterated separately in the following way.

```

for n = 2:nt-1
    u(1,n+1) = u(1,n-1) - cfl * (u(2,n) - u(nx-1,n));
    u(nx,n+1) = u(nx,n-1) - cfl * (u(2,n) - u(nx-1,n));
end

```

13.4 Theoretical exercises

Exercise 1 - Leapfrog

Study the leapfrog scheme for the advection equation.

1. Give the leapfrog scheme (centred scheme with 2nd order accuracy in space and time).
2. Derive the stability condition.
3. Discuss the computational mode and how it can be avoided.

Exercise 2 - Upwind

Study the upwind scheme for the advection equation.

1. Give the upwind scheme (uncentred scheme with 1st order accuracy in space and time).
2. Derive the stability condition.

Exercise 3 - Euler forward

Study the Euler forward scheme for the diffusion equation.

1. Derive the stability criterion of the Euler forward scheme for the diffusion equation:

$$\frac{u_j^{n+1} - u_j^n}{\Delta t} = \mu \frac{u_{j+1}^n - 2u_j^n + u_{j-1}^n}{(\Delta x)^2}.$$

2. Discuss how the time step should be chosen. Why is it good to choose a smaller time step than that given by the stability criterion? Hint: Study how the amplification factor depends on the wavelength, especially the highest frequencies.

13.5 Experimental exercises

Exercise 4 - Advection

Study the advection equation using a simple numerical model. Write a program that can solve the advection equation with two different schemes: the leapfrog scheme and the upwind scheme.

1. Run the program with the resolution $\Delta x = 0.1$ and the CFL-numbers 0.9, 1.0 and 1.1. Use a cosine wave as initial condition:

$$u(x, t = 0) = \cos(2\pi x).$$

Solve the problem both with the leapfrog scheme and the upwind scheme, initialising the leapfrog scheme with a single Euler forward step. Plot the results obtained with both schemes and the analytic solution in the same figure. Comment on both the phase error and the amplitude error. Also show how the relative error develops in time.

2. Run the program with the resolution $\Delta x = 0.02$ and the CFL-number 0.9. Use a cosine pulse as initial condition:

$$u(x, t = 0) = \begin{cases} \frac{1}{2} + \frac{1}{2} \cos [10\pi(x - 0.5)], & \text{for } 0.4 \leq x \leq 0.6 \\ 0, & \text{elsewhere} \end{cases}$$

Solve the problem both with the leapfrog scheme and the upwind scheme. Initialise the leapfrog scheme both with a single Euler forward step, and with a constant step: $u_j^1 = u_j^0$. Try to identify the computational mode. (For this, 3D plots of u as a function of x, t are useful.)

Exercise 5 - Diffusion

Study the diffusion equation using a simple numerical model. Write a program that can solve the diffusion equation using the Euler forward scheme. Set $\Delta x = 0.05$ and try with three different time steps: the critical value $(\Delta x)^2/2\mu$ permitted by the stability criterion, a value slightly larger than the critical one, and half the critical value. Also run the program with two different initial conditions:

- rectangular pulse:

$$u_i^1 = \begin{cases} 1, & \text{for } 0 \leq x \leq 0.5 \\ 0, & \text{for } 0.5 < x < 1 \end{cases}$$

- spike: $u = 1$ in a single grid point at $x = 0.5$, and $u = 0$ in all other grid points.

Exercise 6 - Shallow-Water model

Study one-dimensional gravity waves. Gravity waves can be described by the shallow-water equations.

1. Write a program solving these equations with the leapfrog scheme on an unstaggered grid. Set $H = g = 1$. Run the program with $\Delta x = 0.025$ and the CFL-number 0.9. (The CFL-number is defined as $c \cdot \Delta t / \Delta x$, where $c = (gH)^{1/2}$.) Initialise the leapfrog scheme with a single Euler forward step, and use the following initial conditions which describes a travelling pulse:

$$\begin{aligned} h(x, t = 0) &= \begin{cases} \frac{1}{2} + \frac{1}{2} \cos [10\pi(x - 0.5)], & \text{for } 0.4 \leq x \leq 0.6 \\ 0, & \text{elsewhere} \end{cases} \\ u(x, t = 0) &= h(x, t = 0) \end{aligned}$$

Try to interpret the results physically.

2. Rewrite the program using an staggered grid, with h and u defined in different points. Run the program and try to find the stability limit for the time step. Then choose the time step 10 % smaller than the stability limit, and use the travelling pulse as initial condition. Use *both* the resolution of the previous subexercise and the *half* resolution. Compare the accuracy of the solution with the previous solution obtained on an A-grid. Discuss the difference between the two results and the result from the previous subexercise. Note that Δx is the distance between two height points (and also two velocity points).

13.6 Shallow Water Exercise by Anders Engström

The aim of this exercise is to solve the linearized shallow water equations for some classical atmospheric and oceanographic problems.

13.7 Theory

The linearized shallow water equations in two dimensions including rotation and physical parameterisations are:

$$\frac{\partial u}{\partial t} = +fv - g \frac{\partial h}{\partial x} + F_u \quad (13.1)$$

$$\frac{\partial v}{\partial t} = -fu - g \frac{\partial h}{\partial y} + F_v \quad (13.2)$$

$$\frac{\partial h}{\partial t} = -H \left(\frac{\partial u}{\partial x} + \frac{\partial v}{\partial y} \right) + F_h \quad (13.3)$$

Physical parameterisations, F_u , F_v and F_h may for instance be horizontal diffusion and/or drag/stress forcings. In the current exercise realistic values of g , H and f should be used in order to gain understanding of atmospheric and oceanographic problems.

13.8 Tools

The exercises are done using Matlab. Since the calculations needed to perform the exercise are quite demanding it is strongly recommended to use vector/matrix notation in your m-files. Use a single Euler forward step the first timestep and the use leap-frog. It is also highly recommended that you read chapter 8 in the *Numerical Methods in Meteorology and Oceanography* compendium. Also, for the two-dimensional shallow-water model, try to avoid growing variables inside loops since this will make your computer run out of memory fast.

13.9 Report

In order to complete the shallow water exercise each student should write a *concise* report. This report should live up to general MISU demands. Include only selected figures and illustrations that are relevant. Long mathematical derivations and parts of the code are not welcome in the report. However, equations and references needed to understand the report should be included.

13.10 Exercises

13.10.1 1D-model

Here we develop a 1D shallow water model that includes rotation (coriolis) and diffusion on a staggered grid.

1. Write the code for the model. To do this you need to add an extra velocity variable to the 1D model developed earlier in the course and, if not already done so, rewrite your schemes on staggered grid. Use closed boundary conditions.
2. Run the model without rotation ($f = 0$) and with the following initial conditions:

$$u(x, 0) = 0 \quad (13.4)$$

$$v(x, 0) = 0 \quad (13.5)$$

$$h(x, 0) = h_0 e^{-(x/L_W)^2}, \quad (13.6)$$

where $-L/2 \leq x \leq L/2$ and $L_W \approx L/7$. Describe your results. What is the appropriate domain size L ? Motivate your choice based on the statements in Section 13.7.

3. Study Rossbys adjustment to geostrophic balance (Holton chapter 7.6) by running the same experiment with a realistic rotation. What should you set f to? Motivate your choice based on what you know of the validity of the geostrophic approximation and the Rossby number.
4. Change your initial conditions to

$$u(x, 0) = 0 \quad (13.7)$$

$$v(x, 0) = 0 \quad (13.8)$$

$$h(x, 0) = \begin{cases} h_0 & \text{if } |x| \leq L_W \\ 0 & \text{if } |x| > L_W \end{cases} \quad (13.9)$$

What occurs? Explain the new phenomena. What happens at the boundaries?

5. How do gravity waves affect the results? Try running the same experiment with a relaxation zone (also called sponge zone) at the boundaries and explain the difference. The relaxation can be parameterised in the following way

$$(u_d, v_d) = \left(1 - d \cdot \frac{dt}{\tau}\right) (u, v) \quad (13.10)$$

where (u_d, v_d) is the new damped velocity, d is the value of the sponge at the corresponding grid point (ranging exponentially from 0 to 1) and τ is the damping time given in seconds. Choose d so that damping only occurs near the boundaries. What should τ be?

Explain what the relaxation zone might represent. Also consider why limited area models might need relaxation zones.

6. Apply the Aselin-filter to previous experiment. Do you see any difference? Comment on this.

13.10.2 2D-model

Here we develop a 2D shallow water model that includes rotation and diffusion on an Arakawa **C-grid**.

1. Write the code for the model. (If your previous code is well structured, you can rewrite it for the two-dimensional case). Read section 13.12 before writing the code. And also, try to write it in incremental form, which is explained in section 13.12.
2. Study Rossbys adjustment to geostrophic balance in two dimensions with the following initial conditions:

$$u(x, y, 0) = 0 \quad (13.11)$$

$$v(x, y, 0) = 0 \quad (13.12)$$

$$h(x, y, 0) = h_0 e^{-(x/L_W)^2 - (y/L_W)^2}, \quad (13.13)$$

3. Run the experiment with $f = 0$ and verify your assumptions.
4. Add and evaluate the diffusion at time-step n then at time-step $n - 1$. Describe the discrepancies between the two cases.

$$\frac{\partial u}{\partial t} = \dots + \mu \nabla^2 u \quad (13.14)$$

$$\frac{\partial v}{\partial t} = \dots + \mu \nabla^2 v \quad (13.15)$$

5. Add a two-dimensional relaxation zone at the boundaries, analogous to (10). Do some experiments with different values of f (maybe try out the extremes and some realistic values). Explain what you see.

13.11 Optional exercises

Chose one or do both.

13.11.1 Non-Linear

Rewrite your code into a non-linear shallow water model as described section 8.4.1 and 8.4.2 in the *Numerical Methods in Meteorology and Oceanography* compendium. Include topography using

$$H = h_m - h_T \quad (13.16)$$

Use some variable topography and look at what happens. You can for example use

$$h_T(x, y) = -h_0 e^{-(x/L_W)^2 - (y/L_W)^2} \quad (13.17)$$

Play around or ask for a interesting problem to study.

13.11.2 Spectral model

Write a spectral 1D shallow water model. Use Matlabs FFT routines to move from physical space to spectral space. How do you take the x-derivative of something in spectral space?

13.12 General code structure

This is a general code structure that makes it easy to search model for errors. Try to use the same conventional variable names as in the previous numerical methods lab.

Important is that you try to write your code in incremental form as shown below. That is, add each part of the equations separately.

```
% -----
% Model
% -----  
  
% constants  
g = ...  
...  
  
% set up grid and resolution  
nx = ...  
...  
  
% set up the field variables  
u = zeros(...);  
...  
  
% other stuff you feel is necessary  
...  
  
% set initial conditions  
...  
  
% numerical routine  
  
for t = 1:nt  
  
    % coriolis force  
    du = du + ...  
    ...  
  
    % pressure gradient force  
    du = du - ...  
    ...
```

```
% other stuff, diffusion perhaps  
du = du + ...  
  
% calculate free surface height  
dh = dh - ...  
  
% timestep  
u(...,n+1) = u(...,n-1) + dt*du  
...  
end
```


Chapter 14

Exams at Stockholm University 1999-2008

Tentamen på Numeriska metoder inom meteorologin och oceanografin, 4p, inom meteorologi påbyggnadskurs, ME3570.

Fredagen den 17 september 1999, kl. 9.15–15.15

1. Betrakta funktionen $u(x)$. Härled med hjälp av Taylorutveckling noggranheten av centrerad differens. (6p).

$$\frac{\partial u}{\partial t} + c \frac{\partial u}{\partial x} = 0$$

2. Diskretisera vågekvationen $\frac{\partial u}{\partial t} + c \frac{\partial u}{\partial x} = 0$ med centrerat schema i rummet och för två olika scheman i tiden a) framåt-schema (Euler) och b) Leap-frog. (6p).

3. Utför stabilitetsanalys och ange dess CFL-villkor för Euler fallet. (7p).

4. Räkna ut den numeriska fashastighetens noggranhets och jämför med den verkliga för leap-frog fallet. För vilka våglängder är det minst respektive störst skillnad mellan den analytiska fashastigheten och den numeriska. (7p).

5. Integrerera numeriskt advektionekvationen med centrerat schema för rummet och leap-frog under 8 tidssteg ($n=8$). Integrera sen ett tidssteg med Euler och fortsätt sen med ytterligare 8 tidssteg. Gör detta för två fall med Initialvilkoren för a) $u_j^{n=0} = 1$ och $u_j^{n=1} = 0$ och b) $u_j^{n=0} = 1$ och $u_j^{n=1} = 1$. Beskriv de två simulationerna. (7p).

6. Diskretisera nedanstående ekvationer med centrerade scheman för A och C-gridd. Ledtråd: A-gridden ligger u, v, φ i samma punkter och i C-gridden ligger u, v, φ i olika punkter. Vad är det som saknas för att ekvationssystemet ska kunnas integreras i tiden som en modell. (7p).

$$\frac{\partial u}{\partial t} - fv = -\frac{\partial \varphi}{\partial x} + A_H \nabla^2 u$$

$$\frac{\partial u}{\partial x} + \frac{\partial v}{\partial y} + \frac{\partial w}{\partial z} = 0$$

Tentamen i Numeriska metoder inom meteorologin och oceanografin, ME3580.

Fredagen den 3 november 2000, kl. 9.00–15.00

1. Betrakta funktionen $u(x)$. Härled med hjälp av Taylorutveckling noggrannheten av framåtdifferens. (6p)
2. Betrakta advektionsekvationen

$$\frac{\partial u}{\partial t} + c \frac{\partial u}{\partial x} = 0$$

där $u = u(x, t)$ och c fashastigheten. Låt oss nu betrakta en av många möjliga diskretiseringar av advektionsekvationen som är

$$\frac{u_j^{n+1} - \frac{1}{2}(u_{j+1}^n + u_{j-1}^n)}{\Delta t} + c \frac{u_{j+1}^n - u_{j-1}^n}{2\Delta x} = 0$$

Utför stabilitets analys och diskutera. (6p)

3. Betrakta värmeekvationen

$$\frac{\partial u}{\partial t} = A \frac{\partial^2 u}{\partial x^2} ; \quad A > 0$$

diskretisera med centrerat schema i tiden och högerleddet tas i tidssteget $n-1$. Utför stabilitetsanalys med hjälp av den analytiska lösningen och ange stabiltetsvillkor samt ytterligare egenskaper hos schemat. (6p)

4. Diskretisera nedanstående ekvationer i rummet där u , v och h inte varierar med y med centrerade scheman för A-grid.

$$\frac{\partial u}{\partial t} - fv = -g \frac{\partial h}{\partial x}$$

$$\frac{\partial v}{\partial t} + fu = 0$$

$$\frac{\partial h}{\partial t} + H \frac{\partial u}{\partial x} = 0$$

Ansätt våglösningar av typen $e^{i(kj\Delta x - \omega t)}$ och härled den numeriska fashastigheten och diskutera den och jämför med den analytiska fashastigheten. (6p)

5. Erlands Shallow water teori (6p)

Meteorologiska institutionen Stockholms universitet
Kristofer Döös och Erland Källén



Tentamen i Numeriska metoder inom meteorologin och oceanografin, ME3580.

Torsdagen den 1 november 2001, kl. 9.00–15.00

1. Consider the function $u(x)$. Derive with help of Taylor expansion the order of accuracy of the backward scheme

(6p)

2. Consider the advection equation in two dimensions

$$\frac{\partial u}{\partial t} + c \frac{\partial u}{\partial x} + c \frac{\partial u}{\partial y} = 0$$

where $u = u(x, y, t)$ and c the phase speed.

- a) Discretise with centered scheme in time and space (leap frog).
 b) Make a stability analysis and find under what condition the scheme is stable for the case when $\Delta x \neq \Delta y$.
 c) Find the stability criterion for the case when $\Delta x = \Delta y$

Note: $e^{i\alpha} + e^{-i\alpha} = 2 \cos(\alpha)$ and $e^{i\alpha} - e^{-i\alpha} = 2i \sin(\alpha)$

(6p)

3. Consider the Poisson equation

$$\nabla^2 \Phi = a(x, y)$$

- a) Discretise with a centered scheme in space of the second order accuracy
 b) Discuss how the Poisson equation can be solved iteratively for a given $a(x, y)$
 c) What type of boundary conditions are required in order to solve the equation numerically?

(6p)

4. Discretise the following set of equations both on a B and a C-grid. Show on the grids the different schemes and discuss the advantages and disadvantages of the two grids for this discretisation.

$$\frac{\partial u}{\partial t} + u \frac{\partial u}{\partial x} + v \frac{\partial u}{\partial y} - fv = -g \frac{\partial h}{\partial x} + A \nabla^2 u \quad (1)$$

$$\frac{\partial v}{\partial t} + u \frac{\partial v}{\partial x} + v \frac{\partial v}{\partial y} + fu = -g \frac{\partial h}{\partial y} + A \nabla^2 v \quad (2)$$

$$\frac{\partial h}{\partial t} + u \frac{\partial h}{\partial x} + v \frac{\partial h}{\partial y} + h \left(\frac{\partial u}{\partial x} + \frac{\partial v}{\partial y} \right) = 0 \quad (3)$$

Hint for Equation (3): rewrite before discretisation

(6p)

5. The conservation of potential vorticity for three dimensional motion can be expressed as

$$\frac{d}{dt} \left(\frac{(\mathbf{\hat{u}} + 2\mathbf{\hat{U}}) \cdot \nabla \lambda}{\rho} \right) = 0$$

where λ is a conserved quantity that follows the motion of the air

- a) Suggest a physical quantity λ that is suitable to be used in atmospheric contexts. Discuss why.

(2p)

- b) Show how the conservation of potential vorticity can be simplified for a barotropic atmosphere (shallow water model) in a front region. Assume that the Coriolis parameter is constant.

(4p)

Kunstnare Lars och Birgitta Kallen



Tentamen i Numeriska metoder inom meteorologin och oceanografin, ME3580.

Torsdagen den 31 oktober 2002, kl. 9.00–15.00

1. Betrakta funktionen $u(t)$. Härded med hjälp av Taylorutveckling noggrannheten av leap-frog schemat. (3p)

2. Betrakta ekvationen

$$\frac{\partial T}{\partial t} = A \frac{\partial^2 T}{\partial x^2} - \gamma T, \quad A > 0 \text{ och } \gamma > 0$$

Diskretisera med Euler schema i tiden och högerledet tas i tidssteget n. Utför stabilitetsanalys med hjälp av den analytiska lösningen och ange stabilitetsvillkor samt ytterligare egenskaper hos schemat.

Hjälp: $e^{i\alpha} + e^{-i\alpha} = 2 \cos(\alpha) \quad \text{och} \quad e^{i\alpha} - e^{-i\alpha} = 2i \sin(\alpha)$ (6p)

3. Betrakta Laplaceekvationen $\nabla^2 \Phi = 0$

- a) Diskretisera ekvationen i rummet. (1p)

- b) Sätt $\Delta x = \Delta y$ och skriv det enklaste iterativa schemat (Jacobi iteration). (1p)

- c) Sätt upp en grid på 4 x 4. (1p)

- c) Sätt initialt $\Phi = 0$ och randvärdena till $\Phi = 1$ och iterera 3 gånger och ange alla värden. (1p)

- d) Upprepa men med ett snabbare iterationschema (Gauss-Seidel eller SOR). (2p)

4. Betrakta ekvationerna

$$\frac{\partial u}{\partial t} = -g \frac{\partial h}{\partial x}$$

$$\frac{\partial v}{\partial t} = -g \frac{\partial h}{\partial y}$$

$$\frac{\partial h}{\partial t} + H_0 \left(\frac{\partial u}{\partial x} + \frac{\partial v}{\partial y} \right) = 0$$

- a) Härded dispersionsrelationen genom att ansätta våglösningar. (3p)

- b) Diskretisera ekvationerna i rummet på en A-grid och härded dispersionsrelationen. (2p)

- c) Diskretisera ekvationerna i rummet på en C-grid och härded dispersionsrelationen. (2p)

- d) Diskutera skillnaderna mellan de tre dispersionsrelationerna. (2p)

5. Utgå från shallow-water ekvationerna på formen

$$\frac{\partial u}{\partial t} + u \frac{\partial u}{\partial x} + v \frac{\partial u}{\partial y} - fv = -g \frac{\partial h}{\partial x}$$

$$\frac{\partial v}{\partial t} + u \frac{\partial v}{\partial x} + v \frac{\partial v}{\partial y} + fu = -g \frac{\partial h}{\partial y}$$

$$\frac{d(h - h_B)}{dt} + (h - h_B) \left(\frac{\partial u}{\partial x} + \frac{\partial v}{\partial y} \right) = 0$$

- a) Härded en ekvation för bevarandet av potentiell virvel ur shallow water systemet ovan. (4p)

- b) Diskutera hur denna virvelekvation eventuellt skiljer sig från den kvasi-geostrofiska motsvarigheten (Rossby's potentiella virvelekvation) (2p)

2003

Kristofer Döös och Erland Källén, Meteorolgiska institutionen, Stockholms universitet

Tentamen i numeriska metoder inom meteorologin och oceanografin, ME3580

Torsdagen den 30 oktober 2003, kl. 9.00-15.00

Betrakta ekvationssystemet:

$$\frac{\partial u}{\partial t} = -g \frac{\partial h}{\partial x}$$

$$\frac{\partial h}{\partial t} = -H \frac{\partial u}{\partial x}$$

där g är gravitationen, H djupet, u hastigheten och h ytperturbationen.

1. Lös ut analytiskt en ekvation för h . (1p)
2. Ansätt våglösningar och räkna ut den analytiska fashastigheten. (1p)
3. Diskretisera ekvationerna med centrerade scheman i tid och rum för en A-gridd (u och h i samma gridpunkter). (1p)
4. Räkna ut noggranheten på dessa scheman. (1p)
5. Räkna ut den numeriska fashastigheten och diskutera skillnaden med den analytiska fashastigheten. (1p)
6. Utför stabilitetsanalys. (2p)
7. Vad behövs för initialvilkor och hur kan modellen integreras första tidssteget? (1p)
8. Vad krävs för randvilkor? (1p)
9. Sätt upp en numerisk modell för dessa ekvationer med IM punkter i x -led och beskriv hur den integreras i tiden för NT tidssteg. Ledtråd: skriv en skiss ungefär som en matlab eller fortran kod. (3p)
10. Vad förändras om modellen är på en alternerande gridd där u och h inte är i samma punkter. (3p)
11. Vad förändras om modellen dessutom är i två dimensioner? (3p)
12. Vad förändras om coriolistermen dessutom är med? (3p)
13. Vad förändras om advektionstermerna dessutom är med? (3p)

Formelsamling:

Taylorserien för $f(x)$ runt $x = a$ är $f(x) = f(a) + (x - a)f'(a) + \frac{1}{2}(x - a)^2 f''(a) + \dots + \frac{1}{n!}(x - a)^n f^{(n)}(a)$
 $e^{i\alpha} - e^{-i\alpha} = 2i \sin \alpha$

Shallow water teoriuppgiften: Utgå från de horisontella rörelseekvationerna på formen

$$\frac{\partial u}{\partial t} + u \frac{\partial u}{\partial x} + v \frac{\partial u}{\partial y} + w \frac{\partial u}{\partial z} - fv = -\frac{1}{\rho} \frac{\partial p}{\partial x}$$

$$\frac{\partial v}{\partial t} + u \frac{\partial v}{\partial x} + v \frac{\partial v}{\partial y} + w \frac{\partial v}{\partial z} + fu = -\frac{1}{\rho} \frac{\partial p}{\partial y}$$

samt hydrostatiskt

$$\frac{\partial p}{\partial z} = -g\rho$$

- a) Visa att tryckgradienttermen i de horisontella rörelseekvationerna kan skrivas enbart som funktion av höjden på en fri yta i "shallow-water" approximationen. (4p)
- b) Ange det vilkor under vilket vertikaladvektionstermerna kan sättas till noll. (2p)

2004

Tentamen i numeriska metoder inom meteorologin och oceanografin, ME3580, fredagen den 29 december 2004, kl. 9.00-15.00 av *Kristofer Döös och Erland Källén, Meteorologiska institutionen, Stockholms universitet*

De lineariserade shallow water ekvationerna kan skrivas:

$$\frac{\partial u}{\partial t} - fv = -g \frac{\partial h}{\partial x} \quad (14.1)$$

$$\frac{\partial v}{\partial t} + fu = -g \frac{\partial h}{\partial y} \quad (14.2)$$

$$\frac{\partial h}{\partial t} + H \left(\frac{\partial u}{\partial x} + \frac{\partial v}{\partial y} \right) = 0 \quad (14.3)$$

där $g = 10m/s^2$, $H = 10km$, $f = 10^{-4}s^{-1}$.

1. Härled en dispersionsrelation för våglösningarna till systemet ovan. (3p)
2. Diskutera den relativa betydelsen av rotation och gravitation för vågrörelser. För vilken våglängd är rotations- och gravitationseffekten jämförbara för atmosfäriska förhållanden? (3p)
3. Diskretisera ekvationerna 14.23-14.25 i tid och rum med centrerade scheman på en C-grid (u , v och h i olika punkter) (2p).
4. Vad behövs för typ av initialvillkor och hur kan den numeriska modellen integreras första tidssteget? (1p)
5. Vad krävs för typ av randvillkor för den numeriska modellen? (1p)
6. Räkna ut noggrannheten på de finita diffenserna. Är de olika? (3p)
7. Räkna ut den numeriska dispersionsrelationen för fallet då u , v och h ej beror på y . Diskutera skillnaden med den analytiska dispersionsrelationen från uppgift 1 då $l = 0$. (3p)
8. Beskriv hur en numerisk modell baserad på de diskretiserade ekvationerna från uppgift 3 ser ut med IMT punkter i x -led, JMT punkter i y -led och beskriv hur den integreras i tiden för NT tidssteg. Ledtråd: skriv en skiss ungefärlig som en matlab eller fortran kod. (3p)
9. Utför stabilitetsanalys för fallet då u , v och h ej beror på y och $f = 0$. (4p)
10. Inkludera de icke-linjära termerna i shallow water ekvationerna och skriv om så att de icke-linjära termerna delas upp på den absoluta potentiella virveln och en gradient av kinetiska energin. (3p)
11. Diskretisera dessa ekvationerna på en C-gridd. Visa att det finns flera möjliga diskretiseringar. (4p)

Formelsamling: $e^{i\alpha} - e^{-i\alpha} = 2i \sin \alpha$ och $e^{i\alpha} + e^{-i\alpha} = 2\cos \alpha$ och $2\sin^2(\alpha/2) = 1 - \cos \alpha$

Taylorserien för $f(x)$ runt $x = a$ är $f(x) = f(a) + (x-a)f'(a) + \frac{1}{2}(x-a)^2f''(a) + \dots + \frac{1}{n!}(x-a)^n f^{(n)}(a)$

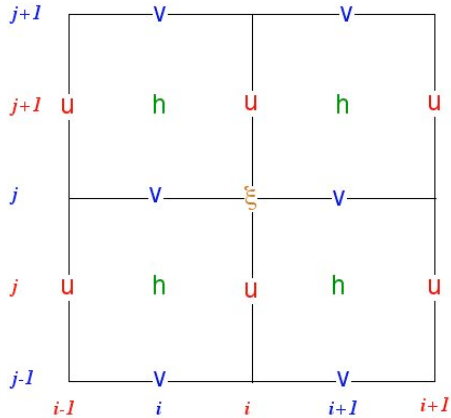


Figure 14.1: C-grid.

2005

Tentamen i numeriska metoder inom meteorologin och oceanografin, ME3580, torsdagen den 3 november 2005, kl. 9.00-15.00 av Kristofer Döös och Erland Källén, Meteorologiska institutionen, Stockholms universitet

Consider the partial differential equation (PDE):

$$\frac{\partial T}{\partial t} = A \nabla^2 T \quad \text{where } A > 0 \text{ and } \nabla^2 \equiv \frac{\partial^2}{\partial x^2} + \frac{\partial^2}{\partial y^2}$$

- 1) Find a solution for $T(x, y, t)$ and describe what it could represent physically. (N.B. Nothing to do with numerical methods!) (2p)
- 2) Is the PDE elliptic, hyperbolic or parabolic? Show how you determine this. Clue: use only one dimension in space. (2p)
- 3) Discretise the time derivative with centered difference and the laplace with centered difference at time step n-1. (2p)
- 4) Derive the order of accuracy of the two schemes with help of Taylor series. (2p)
- 5) Make a stability analysis. (2p)
- 6) Is there a numerical mode? Why? How do you suppress it? (2p)

Consider the non-linear shallow water equations:

$$\frac{\partial u}{\partial t} - \xi h v = - \frac{\partial H}{\partial x} \tag{14.4}$$

$$\frac{\partial v}{\partial t} + \xi h u = - \frac{\partial H}{\partial y} \tag{14.5}$$

$$\frac{\partial h}{\partial t} + \frac{\partial(hu)}{\partial x} + \frac{\partial(hv)}{\partial y} = 0 \tag{14.6}$$

where $\xi \equiv \left(f + \frac{\partial v}{\partial x} - \frac{\partial u}{\partial y} \right) / h$ and $H \equiv gh + \frac{1}{2} (u^2 + v^2)$

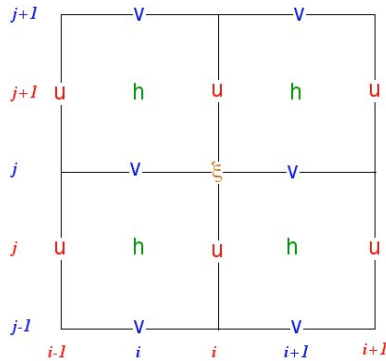


Figure 14.2: C-grid.

- 7) Discretise the equations 14.4-14.6 with centered schemes on a C-grid (See Figure 14.2 at bottom of the page). (4p)
- 8) Find a second way to discretise the terms ξhv and ξhu . (2p)
- 9) What type of initial condition is needed and how can one integrate the first time step? (2p)
- 10) What type of boundary conditions are needed? (2p)
- 11) Describe a numerical model code in matlab or fortran based on these discretised equations with IM grid cells in the x direction and JM in the y direction and how it is integrated in time for NT time steps. (2p)
- 12 a) Linearise eqs 14.4-14.6 around a state of rest with an average shallow water depth D. (3p)
- 12 b) Determine the types of wave motions that can be described with the linearised system given in 12a). If you cannot solve 12a) you can get the answer to 12a), but in this case you will not be given any points for 12a. (3p)

Formulas: $e^{i\alpha} - e^{-i\alpha} = 2i \sin \alpha$ and $e^{i\alpha} + e^{-i\alpha} = 2\cos \alpha$ and $2\sin^2(\alpha/2) = 1 - \cos \alpha$

Taylor series for $f(x)$ about $x = a$ is $f(x) = f(a) + (x - a)f'(a) + \frac{1}{2}(x - a)^2f''(a) + \dots + \frac{1}{n!}(x - a)^n f^{(n)}(a)$
 $a\frac{\partial^2 u}{\partial x^2} + b\frac{\partial^2 u}{\partial x \partial y} + c\frac{\partial^2 u}{\partial y^2} + d\frac{\partial u}{\partial x} + e\frac{\partial u}{\partial y} + fu + g = 0$. If $b^2 - 4ac < 0$ then elliptic; if $= 0$ then parabolic; if > 0 then hyperbolic .

2006

Tentamen i numeriska metoder inom meteorologin och oceanografin, ME3580, torsdagen den 2 november 2006, kl. 9.00-15.00 av *Kristofer Döös och Heiner Körnich, Meteorologiska institutionen, Stockholms universitet*. Tentamen på totalt 30 p. För godkänt krävs 15 p. och väl godkänt 22,5 p.

Betrakta grunt vattenekvationerna på formen

$$\frac{\partial u}{\partial t} + u \frac{\partial u}{\partial x} + v \frac{\partial u}{\partial y} - fv = -g \frac{\partial h}{\partial x} + A \nabla^2 u \quad (14.7)$$

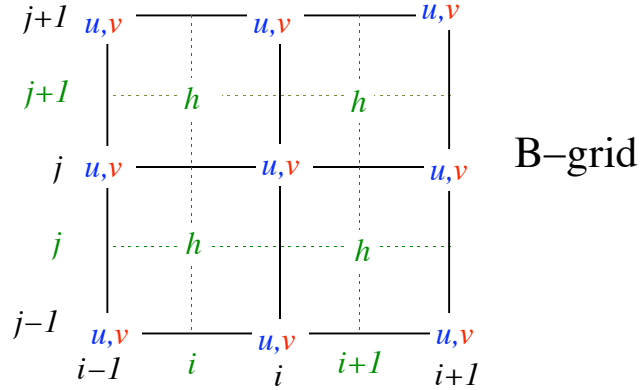
$$\frac{\partial v}{\partial t} + u \frac{\partial v}{\partial x} + v \frac{\partial v}{\partial y} + fu = -g \frac{\partial h}{\partial y} + A \nabla^2 v \quad (14.8)$$

$$\frac{\partial h}{\partial t} + \frac{\partial (hu)}{\partial x} + \frac{\partial (hv)}{\partial y} = 0 \quad (14.9)$$

- 1) Linjarisera ekvationerna (14.23) - (14.25) runt ett medeldjup på D samt gör friktionsfritt. (2p)
- 2) Diskretisera dessa linjarisrade friktionsfria rörelseekvationer med centrerade differenser i både tid och rum på en B-grid (se figur). (2p)
- 3) Förenkla dessa diskretiserade ekvationer för fallet då fallet $f = 0$ och utan y beroende d.v.s. $\partial/\partial y = 0$.(1p)
- 4) Gör en stabilitetsanalys på de diskretiserade ekvationer i uppgift 3. (4p)
- 5) Härlled noggrannheten av den centrerade tidsdifferensen. (2p)
- 6) Hitta en möjlig diskretisering av de ickelinjära advektionstermerna i ekvationerna (14.23) och (14.24). Redovisa dem var och en för sig. (3p).
- 7) Diskretisera även friktionstermerna i ekvationerna (14.23) och (14.24). Redovisa dem var och en för sig. (2p).
- 8) Härlled noggrannheten friktionstermerna. (Räcker med en dimension) (2p)
- 9) Finns det en beräkningsmod (numerisk mod) ? I så fall varför och hur filtreras denna bort? (1p)
- 10) Vad för initial- och randvillkor behövs för att ekvationerna ska kunna integreras? (1p)
- 11) Beskriv hur en numerisk modell bestående av de diskretiserade ekvationerna skulle se ut. Med IM griddceller i x -led och JM i y -led och som integreras i tiden under NT tidsteg. (4p)
- 12) Linjarisera friktionsfria versioner av ekvationerna (1)-(3) runt ett medeldjup på D med en konstant geostrofisk flöde u_b i x -led, dvs. $\vec{u} = (u_b; 0) + (u'; v')$, $h = D + \eta_b + \eta'$. η_b är det geostrofiskt balanserade höjd fältet med $\eta_b \ll D$. (3p)
- 13) Bestäm vilken typ av vågor som beskrivs av de linjarisade ekvationerna i uppgift 10). Hur påverkar bakgrund fashastighet i x -led c_x ? (3p)

Formelsamling: $e^{i\alpha} - e^{-i\alpha} = 2i \sin \alpha$ and $e^{i\alpha} + e^{-i\alpha} = 2\cos \alpha$ and $2\sin^2(\alpha/2) = 1 - \cos \alpha$

Taylorserien för $f(x)$ runt $x = a$ är $f(x) = f(a) + (x - a)f'(a) + \frac{1}{2}(x - a)^2 f''(a) + \dots + \frac{1}{n!}(x - a)^n f^{(n)}(a)$



2007

Tentamen i numeriska metoder inom meteorologin och oceanografin, ME3580, torsdagen den 1 november 2007, kl. 9.00-15.00 av Kristofer Döös och Heiner Körnich, Meteorologiska institutionen, Stockholms universitet. Tentamen på totalt 30 p. För godkänt krävs 15 p. och väl godkänt 22,5 p.

Consider the shallow water equations in vector-form:

$$\frac{\partial}{\partial t} \vec{u}_h + \nabla \frac{\vec{u}_h \cdot \vec{u}_h}{2} + (\xi + f) \vec{k} \times \vec{u}_h = -g \nabla h \quad (14.10)$$

$$\frac{\partial H}{\partial t} + \nabla \cdot (\vec{u}_h H) = 0 \quad (14.11)$$

with the following definitions:

$$\text{the total depth } H = h - h_b, \quad (14.12)$$

$$\text{the surface elevation } h_b = h_b(x, y), \quad (14.13)$$

$$\text{the relative vorticity } \xi = \frac{\partial v}{\partial x} - \frac{\partial u}{\partial y}, \quad (14.14)$$

$$\text{and the horizontal velocity vector } \vec{u}_h = \begin{pmatrix} u \\ v \end{pmatrix} \quad (14.15)$$

- 1) Linearise the equations (14.10) and (14.11) for small amplitude motion around a mean depth $D = D(x, y)$. Derive the solution for the time-independent linear motion. Show that the divergence of this motion is zero and discuss this motion for a spatially varying surface elevation h_b . (4p)
- 2) Use the linear equations to derive the tendency equation for the total energy $E_{tot} = D|\vec{u}_h|^2/2 + gh^2/2$. Assume a closed region with no normal flow across the boundaries: $\vec{u}_h \cdot \vec{n} = 0$, where the vector \vec{n} which is the orthogonal unity vector on the boundary contour. Argue why the area integrated total energy is conserved. Hint: Apply the divergence theorem (2p)

$$\iint_A dA \nabla \cdot \vec{v} = \oint \vec{v} \cdot \vec{n} dr. \quad (14.16)$$

- 3) Discretise the linearised shallow water equations with a flat bottom on a C-grid (see Fig. ??) with Euler forward finite differences in time and centred finite differences in space. (3p)
- 4) What initial and boundary conditions are required. (1p)
- 5) Is there a numerical mode? How can you suppress a numerical mode? (1p)
- 6) Simplify the discretised equations from task 3 for the case when $f = 0$ and for no y dependency. i.e. when $\partial/\partial y = 0$. (1p)
- 7) Make a stability analysis on the equations from previous task. (3p).
- 8) Calculate the truncation error of the Euler forward finite difference. (2p)
- 9) Derive the frequency equation by substituting wave solutions into the linearised shallow water equations for the case when $\partial/\partial y = 0$. Note that this is for the continuous equations with no finite differences. (3p)
- 10) Same as previous task but for the discretised equations with finite differences in space on a C-grid. Use continuous differences in time. Discuss the effects of discretisation on the phase speed. (3p)
- 11) Find two possible discretisations on the C-grid of the non-linear advection terms in the shallow water momentum equations (both the zonal and the meridional momentum equations). (3p)
- 12) In what way is a hydrostatic 3-D model (GCM) different from a shallow water model? What extra equations and terms are there? Discretise these extra terms and equations. (4p).

Formelsamling: $e^{i\alpha} - e^{-i\alpha} = 2i \sin \alpha$ and $e^{i\alpha} + e^{-i\alpha} = 2\cos \alpha$ and $2\sin^2(\alpha/2) = 1 - \cos \alpha$

Taylorserien för $f(x)$ runt $x = a$ är $f(x) = f(a) + (x - a)f'(a) + \frac{1}{2}(x - a)^2f''(a) + \dots + \frac{1}{n!}(x - a)^n f^{(n)}(a)$

2008

Tentamen i numeriska metoder inom meteorologin och oceanografin, ME3580, torsdagen den 30 oktober 2008, kl. 9.00-15.00 av *Kristofer Döös och Heiner Körnich, Meteorologiska institutionen, Stockholms universitet.* Tentamen på totalt 30 p. För godkänt krävs 15 p. och väl godkänt 22,5 p.

Consider the linearised shallow water equations in the quasi-one-dimensional case where u , v and h do not depend on y so that the shallow water equations are reduced to

$$\frac{\partial u}{\partial t} - fv = -g \frac{\partial h}{\partial x} \quad (14.17)$$

$$\frac{\partial v}{\partial t} + fu = 0 \quad (14.18)$$

$$\frac{\partial h}{\partial t} + H \frac{\partial u}{\partial x} = 0 \quad (14.19)$$

- 1) Derive the dispersion relationship (frequency equation) by substituting wave solutions into 14.17- 14.19. (2p)
- 2) Discretise Eqs. 14.17- 14.19 in space on a B-grid (see Figure on next page) and keep the continuos derivatives in time. (1p)
- 3) Derive the numerical dispersion relationship for these discretised equations in space. (3p)
- 4) Describe the differences between these model waves and the analytical continuos waves (2p)
- 5) Discretise the equations in task 2 with centred finite differences in time (leap-frog). (1p)
- 6) Make a stability analysis on the equations in previous task. (5p).
- 7) Derive the numerical dispersion relationship from the disrcetised equation from task 5 (this time with finite differences in time). (4p)
- 8) What initial and boundary conditions are required? How can you start to integrate the first time step? (1p)
- 9) Is there a numerical mode? Why? How can you suppress a numerical mode? (1p)
- 10) Calculate the truncation error of the finite difference in space of the continuity equation from task 2. (2p)
- 11) Consider the continuity equation with pressure as vertical coordinate

$$\frac{\partial u}{\partial x} + \frac{\partial v}{\partial y} + \frac{\partial \omega}{\partial p} = 0 \quad (14.20)$$

Discretise it on a B-grid and explain how it can be integrated. (2p)

- 12) Derive the linearised potential vorticity equation

$$\frac{\partial}{\partial t} \left[\xi - \frac{f}{H} h \right] = 0 \quad (14.21)$$

from the equations 14.17- 14.19. Discuss the relationship between the vorticity and the surface elevation implied by equation 14.21. (3p)

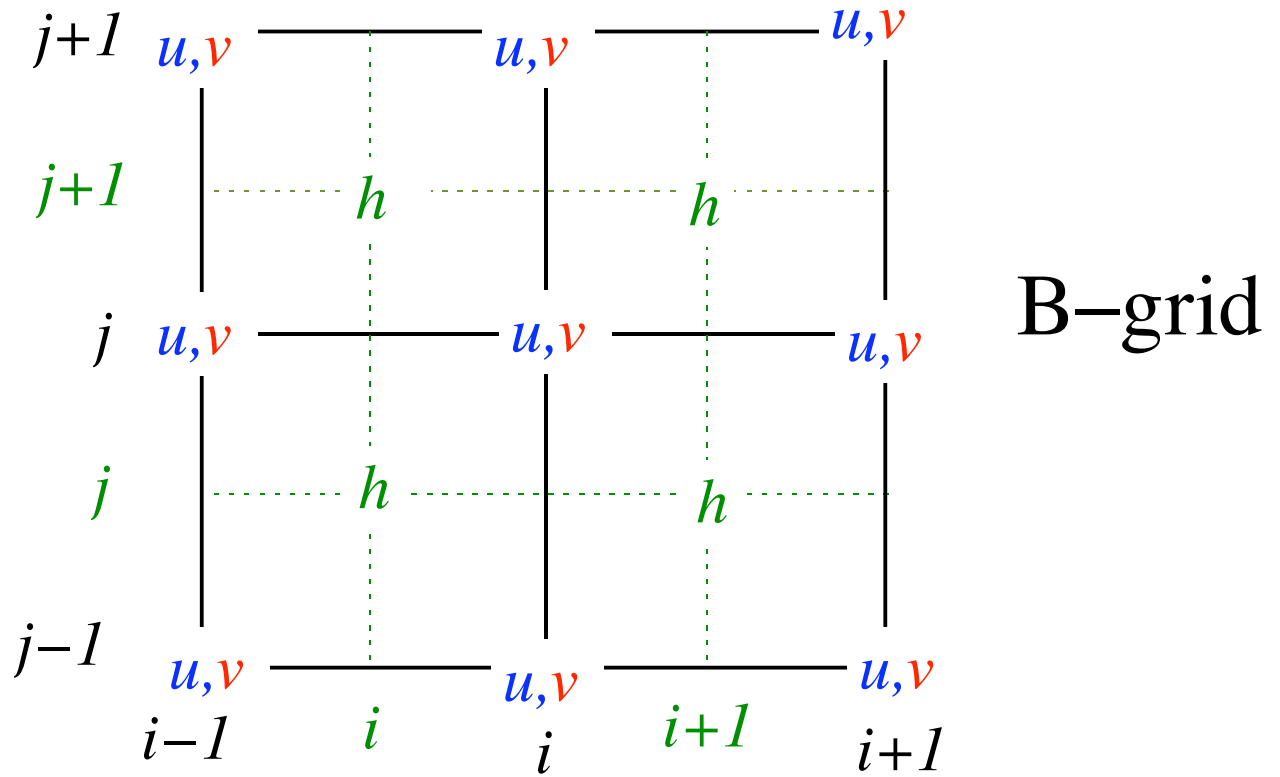
- 13) Assume that the real part of the wave solution for $\eta = h - H$ is given as

$$\eta = \eta_0 \cos(kx - \sigma t). \quad (14.22)$$

Express the wave solution for the vorticity and the divergence in terms of the amplitude η_0 . Which motion type (divergence or vorticity) has a larger amplitude? Use the fact $\sigma > f$. (3p)

Formulas: $e^{i\alpha} - e^{-i\alpha} = 2i \sin \alpha$ and $e^{i\alpha} + e^{-i\alpha} = 2 \cos \alpha$ and $2 \sin^2(\alpha/2) = 1 - \cos \alpha$

The Taylor series for $f(x)$ around $x = a$ is $f(x) = f(a) + (x-a)f'(a) + \frac{1}{2}(x-a)^2f''(a) + \dots + \frac{1}{n!}(x-a)^n f^{(n)}(a)$



2010

Tentamen i numeriska metoder inom meteorologin och oceanografin, MO7004, tisdagen den 28 september 2010, kl. 9.00-15.00 av *Kristofer Döös, Meteorologiska institutionen, Stockholms universitet*. Tentamen på totalt 100 poäng. För betyg A krävs minst 90 p., B ges mellan 89 och 80p, C: 65-79, D:55-64, E:50-54, Fx:45-49 och under 45 p. ges betyg F.

Betrakta de linjariserade gruntuattenekvationerna på formen

$$\frac{\partial u}{\partial t} - fv = -g \frac{\partial h}{\partial x} \quad (14.23)$$

$$\frac{\partial v}{\partial t} + fu = -g \frac{\partial h}{\partial y} \quad (14.24)$$

$$\frac{\partial h}{\partial t} + D \left(\frac{\partial u}{\partial x} + \frac{\partial v}{\partial y} \right) = 0 \quad (14.25)$$

där D är medeldjupet.

1) Inkludera de icke-linjära termerna i ekvationerna (14.23) - (14.25). (5p)

2) Skriv om dessa icke-linjariserade gruntuattenekvationer med hjälp av
 $\xi \equiv \left(f + \frac{\partial v}{\partial x} - \frac{\partial u}{\partial y} \right) / h$, $U = uh$, $V = vh$ och $E = gh + \frac{1}{2} (u^2 + v^2)$. (7p)

3) Diskretisera de linjariserade rörelseekvationer (14.23) - (14.25) med centrerade differenser i rummet på en A-grid (se figur) och Euler framåt i tiden. (7p)

4) Hitta en möjlig diskretisering på en A-grid även för de icke-linjära termerna för de tre icke-linjariserade gruntuattenekvationerna. Redovisa separat varje term. (10p)

5) Härled dispersionsrelationen för (14.23) - (14.25) genom att ansätta våglösningar. (10p)

6) Härled den numeriska dispersionsrelationen för de diskretiserade linjariserade ekvationerna från uppgift 3 genom att ansätta diskretiserade våglösningar. Använd kontinuerliga derivater i tiden och antag att det inte finns någon variation i y-led. Diskutera skillnaden mellan den numeriska och analytiska dispersionsrelationen från föregående uppgift. (15p)

7) Härled noggrannheten av de finita differenserna av ekvationerna i uppgift 3. Är de alla lika exakta? (10p)

8) Gör en stabilitetsanalys på de diskretiserade ekvationer i uppgift 3 för fallet då $f=0$. (16p)

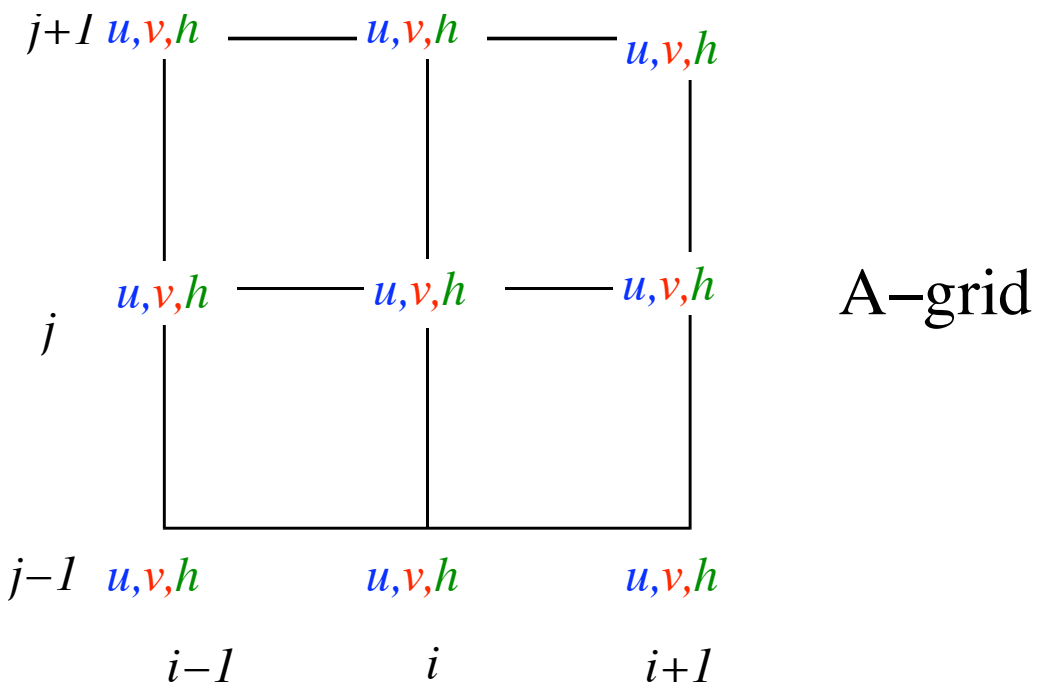
9) Finns det en beräkningsmod (numerisk mod)? Motivera! (5p)

10) Vad för initial- och randvillkor behövs för att ekvationerna ska kunna integreras? (5p)

11) Skulle du valt ha de finita differenserna i uppgift 3 om du hade satt upp en linjära gruntvattenmodell? Skulle du föredragit en annan uppsättning? Argumentera för för- och nackdelarna mellan din och den givna modellen i uppgift 3. (10p)

Formelsamling: $e^{i\alpha} - e^{-i\alpha} = 2i \sin \alpha$ and $e^{i\alpha} + e^{-i\alpha} = 2\cos \alpha$ and $2 \sin^2(\alpha/2) = 1 - \cos \alpha$

Taylorserien för $f(x)$ runt $x = a$ är $f(x) = f(a) + (x-a)f'(a) + \frac{1}{2}(x-a)^2f''(a) + \dots + \frac{1}{n!}(x-a)^n f^{(n)}(a)$



Bibliography

- Asselin, R. A., 1972: Frequency filter for time integrations. *Mon. Weather Rev.*, 100, 487-490.
- Kalnay, Eugenia, 2003: *Atmospheric Modeling, Data Assimilation and Predictability*. Cambridge University Press, 341pp.
- Mesinger and Arakawa, 1976: GARP Publication Series No. 17, WMO.
- Robert, A., 1969: The integration of a spectral model of the atmosphere by the implicit method. *Proc. of the WMO/IUGG Symp. on NWP*, Tokyo, Japan Meteor. Agency, VII, 19-24.
- Sadourny, R., 1975: The dynamics of finite-difference models of the shallow-water equations. *J. Atmos. Sci.*, 32, 680-689.
- Sadourny, R., 1975: Compressible model flows on the sphere. *J. Atmos. Sci.*, 32(11):2103-2110.
- Simmons, A.J. and D.M. Burridge, 1981. An Energy and Angular-Momentum Conserving Vertical Finite-Difference Scheme and Hybrid Vertical Coordinates. *Monthly Weather Review*. 109, 4, 758-766.